Programme de Recherche Interorganisme
Pour une Meilleure Qualité de l'Air à l'Echelle Locale - 2

PRIMEQUAL-2

Proposition de Recherche

Etude de la contribution de l'aérosol organique en tant que source d'acide nitreux (Acronyme: SHONO)

Rapport final

Coordinateur :

GEORGE Christian
Directeur de Recherche CNRS
Laboratoire d'Application de la Chimie à l'Environnement
43, boulevard du 11 novembre 1918
F-69622 VILLEURBANNE

Partenaire:

WORTHAM Henri
Professeur, Université de Provence
Laboratoire Chimie et Environnement
(Case courrier 29)
3 Place Victor Hugo
13331 Marseille Cedex 03

Décembre 2005

Nitrous acid is an important source of hydroxyl radical and there is therefore a keyplayer in atmospheric chemistry. In this project, we investigated the heterogeneous and multiphase chemistry of NO_2 on solid and organic surfaces and identified that these reactions are acting as HONO sources. The reaction on liquid surfaces were strongly depending on the pH and were more efficient at high pH meaning that btheir atmospheric implications will be limited. However, we demeonstrated for the first time that HONO can be efficiently produced by photoinduced processe on surfaces and that this source will be the major OH source in the planetray boundary layer. This is a key finding of this project.

L'acide nitreux est une gaz important car c'est une source importante de radicaux OH. Ce gaz est donc élement crucial pour une bonne description de la chimie atmosphérique. Dans ce projet nous avons étudié quelques sources d'acide nitreux à travers la chimie hétérogène et multiphasique du dioxyde d'azote sur des surfaces organiques liquides et solides. Nous avons ainsi pu montrer que la chimie sur des milieux liquides étaient fortement dépendantes du pH (plus actif dans des milieux alcalains) et avait donc une implication atmosphérique limitée. Par contre, nous avons identifié pour la première fois une source photochimique d'acide nitreux. L'importance de ce nouveau chemin réactionnel est tel que cette source de HONO représent la source principale de radicaux OH dans la couche limite planétaire. Il s'agit d'une découverte majeure issue de ce projet.

Résumé

En 1986, dans leur ouvrage "Atmospheric Chemistry: Fundamentals and experimental techniques", devenu un classique dans le domaine, Barbara Finlayson-Pitts et James Pitts concluent en ces termes un des passages concernant l'acide nitreux: "HONO est certainement une espèce clé dans la troposphère à travers sa photolyse, cependant ses sources sont hautement incertaines. Ceci est clairement un domaine d'études futures" [*Finlayson-Pitts et Pitts*, 1986].

Près de vingt ans après, cette affirmation est toujours d'actualité puisque les sources d'acide nitreux restent encore mal décrites et ce malgré des progrès significatifs! En effet, de nombreuses réactions (homogènes et hétérogènes) ont été proposées en tant que source d'acide nitreux. Néanmoins, elles ne permettent pas de décrire pleinement les vitesses de conversion entre l'azote à l'état d'oxydation +IV (soit NO_2) et +III (soit HNO_2) observées sur le terrain [*Lammel et Cape*, 1996] et ce surtout durant la journée.

Or simuler correctement les sources d'acide nitreux est nécessaire car ce gaz peut jouer un rôle très important lors d'épisodes de pollution photochimique. En effet, HNO_2 est photolysé très rapidement (avec des temps de vie de l'ordre de l'heure au lever du soleil) libérant ainsi du monoxyde d'azote et des radicaux hydroxyle (OH). Dès leur formation, ces derniers vont débuter les cycles d'oxydation des hydrocarbures et la conversion de NO vers NO_2 et ainsi la production photochimique d'ozone. Ainsi la photolyse d'acide nitreux peut influencer les pics de pollution observés dans nos grandes agglomérations [*Cox et Jenkin*, 1987; *Jenkin et al.*, 1988] car pouvant être une source majeure de radicaux OH.

En effet, l'acide nitreux est observé principalement en milieu urbain car une de ses sources importantes est liée à la chimie de NO_2 sur les aérosols carbonés. Or très récemment, *Ammann et al.* ont montré que le dioxyde d'azote réagissait principalement avec les composés organiques adsorbés sur les aérosols mais aussi avec les aérosols organiques obtenus lors de la condensation des gaz d'échappement. Ces mêmes auteurs ont pu montrer que les organiques impliqués dans ces réactions sont des dérivés (plus ou moins complexes) du phénol [*Gutzwiller et al.*, 2000; *Gutzwiller et al.*, 2001].

Cela a ouvert une toute nouvelle orientation de recherche, car de telles espèces aromatiques sont ubiquistes et forment une fraction importante de la matière organique condensée présente dans l'atmosphère. Ainsi, il convient de pouvoir quantifier l'importance d'une telle source d'acide nitreux.

Pour cela nous avons étudié les réactions entre NO_2 et une série de composés organiques représentatives de l'aérosol troposphérique afin d'identifier de nouvelles sources d'acide nitreux. Ces travaux ont été menés à la fois sur des substrats solides et liquides (aqueux et organiques) afin d'explorer la plus large gamme possible de conditions atmosphériques. Ceci sera possible grâce à l'emploi de techniques expérimentales complémentaires: les tubes à écoulement à film tombant et à paroi enduite. Les résultats expérimentaux seront ensuite intégrés dans un code chimique 0-D afin d'estimer leur impact sur une masse d'air donnée.

Nous avons ainsi mesuré les vitesses de capture de NO_2 sur différents milieux liquides (aqueux et organiques). Ces vitesses de capture sont reliées à la fois à la solubilité du gaz dans le liquide considéré mais aussi à la réactivité en solution. Cette réactivité était dans le cadre de ces travaux à la présence composés organiques (de type dérivés phénoliques). De nos études, il a donc été possible de déterminer la

solubilité (le cas échéant) et les vitesses de réactions entre NO_2 et ces dérivés phénoliques (ou différents mélanges de composés organiques). Il en résulte que cette réaction produit effectivement des ions nitrites (et donc de l'acide nitreux) mais de manière fortement dépendante du pH. Cette dépendance malheureusement limite fortement l'implication de cette chimie en tant que source d'acide nitreux. Cette chimie s'avère ainsi être très importante dans le cadre d'aérosol organiques tels que ceux issus de processus de combustion de biomasse.

Devant cette limitation, nous avons en complément étudié la photochimie de surfaces organiques et démontré ainsi, pour la première fois, que NO_2 était converti de manière photochimique sur des surfaces organiques telles que celles présentes de manière ubiquiste dans l'environnement (végétation, bâti, sols, etc…). Cette photochimie converti très efficacement NO_2 en HONO. Cette source est tellement importance, qu'après photodissociation de l'acide nitreux en OH, il s'agit de la source principale de ces radicaux dans la couche limite planétaire. Il s'agit d'une découverte majeure issue de ce projet.

Etude de la contribution de l'aérosol organique en tant que source d'acide nitreux (Acronyme: SHONO)

Rapport final

I. Problématique

Pourquoi l'acide nitreux est-il un élément important dans les cycles d'oxydation?

Ce gaz est généralement présent à de très faibles concentrations (typiquement de l'ordre du ppbv et avec des maxima de l'ordre de 10 ppbv) et ne correspond qu'à une très faible fraction des oxydes d'azote. Par contre, la photochimie de cet acide est des plus importantes. En effet, HNO_2 se photodissocie selon [*Cox*, 1974]:

$$HNO_2 + h\nu \xrightarrow{\lambda \leq 400nm} OH + NO \qquad (1)$$

libérant ainsi des radicaux hydroxyle. La vitesse de photolyse associée varie de l'ordre de l'heure le matin à quelques minutes lorsque le soleil est à son zénith. La photolyse étant le principal mécanisme de dégradation de l'acide nitreux, cette espèce est stable la nuit et peut donc s'accumuler en l'absence de lumière. Par contre, dès le lever du soleil, la photolyse devient le puits principal de cette espèce qui agit alors comme source de OH. Cette source peut être suffisante pour initier plus tôt dans la journée les cycles chimiques pouvant donner lieu ultérieurement à un épisode de pollution photochimique. Selon une étude numérique, la photolyse d'acide nitreux peut multiplier jusqu'à 5 la concentration en OH à 06:00h et contribuer jusqu'à 16% dans la production nette d'ozone photochimique [*Cox et Jenkin*, 1987; *Jenkin et al.*, 1988]. Pour quantifier cette source de radicaux hydroxyle. Il convient d'identifier les réactions chimiques pouvant former de l'acide nitreux.

Les premières sources identifiées d'acide nitreux concernent la chimie homogène en phase gazeuse du monoxyde d'azote, soit [*Chan et al.*, 1976]:

$$NO + OH \rightarrow HNO_2 \qquad (2)$$

Combiné avec la photolyse, cette réaction aboutit à une concentration stationnaire d'acide nitreux (et ce même en plein jour). Par contre, comme cette réaction fait intervenir le radical OH, elle ne va pas être effective la nuit. Or c'est justement la nuit que HNO_2 s'accumule. Une deuxième réaction peut être considérée soit [*Cox et Jenkin*, 1987]:

$$NO + NO_2 + H_2O \rightarrow 2\ HNO_2 \qquad (3)$$

Mais cette réaction est très lente et même à des humidités relatives de 80%, la vitesse de formation d'acide nitreux par cette réaction serait beaucoup trop faible pour expliquer les concentrations réellement observées. Ainsi d'autres réactions ont été proposées qui font intervenir l'eau condensée, soit [*Lee et Tang*, 1988; *Mertes et Wahner*, 1994; *Schwartz et Lee*, 1995]:

$$NO + NO_2 + H_2O \leftrightarrow 2\ HNO_2 \qquad (4,\text{-}4)$$

$$2\ NO_2 + H_2O \leftrightarrow HNO_2 + HNO_3 \qquad (5,\text{-}5)$$

Ces réactions font intervenir l'eau liquide et l'effet catalytique que peut avoir une surface sur une réaction chimique. Or compte tenu des concentrations de monoxyde d'azote et/ou de dioxyde d'azote, il a été montré que ces réactions sont trop lentes pour contribuer de manière significative au bilan d'acide nitreux [*Lee et Schwartz*, 1981a; *Lee et Schwartz*, 1981b]. D'autres réactions en solution peuvent également contribuer à la réduction de l'azote telle que les réactions d'échanges de charges du type [*Pires et al.*, 1994; *Herrmann et al.*, 2000]:

$$NO_2 + O_2^- \rightarrow NO_2^- \quad (6)$$

Là encore, bien que la réaction soit intrinsèquement rapide, les faibles concentrations des réactifs limitent la quantité d'acide nitreux formée. Bien qu'il soit connu que les nuages peuvent contenir des quantités conséquentes d'ions nitrites, cette chimie aqueuse ne semble pas avoir le potentiel pour être une source importance pour le milieu urbain.

Il en va tout autrement si l'on considère, une fois de plus, l'influence de l'automobile. En effet, les gaz d'échappement sont une des rares sources directes d'acide nitreux, qui est observé de manière prépondérante en milieu urbain. D'autre part, les particules émises par les moteurs diesels sont au cœur de très nombreuses questions liées à leur réactivité dans l'atmosphère. De nombreuses études, ont montré que les aérosols carbonés peuvent convertir aisément NO_2 en HNO_2 [*Ammann et al.*, 1998; *Chughtai et al.*, 1994; *De Santis et Allegrini*, 1992; *Gerecke et al.*, 1998; *Kalberer et al.*, 1996; *Lary et al.*, 1999; *Rogaski et al.*, 1997; *Tabor et al.*, 1994; *Vogt et Finlayson-Pitts*, 1994]. D'autres produits ont été observés lors de ces études tels que NO ou N_2O. Les études publiées diffèrent parfois grandement dans leurs conclusions ce qui reflète en fait la difficulté de mener en laboratoire des études sur la suie. En effet, cela soulève de nombreux problèmes tels que : comment produire la suie de manière reproductible? Quelle est sa forme géométrique? Quelle est sa composition de surface? Des réponses à ces questions commencent à être publiées, mais encore maintenant il est commode de décrire cette source sous la forme suivante [*Lammel et Cape*, 1996]:

$$NO_2 + Red_{ads} \leftrightarrow NO_2^- + OX_{ads} \quad (7)$$

où Red_{ads} et OX_{ads} sont respectivement des sites ou des espèces réductrices ou oxydantes adsorbés à la surface de l'aérosol. Il est évident que la surface d'un aérosol carboné est extrêmement complexe. C'est pourquoi l'identification de ces "moteurs chimiques" (soit Red_{ads} et OX_{ads}) est un point très délicat à mener à bien.

Très récemment, Ammann *et al*. ont montré que NO_2 réagissant non seulement avec la suie mais aussi avec les condensats des vapeurs organiques émises par un moteur diesel [*Gutzwiller et al.*, 2000; *Gutzwiller et al.*, 2001]. Cela peut signifier que ces "moteurs chimiques" sont partagés entre les phases particulaire et gazeuse et donc susceptible d'initier la transformation de NO_2 en HNO_2 sur d'autres substrats et dans d'autres conditions (il a par exemple été montré que le bitume est une source d'acide nitreux du fait de la condensation de telles vapeurs [*Ackermann et al.*, 2001]). D'autres part, ces mêmes auteurs ont montré que les espèces mises en jeu étant très vraisemblablement des phénols ou autres aromatiques hydroxylés (noté ici ArOH) qui sont finalement présent dans (presque) tous les aérosols organiques. La réaction produisant l'acide nitreux peut alors s'écrire sous la forme:

$$ArO^- + NO_2 \rightarrow NO_2^- + ArO \quad (8)$$

L'ion nitrite ainsi formé est en équilibre avec son acide HNO_2 suivant une répartition contrôlée par le pH [*Park et Lee*, 1986]. Ce facteur acidité apparaît comme étant très important puisqu'il va également contrôler la quantité d'ions ArO^- présents dans l'aérosol ou le condensat. Les conditions idéales pour la formation d'acide nitreux seraient alors un pH dans la gamme 4-6 qui correspond pleinement à des valeurs observées dans le milieu naturel et pollué.

Tandis que les voies de formation durant la nuit sont qualitativement identifiées. Il en va tout autrement pour les processus aboutissant à la formation d'acide nitreux le jour. En effet, très récemment il a été possible de mesurer avec sensibilités les concentrations de cet acide durant le jour. Or il s'est avéré que ces concentrations

sont très nettement supérieures aux concentrations calculées dans des modèles de chimie atmosphérique. Ainsi il existe une source photochimique produisant de l'acide nitreux avec des taux horaires de l'ordre de 200 à 1800 ppt/hr. Or cette source est préalablement à notre étude non identifiée.

Cette situation est donc très récente et finalement unique puisque nous sommes dans la mesure de mener à bien, peut être pour la première fois, une étude liée aux sources d'acide nitreux et ce dans des conditions idéales de reproductibilité devant aboutir à une estimation directement utilisable de l'importance de cette source de HNO_2.

Pour cela il convient de savoir:

- dans quelles conditions (par exemple de pH), la réaction (8) peut-elle avoir lieu?
- quelles sont les vitesses de réaction?
- quels sont les produits?

Ce sont là des paramètres essentiels pour estimer le facteur source mais qui sont à l'heure actuelle totalement inconnus.

Ainsi nous avons souhaité:

- étudier les réactions multiphasiques (allant de milieux riches en eau à des milieux riches en composés organique) et hétérogènes (sur des supports solides) entre NO_2 et les espèces listées dans le tableau I
- de simuler l'importance de cette chimie à travers des modèles 0-D

L'objectif général de cette demande est d'étudier de manière approfondie l'impact que peuvent avoir les sources d'acide nitreux nouvellement identifiées. Le but du projet vise à fournir les données physico-chimiques nécessaires à l'évaluation de l'importance de ces réactions et à donner les moyens pour leur simulation ultérieure dans des codes de chimie atmosphérique.

Les réactions considérées peuvent généralement s'écrire sous la forme:

$$ArO^- + NO_2 \rightarrow NO_2^- + ArO, \qquad (8)$$

l'ion nitrite étant en équilibre avec l'acide nitreux.

L'approche expérimentale réside dans l'utilisation de techniques de laboratoire standards et validées et doit aboutir à des résultats directement utilisables par la communauté scientifique.

II. Méthodologies expérimentales

Comme cela a déjà été décrit, nous avons cherché à caractériser la réactivité multiphasique de NO_2 envers:

- les constituants isolés de l'aérosol organique,
- le mélange de ces constituants afin d'étudier l'impact de l'aérosol à travers l'emploi d'un "proxy" simple de l'aérosol organique mais qui maintient la proportionnalité des fonctionnalités chimiques telles qu'elles ont été établies par Fuzzi *et al.* [*Fuzzi et al.*, 2001].

Afin de pouvoir être applicable dans la plus large gamme de conditions possibles, ces réactions devront être étudiées sur des substrats liquides (aqueux et/ou organiques) et solides. Ceci sera possible grâce à l'emploi de techniques expérimentales complémentaires: les tubes à écoulement à film tombant et à paroi enduite. Les résultats expérimentaux seront ensuite intégrés dans un code chimique 0-D afin d'estimer leur impact sur une masse d'air donnée. Ces approches sont décrites ci-dessous.

II.a Technique du tube à écoulement à film tombant

L'incorporation et la transformation d'un composé gazeux minoritaire dans une phase liquide est un processus hétérogène résultant de la convolution de plusieurs mécanismes [*Schwartz*, 1986]:

- transport de masse dans la phase gazeuse vers l'interface,
- transport de masse à travers l'interface,
- transport de masse en phase liquide,
- établissement de possibles réactions chimiques.

Le principe général de mesure de ces cinétiques de capture consiste à exposer une phase liquide à une phase gazeuse contenant le gaz en traces à étudier. Pour pouvoir mesurer ces coefficients de manière directe, il est nécessaire de répondre aux deux critères suivants:

- séparer le transport de masse à l'interface des phénomènes de diffusion dans les phases gazeuse et liquide et des réactions secondaires (ionisation, hydrolyse,...),
- travailler avec une interface parfaitement caractérisée et constamment renouvelée de manière à minimiser les phénomènes de contamination et de saturation de l'interface.

Afin de répondre à ces critères, nous avons retenu la technique standard du tube à écoulement à film tombant. Dans ce cas, la phase liquide exposée au gaz prend la forme d'un film liquide tombant le long des parois internes d'un tube à écoulement vertical.

Dans ce montage (figure 1), la phase liquide exposée au gaz prend la forme d'un film liquide tombant le long des parois internes d'un tube à écoulement vertical. Ainsi la surface exposée est de l'ordre de quelques dizaines de cm^2 ainsi cette technique se révèle être sensible pour des cinétiques de capture lentes.

Le dispositif utilisé consiste en un tube à écoulement vertical (ayant un diamètre interne d=12 mm) dont les parois internes sont recouvertes d'un film liquide tombant doucement sous l'action de la gravité. L'épaisseur f du film est peut être calculée dans le cas d'un fluide Newtonien [*Behnke et al.*, 1997b; *Danckwerts*, 1970b] grâce à l'équation suivante:

$$f = \sqrt[3]{\frac{3\mu F_l}{\pi g d \rho}} \qquad (9)$$

où μ est la viscosité du liquide et ρ sa masse volumique, F_l est le débit liquide et g l'accélération gravitationnelle. Dans nos conditions expérimentales, l'épaisseur calculée est de l'ordre de 100µm. Le liquide est injecté dans le système de manière à ce qu'il s'écoule doucement afin d'éviter la formation de "vagues" à la surface du film qui rendraient turbulent le transport en phase gazeuse au voisinage immédiat de l'interface. L'ensemble du système est thermostaté permettant des études en fonction de la température entre 0 et 30°C. Ce domaine d'étude est restreint par les propriétés physico-chimiques de l'eau.

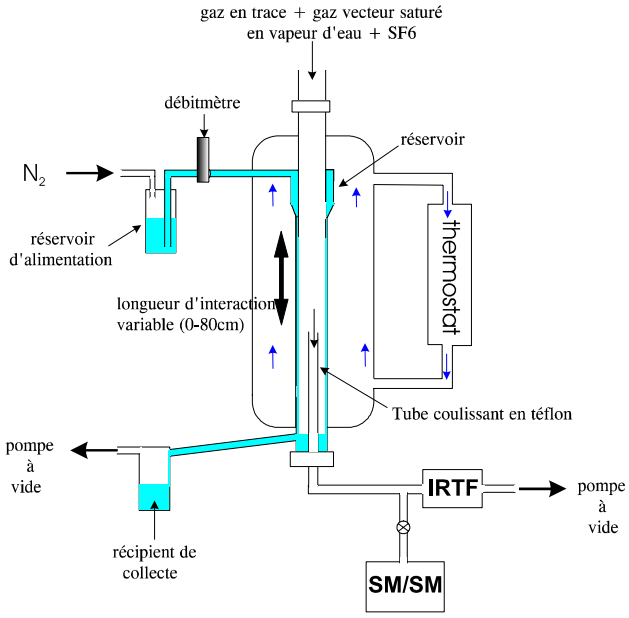

Figure 1: Vue générale du tube à écoulement à film tombant

Dans ce dispositif qui peut être opéré tout aussi bien à pression normale que réduite, le suivi cinétique de l'incorporation d'un gaz dans le film liquide se fait en analysant la disparition de cette espèce en fonction du temps d'interaction t entre les deux phases. Les moyens analytiques utilisés sont ceux déjà décrits soit les spectrométries de masse et infrarouge. La cinétique mesurée est généralement du premier ordre et peut donc être décrite par:

$$\ln\left(\frac{n - \Delta n}{n}\right) = -k_{film}\, t \qquad (10)$$

où k_{film} est la constante cinétique du premier ordre correspond à la capture par le film. Celle-ci peut être calculée grâce à la théorie cinétique comme étant égale à:

$$k_{film} = \frac{\gamma < c >}{d} \qquad (11)$$

Cette équation met en évidence que la connaissance de k_{film} permet la détermination du coefficient de capture γ. Ainsi, la réalisation de ce dispositif étoffe les moyens expérimentaux dont disposent l'équipe et permettra d'étudier les cinétiques hétérogènes pour des systèmes dont les caractéristiques pourront être bien plus variées qu'auparavant.

II.b La technique du tube à écoulement à paroi induite utilisée au LACE

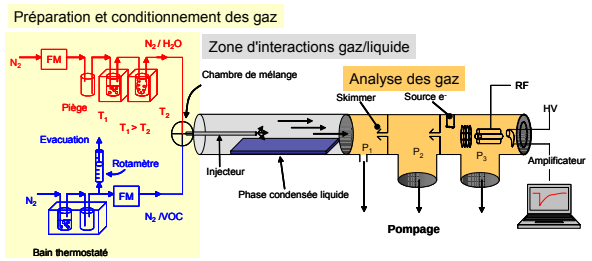

Figure 2: Schéma simplifié du montage utilisé pour l'étude des processus photochimique

Il s'agit d'un montage très similaire à celui schématisé par la figure 2. Il s'agit en fait d'un tube à écoulement horizontal dont les parois internes peuvent être recouvertes d'un film solide, constitué des espèces organiques dont l'étude est souhaitée. Ainsi dans ce cas, le film est statique. Cet ensemble est ensuite placé dans une enceinte permettant une irradiation simultanée du film solide et de la phase gazeuse avoisinante au moyen de différentes lampes permettant un choix dans la gamme spectrale d'irradiation.

II.c La technique du tube à écoulement à paroi induite utilisée au LCE

Le tube à écoulement est constitué de deux tubes en verre de 50 cm de long emboîtés l'un dans l'autre (figure 3). Les gaz réactifs (ici NO_2 dilué dans l'Hélium) sont introduits dans l'espace annulaire ainsi formé. Les faibles dimensions de l'espace annulaire permettent de ne pas être gêné par une éventuelle diffusion en phase gaz trop lente. Les parois internes du tube externe sont recouvertes d'un film de solvant organique, dans lequel on peut ajouter des quantités connues de catéchol. Le système est entièrement thermostaté, afin d'étudier l'influence de la température sur la réaction.

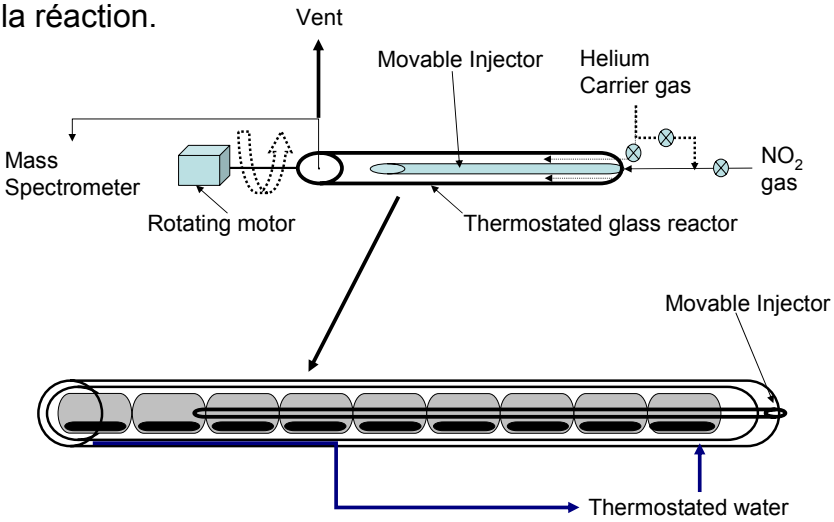

Figure 3 : schéma du tube à écoulement, couplé à spectromètre de masse

La phase gaz est suivie en continu à l'aide d'un spectromètre de masse de type trappe d'ion. Ainsi, l'incorporation de $NO_{2\ gaz}$ dans le film liquide se fait en analysant la disparition du signal de m/z = 46 en fonction du temps (figure 4)

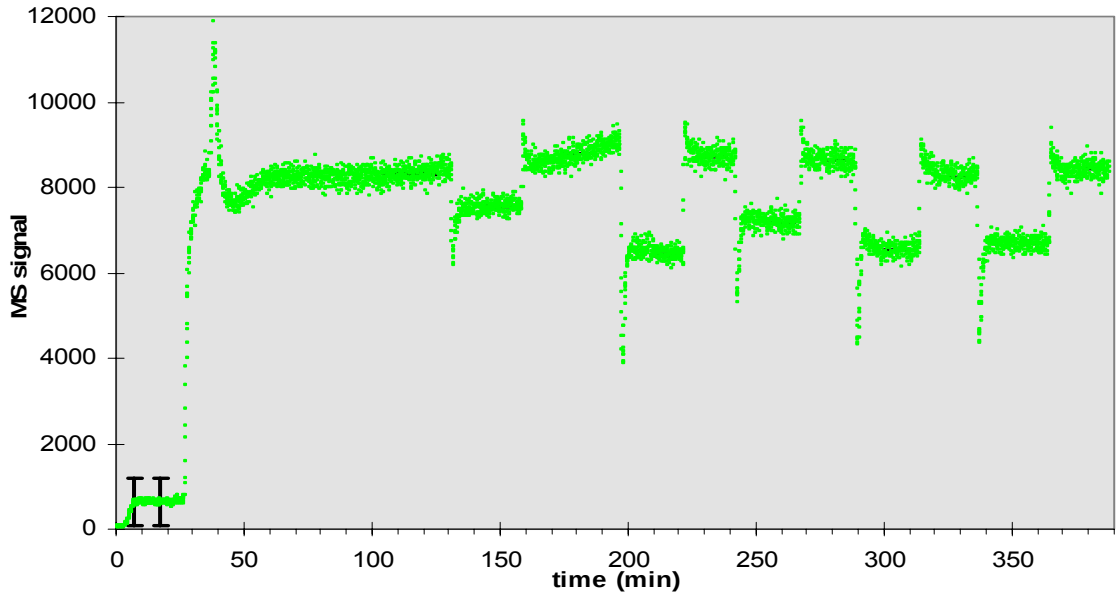

Figure 4 : Suivi du signal m/z = 46 (NO_2) en fonction du temps de contact NO_2-substrat (éthylène glycol + catéchol)

III. Résultats

Ci-dessous, nous ne donnons qu'un aperçu partiel de nos résultats qui sont détaillés dans les publications fournies en annexe 3.

III.a Capture de NO_2 sur des films liquides aqueux

Tous les résultats ci-dessous ont été obtenus à 298K.

La technique du tube à écoulement à film tombant, telle qu'elle a été décrite ci-dessus est construite de telle manière à permettre la mesure de coefficient de capture très faible. Ainsi, la mesure du coefficient de capture du dioxyde d'azote sur un film d'eau pure a été possible malgré la très faible solubilité de ce gaz. Les coefficients de capture mesurés ont été systématiquement inférieurs à 10^{-7} révélant une cinétique très lente, due à l'hydrolyse du dioxyde d'azote qui est une réaction complexe ayant un ordre 2 vis à vis de NO_2. En particulier, nos expériences ont été faites avec une analyse de la phase gazeuse par spectrométrie de masse impliquant une forte concentration en phase gazeuse (de l'ordre de 50 ppm). Ainsi, nos cinétiques de captures ont été de fait influencées par le deuxième ordre présent dans le mécanisme d'hydrolyse. La capture de NO_2 a été étudiée en détail ailleurs, ainsi nous n'avions pas comme objectif d'effectuer une nouvelle analyse de ce processus mais simplement de vérifier l'influence de l'eau sur les cinétiques de capture observées en présence de composés organiques. Ainsi, comme cela sera détaillé ci-dessous la capture sur des films aqueux est au minimum un facteur 5 plus faible qu'en présence d'autres composés réactifs.

III.b Capture de NO_2 sur des films liquides aqueux contenant des composés organiques.

Le système chimique devient apparemment plus simple avec l'ajout en solution de réactifs organiques (de types dérivés phénolique). Nous avons ainsi étudié en détail la capture de NO_2 sur des films liquides contenant du catéchol. La figure 5 montre l'évolution du coefficient de capture de NO_2 sur des films aqueux contenant du catéchol à différents pH. Il est évident que la vitesse de capture est fortement augmentée comparé à un film d'eau pure démontrant que la présence de catéchol introduit un nouveau chemin réactionnel, en solution, pour la conversion du dioxyde d'azote.

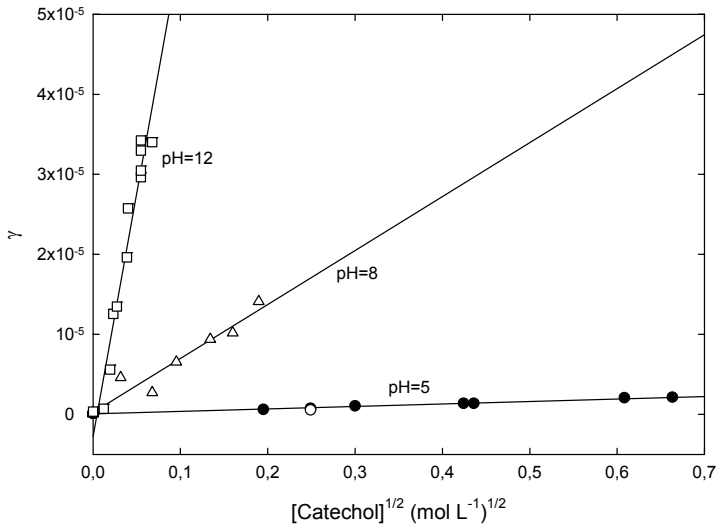

Figure 5: Coefficients de capture de NO2 sur des films aqueux contenant du catechol.

Ainsi dans cette situation, en plus de la réaction de

disproportionation ayant lieu dans l'eau, il se produit d'autres réactions avec les dérivés phénoliques (dénotés ArOH ci-dessous)

$$NO_2 + ArOH \rightarrow HONO + ArO^{\cdot} \quad (12)$$
$$NO_2 + ArO^{-} \rightarrow NO_2^{-} + ArO^{\cdot} \quad (13)$$

où ArOH est la forme moléculaire du composés phénolique (en l'occurrence la catéchol) et ArO^- la formé déprotoné (ou basique).

Puisque la vitesse de capture sur l'eau pure apparaît comme négligeable par rapport à celles observés avec les films contenant du catéchol

$$\gamma = \frac{4HRT\sqrt{kD}}{< c >} \quad (14)$$

où H est la constante de Henry de NO_2, R la constante des gaz parfait, D le coefficient de diffusion en solution de NO_2, T la température et k la constante de réaction de pseudo-premier ordre. La figure 6 montre l'évolution du coefficient de capture de NO_2 en fonction de la racine carrée de la concentration en catéchol. Dans cette représentation, un comportement linéaire est observé validant ainsi non seulement l'emploi de l'équation ci-dessus mais aussi le fait que la capture de NO_2 est exclusivement due à la réaction avec le catéchol. Dans une telle situation, les constantes cinétique de deuxième ordre entre NO_2 et les dérivés phénoliques peuvent être obtenus grâce à :

$$k_X^{II} = \left[\frac{\gamma \cdot \frac{< c >}{4}}{H_{NO2} \cdot R \cdot T} \right]^2 \cdot \frac{1}{[X] D_{NO2}} \quad (15)$$

où k_X^{II} est cette constante de deuxième ordre et [X] la concentration en solution du dérivé phénolique. Le tableau présente nos résultats dont de nombreux ont été obtenu en collaboration avec Markus Ammann à Villigen (Suisse). Ces constantes cinétiques peuvent ensuite être utilisées à des fins de modélisation de cette chimie.

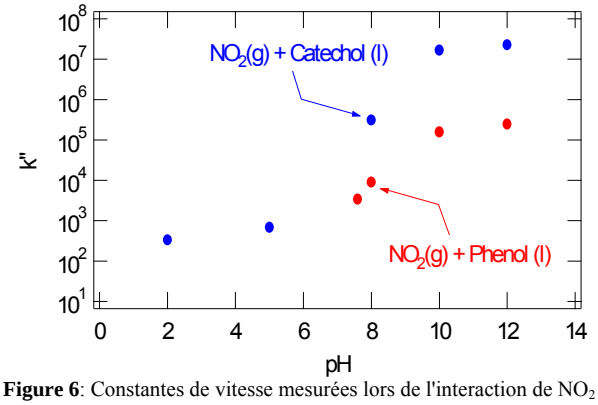

Figure 6: Constantes de vitesse mesurées lors de l'interaction de NO_2 avec des solutions de catéchol et de phénol.

Tableau I Données concernant les constantes de vitesses

	composé		*CASno*	*Reaction*	k^{II} ($M^{-1}s^{-1}$) *pK*	*Ce travail (en collaboration avec M. Ammann)*
	catechol	1,2-dihydroxybenzene	120-80-9	$C_6H_4(OH)_2 + H2O = C_6H_4(OH)O^- + H_3O^+$	pK_1 = 9.3 a	**9.1**
1a				$C_6H_4(OH)_2 + NO_2 = C_6H_4(OH)O + HONO$	$k_{1,1}$	**$1x10^4$**
1b				$C_6H_4(OH)O^- + NO_2 = C_6H_4(OH)O + NO_2^-$	$k_{1,2}$	**$1.3x10^8$**
	guaiacol	2-methoxyphenol	90-05-1	$C_6H_4(OCH_3)OH + H_2O = C_6H_4(OCH_3)O^- + H_3O^+$	pK_2 =9.9 b	**9.8**
2°				$C_6H_4(OCH_3)OH + NO_2 = C_6H_4(OCH_3)O + HONO$	$k_{2,1}$	**< 10^4**
2b				$C_6H_4(OCH_3)O^- + NO_2 = C_6H_4(OCH_3)O + NO_2^-$	$k_{2,2}$	**$1.5x10^8$**
	syringol	2,6-dimethoxyphenol	91-10-1	$C_6H_3(OCH_3)_2OH + H_2O = C_6H_3(OCH_3)_2O^- + H_3O^+$	pK_3 =10.2 c	**9.8**
3°				$C_6H_3(OCH_3)_2OH + NO_2 = C_6H_3(OCH_3)O + HONO$	$k_{3,1}$	**$1.5x10^5$**
3b				$C_6H_3(OCH_3)_2O^- + NO_2 = C_6H_3(OCH_3)O + NO_2^-$	$k_{3,2}$	**$4.5x10^8$**
4b	**quinol**	1,4-benzenediol	123-31-9	$C_6H_4(OH)O^- + NO_2 = C_6H_4(OH)O + NO_2^-$	$k_{4,2} = 1.1x10^9$ d	
5b	**m-guaiacol**	3-methoxyphenol	150-19-6	$C_6H_4(OCH_3)O^- + NO_2 = C_6H_4(OCH_3)O + NO_2^-$	$k_{5,2} = 1.8x10^7$ e	
6b	**mequinol**	4-methoxyphenol	150-76-5	$C_6H_4(OCH_3)O^- + NO_2 = C_6H_4(OCH_3)O + NO_2^-$	$k_{6,2} = 2.1x10^8$ f	
7b	**resorcinol**	1,3-benzenediol	108-46-3	$C_6H_4(OH)O^- + NO_2 = C_6H_4(OH)O + NO_2^-$	$k_{7,2} = 1.3x10^7$ g	

a a Kimura et al. JACS 105, 2063-2066, 1983; other literature range 9.0-9.5
b Zeev et al., JPC 89, 3359-3363, 1985; other literature range 9.2-10.0
c Chapoteau et al. JOC 54, 861-867, 1989
d Alfassi et al. JPC, 90, 4156-4158, 1986
e Alfassi et al. J. Phys. Chem. 90, 4156-4158, 1986
f Alfassi et al. J. Phys. Chem. 94, 8800-8805, 1990
g Gutzwiller et al. JPC 2002

En complément des expériences réalisées au LACE, le LCE a mis en évidence la formation d'acide nitreux HONO lors de la réactivité de NO_2 gaz sur le catéchol dilué dans l'eau.

L'objectif était de déterminer le rendement de la réaction suivante :

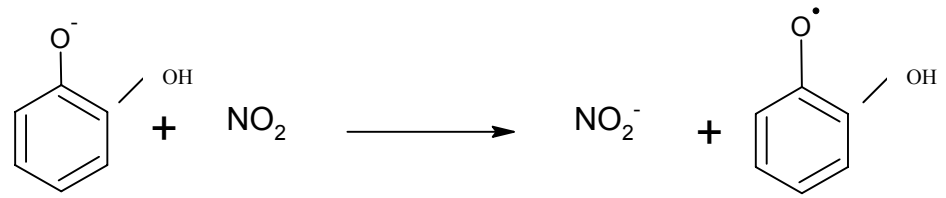

Méthodologie : La réaction a été étudiée en exposant une solution aqueuse contenant du catéchol en excès (dans des proportions variant de $0{,}9.10^5$ à 3.10^5) par rapport aux concentrations de $NO_{2(g)}$. La technique utilisée a été le barbotage, et le $NO_{2(g)}$ restant après barbotage été piégé, et dosé par la méthode de Saltzmann, en chromatographie ionique, qui permet la détection de très faibles quantités de NO_2.

Les résultats ont montré que sur 14 expériences réalisées à 300K, le rendement de formation de HONO par la réaction est de 97% (± 38%). L'incertitude indiquée tient compte de l'ensemble des incertitudes analytiques. Il semble donc que lors de la réaction de $NO_{2(g)}$ sur le catéchol dilué dans l'eau, une mole de $NO_{2(g)}$ produise une mole de HONO.

III.c. Capture de NO_2 sur film liquide organique

Le n-octanol et l'éthylène glycol ont été utilisés comme supports modèles pour l'aérosol organique, car ils présentent des propriétés de viscosité proches de l'aérosol organique (Rudich, 2003). De plus, chacun de ces deux solvants a des propriétés de solubilité dans l'eau très différentes : le n-octanol est hydrophobe, alors que l'éthylène glycol est hydrophile.

1/ Tests de la réactivité des solvants

Les premières expériences ont été réalisées sur chacun des films organiques, en absence de catéchol, afin de déterminer une éventuelle réactivité de $NO_{2\ gaz}$ sur le film. Les résultats obtenus montrent que l'octanol présente une réactivité significative, alors que l'éthylène glycol présente une très faible réactivité (comparable à celle de l'eau, voir les résultats du LACE).

2/ Réactivité de $NO_{2\ gaz}$ sur le catéchol dilué dans un solvant organique

2.1 Influence de la présence du catéchol dans l'éthylène glycol

Les expériences de réactivité de $NO_{2\ gaz}$ sur le catéchol dilué dans un solvant organique ont donc été menées sur le film organique le moins réactif, à savoir l'éthylène glycol. En écrivant la loi de conservation de la matière au cours du parcours de $NO_{2\ gaz}$ à travers le tube, Schwartz (1986) a montré :

i) le temps de contact t est proportionnel à la longueur L du tube sur laquelle la réaction a lieu :

$$t = \frac{\pi r^2 L}{F_g} \tag{16}$$

où r est le rayon du tube (en cm), et F_g est le débit de gaz (en ml/min)

ii) Ce temps de contact t est relié au rapport des concentrations de gaz à la distance L (C_L) et à la distance L=0 (C_0) (pas de réaction) par l'équation suivante :

$$\ln\left(\frac{C_0}{C_L}\right) = \frac{\gamma_{obs}\langle c\rangle}{2r} \times t \tag{17}$$

où $\langle c\rangle$ est la vitesse moléculaire moyenne de $NO_{2\ gaz}$ à 293 K= 36 731,7 cm/s, γ_{obs} est le coefficient de capture de $NO_{2\ gaz}$ par la surface.

Le tracé de ln (C_0/C_L) en fonction de t donne donc une droite de pente $k_{wall} = \frac{\gamma_{obs}\langle c \rangle}{2r}$

Les résultats obtenus lors de ces expériences, ont montré que la présence de catéchol augmente la réactivité du solvant (figure 7)

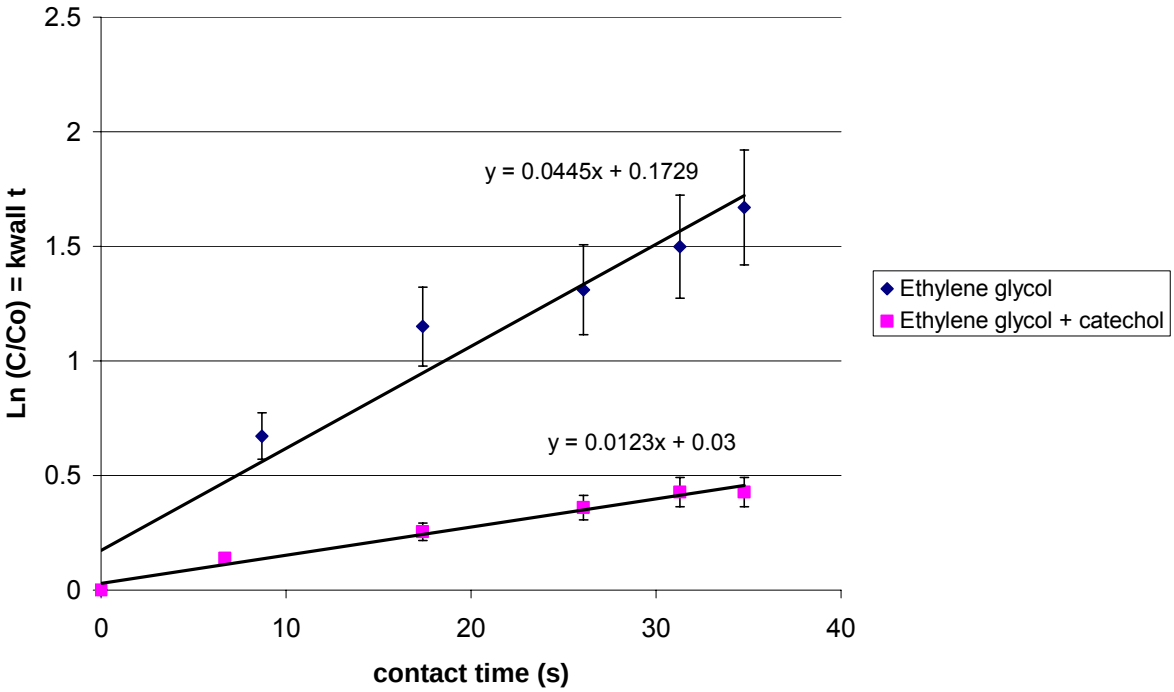

Figure 7 : influence de la présence de catéchol (0.1 M) dans l'éthylène glycol sur la réactivité de $NO_{2\ gaz}$, à 293 K

2.2 Influence des concentrations de catéchol

Pour des concentrations de catéchol en excès par rapport à celles de $NO_{2\ gaz}$, on a une cinétique d'ordre 1 par rapport à $NO_{2\ gaz}$, de constante de vitesse kI = kII[catéchol]. Le coefficient de capture est relié à la constante de vitesse kI par :

$$\gamma_{obs} = \frac{4K_H RT\sqrt{k_I D_l}}{< c >} = \frac{4K_H RT\sqrt{k_{II}[catéchol] D_l}}{< c >}$$

D_L est le coefficient de diffusion de NO_2 dans le solvant, K_H est la constante d'équilibre de NO_2 entre la phase gazeuse et la phase liquide.
Ainsi, en faisant varier les concentrations (en excès) de catéchol dans l'éthylène glycol, on peut tracer le graphe de γ_{obs} en fonction de $\sqrt{[catéchol]}$, qui est une droite de pente $\frac{4K_H RT\sqrt{k_{II} D_l}}{\langle c \rangle}$. Les résultats ont montré que nous obtenons une courbe possédant plusieurs domaines de linéarité (figure 8)

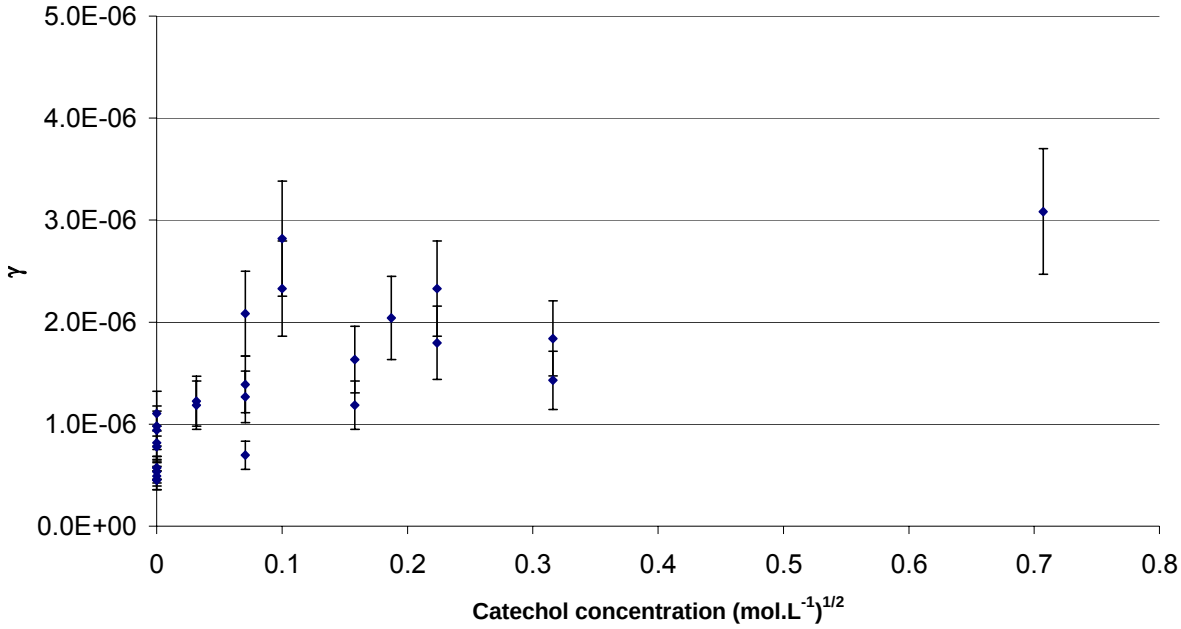

Figure 8: Influence de la concentration de catéchol sur le coefficient de capture

L'interprétation de ce résultat est en cours. Néanmoins, la comparaison avec les résultats obtenus en remplaçant le solvant organique par l'eau (réalisés au LACE) montre que pour de faibles concentrations, le catéchol est assez réactif, mais lorsqu'on augmente les concentrations, la réactivité de $NO_{2\ gaz}$ est comparables aux expériences dans l'eau réalisées à pH=5, représentatifs des pH mesurés dans l'atmosphère.

2.3 Produits de réaction

L'ensemble des expériences de réactivité de $NO_{2\ gaz}$, sur le catéchol dilué dans l'éthylène glycol a montré l'apparition d'eau lors de la réaction (figure 9).

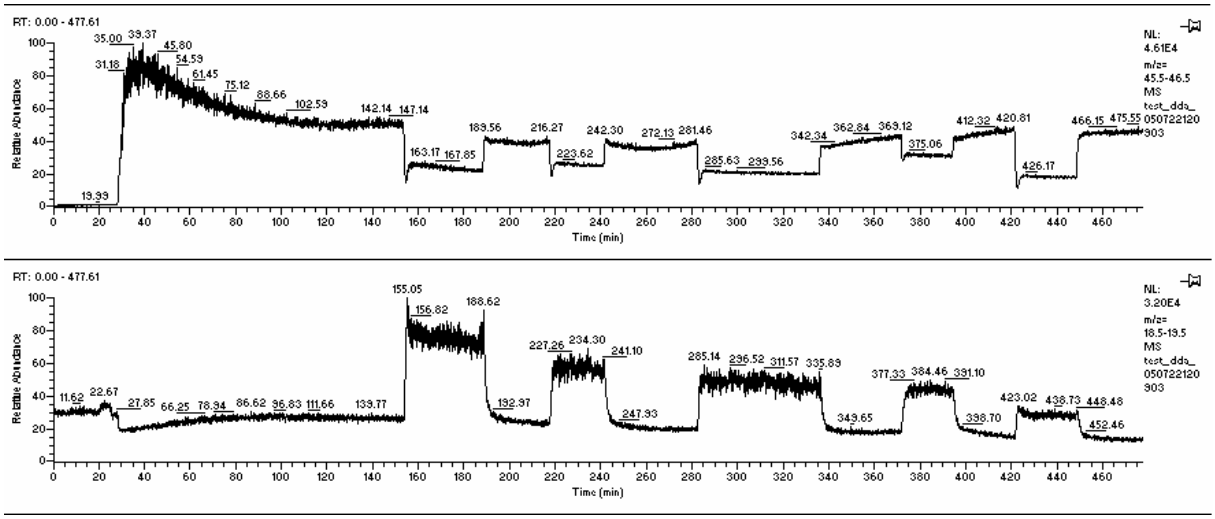

Figure 9 : Apparition d'un pic à 19 amu (H_2O $_{gaz}$) simultanément à la disparition du pic à 46 amu (NO_2 $_{gaz}$).

Ce résultat reste à être confirmé par des expériences sur du catéchol deutéré (en cours), mais cela pourrait être une première piste pour expliquer les mécanismes réactionnels.

III.d Modélisation de la chimie multiphasique

En collaboration avec H. Herrmann (IFT – Leipzig), nous avons développé un code chimique "CAPRAM2.4: MODAC Mechanism" dont l'état actuel est décrit par la figure 11, et qui prend en compte à la fois la phase gazeuse et une phase condensée (brouillards, nuages, ou aérosols déliquescents), et leurs interactions.

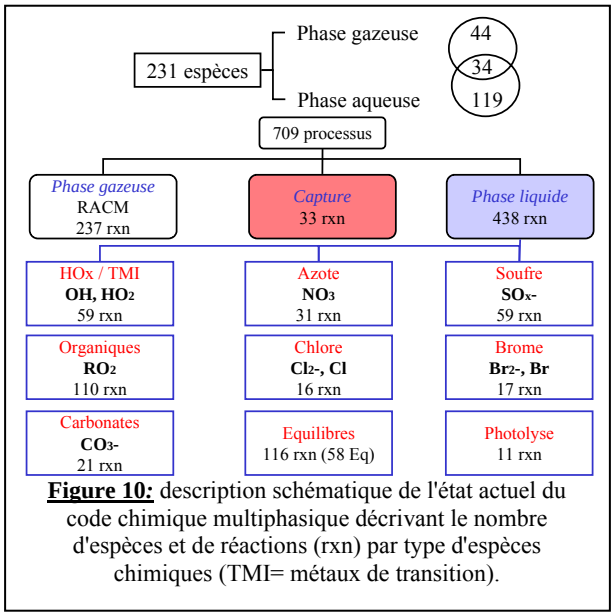

Figure 10: description schématique de l'état actuel du code chimique multiphasique décrivant le nombre d'espèces et de réactions (rxn) par type d'espèces chimiques (TMI= métaux de transition).

Ce modèle utilise le code RACM, soit "Regional Atmospheric Chemistry Mechanism"(développé par Stockwell [*Stockwell et al.*, 1997]) pour la simulation de la chimie en phase gazeuse qui est un standard qui plus est, il a été testé sur des résultats de chambres de simulations.

L'adjonction à RACM d'un module de chimie hétérogène et/ou multiphasique est donc un point crucial pour le développement d'un outil de modélisation performant. La structure du code chimique est basée sur un traitement explicite de l'ensemble des espèces chimiques considérées, des radicaux potentiellement impliqués dans des processus d'oxydation (OH, NO_3, SO_4^-, CO_3^-, Cl_2^-,…), ainsi que l'implication des métaux de transition, du pH et des effets de ce dernier sur les cinétiques d'oxydation. Un traitement relativement complet et détaillé de l'oxydation du soufre est également

pris en compte. Ce code chimique considère d'ores et déjà un panel relativement important de réactions impliquant des COV (limités cependant à des espèces ayant au plus deux atomes de carbone) tels que les aldéhydes (formaldéhyde, acétaldéhyde, glyoxal) et alcools (méthanol, éthanol). Toutes ces caractéristiques en font un modèle très souple d'emploi. De plus, du fait du caractère relativement exhaustif des oxydants considérés, ce schéma réactionnel est applicable à un grand nombre de situations, allant de l'aérosol déliquescent à la chimie des nuages. Ainsi, le couplage de ce code à RACM donne un outil très pertinent pour la simulation des processus multiphasiques troposphériques.

Ainsi, ce code a été étendu afin d'inclure la chimie multiphasique de composés aromatiques. En particulier, nous avons considéré les espèces suivantes: benzène, toluène, ortho-, meta-, para-xylène, ortho- et para- crésol et phénol. Après leur transfert dans la phase condensée, ses aromatiques vont réagir en subissant une attaque primaire de différents radicaux (Cl_2^-, Br_2^-, CO_3^-, NO_3, OH ou SO_4^-). Le mécanisme en découlant est multiple puisque cette réaction peut se dérouler à travers des processus d'échange de charge, d'arrachement d'atome d'hydrogène (sur le cycle aromatique mais aussi sur les différentes ramifications) et finalement par une addition sur les insaturations. Cependant afin de simplifier le code, nous avons considéré que tous les radicaux réagissent de la même manière et uniquement sur le cycle aromatique. L'ensemble des réactions impliquant les aromatiques (et l'ensemble des données nécessaires, soit les constantes de Henry, …) a été incluse dans le code “CAPRAM 2.4, MODAC mechanism” qui permet désormais de simuler la chimie de ces aromatiques.

Nous avons appliqué ce code afin de comprendre si cette chimie additionnelle a une influence sur le budget des NO_x à travers les réactions suivantes:

$$ArO^- + NO_2 \rightarrow ArO + NO_2^-, \quad (18)$$

$$NO_2^- + H^+ \rightarrow HNO_2.$$

La figure 12 montre nos résultats soulignant une formation additionnelle d'acide nitreux dès lors que le contenu en aromatique des aérosols dépasse un certain seuil se situant aux alentours de 10^{-5} M. Ces résultats montrent que cette chimie additionnelle des aromatiques crée de nouveaux chemins réactionnels mais dans des conditions très particulière.

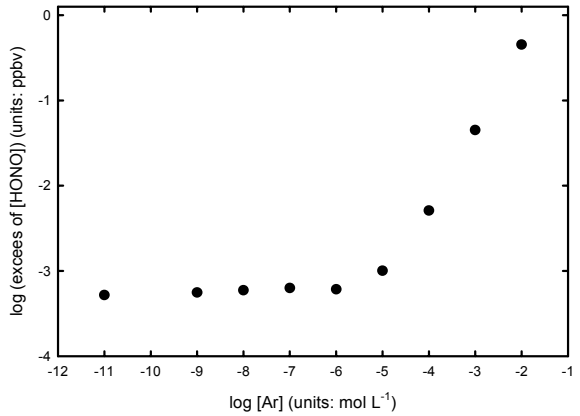

Figure 11: Excès d'acide nitreux en fonction du contenu en aromatique des aérosols. Cet excès est défini comme étant la différence entre des simulations sans chimie des aromatiques et le mécanisme complet.

III.e Capture photo-induite du dioxyde d’azote

Les conditions particulières dans lesquelles cette chimie produisant de l’acide nitreux a lieu, ne permet pas d’expliquer les sources observées de cet acide. De plus, il a été mis en évidence récemment que HONO était produit de manière photochimique en plein jour. C’est pourquoi, nous avons également étudié la conversion de NO2 sur des surfaces organiques solides mais sous l’action de la lumière. Les expériences ci-dessous ont été faites principalement avec un réacteur à écoulement à paroi enduite avec un suivi par spectrométrie de masse de la phase gazeuse.

III.e.1 Test dans l'obscurité

En l'absence d'humidité, la capture de NO_2 dans l'obscurité sur les parois en Pyrex de notre réacteur était au delà de la sensibilité de notre système avec une analyse par spectrométrie de masse de NO_2. Ceci signifie que le coefficient de capture était au-dessous de la limite de détection de 10^{-7}. Seulement une adsorption physique a été observée impliquant que la surface exposée par le tube à écoulement a été rapidement couverte et saturée par des molécules de NO2. À ce stade, plus de la capture de NO2 s'arrête. Nous avons également observé que cette capture était en fait une adsorption physique de ce gaz sur les parois qui s'avère être totalement réversible permettant la mesure des isothermes d'adsorption et de désorption.

Ainsi, en l'absence d'humidité et dans l'obscurité, nous n'avons pas observé de réaction chimique sur le verre. Des tests semblables ont été effectués sur différentes surfaces organiques constituées de catéchol, anthracène, benzophénone, anthrarobine. Comme illustration, les données brutes pendant une expérience sur une surface pure de catéchol sont montrées dans la figure 12. Quand la surface organique a été exposée à du NO_2 gazeux, nous avons observé immédiatement une diminution rapide du signal de spectrométrie de masse à m/z 46 (c.-à-d., correspondant à la masse NO_2 moléculaire) qui ensuite retourne avec un certain délai (quelques minutes) à son niveau original. Ceci signifie à nouveau que les surfaces organiques ont été très rapidement saturées avec les molécules NO_2, comme une surface de verre. Dans notre système, l'injection des gaz (comme NO_2) est mobile et permet d'exposer la surface soit à un gaz vecteur pure soit au gaz réactif. En l'absence de ce dernier, nous avons observé une augmentation rapide du signal à m/z 46. Ceci correspond à la désorption des molécules NO_2 physiquement adsorbées. En intégrant la surface sous ces courbes d'adsorption et de désorption, nous pouvons déterminer le nombre de molécules adsorbées ou désorbées. Nous avons observé que les quantités étaient, dans l'incertitude expérimentale, égale ce qui signifie encore une fois que dans des conditions sèches, NO_2 s'adsorbe seulement physiquement sur ces surfaces organiques pures. Comme NO_2 s'adsorbe seulement physiquement (sans réaction chimique) sur ces surfaces de catéchol, nous ne pouvions pas déterminer les coefficients de capture, qui étaient au dessous de notre limite de détection d'environ 10^{-7}. Des observations semblables ont été faites sur une surface faite en anthrarobin (1,2,10-trihydroxyanthracene) où NO2 s'adsorbe seulement physiquement. Sur l'anthracène, nous avons observé un comportement semblable mais nous avons observé également une réaction lente dans l'obscurité. Dans ce cas, quand la surface est exposée à NO2, sa concentration décroit rapidement mais ne retourne pas complètement à son niveau original mais atteint un plateau dépendant du temps signifiant qu'il y a à terme une désactivation de la surface. Des observations semblables ont été faites dans le cas de la benzophénone, pour lequel

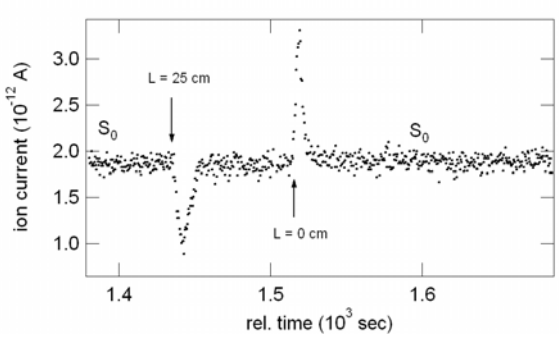

Figure 12. Données brutes démontrant une adsorption physique de NO2 sur les films organiques dans l'obscurité

un coefficient de prise de 0,3 10^{-6} a été déterminé. Tous les résultats sont récapitulés dans le Tableau II.

Tableau II Coefficient de capture de NO2 sur des films organiques solides

Type	RH (%)	$\gamma_{obscurité}$ (10^{-6})	$\gamma_{irradié}$ (10^{-6})
Benzophenone	dry	0.32	0.65
Benzophenone / Catechol	dry	1.26	2.40
Benzophenone / Catechol	14	1.30	2.51
Benzophenone / Catechol	76	3.6	5.1
Catechol	dry	0.07	1.4
Catechol	42	1.1	1.8
Anthracene	dry	0.66	1.2
Anthracene	56	1.9	2.3
Catechol / Anthracene	dry	< 0.1	0.89
Catechol / Anthracene	46	0.67	1.3
Anthrarobin	14	0.24	0.34

Tandis que toutes les expériences décrites ci-dessus étaient exécutées dans des conditions sèches (c.-à-d., rh < 1%), nous avons observé que l'ajout de vapeur d'eau augmentait la capture de NO_2 par au moins un facteur 3 quand l'humidité est supérieure à 40 %. Ceci a été observé pour tous les matériaux étudiés. Il s'avère certainement que l'eau s'adsorbe sur nos films changeant les propriétés des surfaces et sa capacité de réagir. En effet, une inspection visuelle des films a montré que certains étaient déliquescents à humidité élevé. Il semble évident qu'une faction importante d'eau sur les films a une influence sur sa réactivité, car la présence d'une phase aqueuse pourrait augmenter les mécanismes de conversion en phase liquide.

III.e.2 Photochimie de surface

La figure 13 montre les données brutes pour une expérience menée une surface de catéchol quand le réacteur en pyrex a été irradié par des lampes de mercure. Ceci doit être comparé aux données représentées par la figure 12 (expérience correspondante mais dans l'obscurité). Il est évident que dans l'obscurité seulement l'adsorption physique se produise tandis que sous l'irradiation la capture de NO_2 est accrue et engendré par une réaction photochimique.

En fait, dans ce cas la concentration NO_2, une fois exposé à la surface organique dans le réacteur irradié, diminue rapidement et atteint un plateau après quelques secondes. Ce plateau est désormais indépendant du temps impliquant un coefficient de capture constant dans le temps de l'ordre de 10^{-6} donc au moins un ordre de grandeur plus grand que sans lumière.

Les effets induits légers pour les autres produits organiques sont moins prononcés mais principalement évidents par le déplacement n'importe quand de la dépendance dans le coefficient de prise. L'effet principal de la lumière est d'activer

la surface mais aussi d'éliminer tout signe de désactivation des surfaces dans les échelles de temps expérimentales.

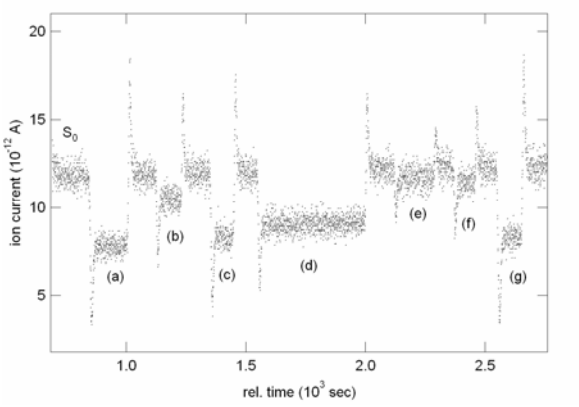

Figure 12. Données brutes pour la capture photoinduite de NO_2 sur des films de caéchol

De plus la lumière engendre non seulement la capture de NO_2 mais permet la formation de produit en phase gazeuse. En effet, l'évolution des signaux en masse à pour m/z = 30 (NO+-ion) et m/z = 46 (NO2+-ion) sont bien décorrélés lorsque NO2 a réagi avec les films organiques irradiés. Ceci a été interprété comme la formation d'un produit interférant avec le signal de la masse 30, tandis que la masse 46 n'a pas été influencée. Les produits potentiels de réaction montrant les signaux de masse à m/z=30 sont NO (d'une photodécomposition de NO_2) ou HONO (de la réduction de NO2). Pour déterminer si le produit formé était HONO ou NO, nous avons inséré un piège enduit de carbonate de sodium dans la ligne de gaz entre le tube d'écoulement et le spectromètre de masse, piégeant les traces de HONO de la phase gazeuse. Avec le piège en ligne, la masse 30 suit la masse 46 ce qui peut être considéré comme évidence indirecte que HONO est photochimiquement formé lors des interactions de NO_2 et des divers films de produits organiques.

Tandis que les expériences avec la détection spectrométrique en masse indiquaient que HONO pourrait être un produit de la réaction photochimique de NO2 avec l'espèce organique étudiée, d'autres expériences ont été exécutées avec une instrumentation spécifique et sensible à HONO. Ces expériences ont confirmés que la photochimie des films organiques était une surface conséquente d'acide nitreux.

IV. Conclusion

Nous avons étudié les réactions entre NO_2 et une série de composés organiques représentatives de l'aérosol troposphérique afin d'identifier de nouvelles sources d'acide nitreux. Ces travaux ont été menés à la fois sur des substrats solides et liquides (aqueux et organiques) afin d'explorer la plus large gamme possible de conditions atmosphériques. Ceci sera possible grâce à l'emploi de techniques expérimentales complémentaires: les tubes à écoulement à film tombant et à paroi enduite. Les résultats expérimentaux seront ensuite intégrés dans un code chimique 0-D afin d'estimer leur impact sur une masse d'air donnée.

Nous avons ainsi mesuré les vitesses de capture de NO_2 sur différents milieux liquides (aqueux et organiques). Ces vitesses de capture sont reliées à la fois à la solubilité du gaz dans le liquide considéré mais aussi à la réactivité en solution. Cette réactivité était dans le cadre de ces travaux à la présence composés organiques (de type dérivés phénoliques). De nos études, il a donc été possible de déterminer la solubilité (le cas échéant) et les vitesses de réactions entre NO_2 et ces dérivés phénoliques (ou différents mélanges de composés organiques). Il en résulte que cette réaction produit effectivement des ions nitrites (et donc de l'acide nitreux) mais de manière fortement dépendante du pH. Cette dépendance malheureusement limite fortement l'implication de cette chimie en tant que source d'acide nitreux. Cette chimie s'avère ainsi être très importante dans le cadre d'aérosol organiques tels que ceux issus de processus de combustion de biomasse.

Devant cette limitation, nous avons en complément étudié la photochimie de surfaces organiques et démontré ainsi, pour la première fois, que NO_2 était converti de manière photochimique sur des surfaces organiques telles que celles présentes de manière ubiquiste dans l'environnement (végétation, bâti, sols, etc…). Cette photochimie converti très efficacement NO_2 en HONO. Cette source est tellement importance, qu'après photodissociation de l'acide nitreux en OH, il s'agit de la source principale de ces radicaux dans la couche limite planétaire. Il s'agit d'une découverte majeure issue de ce projet.

V. Bibliographie

Ackermann, R., A. Geyer, K.-H. Naumann, H. Saathoff, U. Schurath, S. Trick, et U. Platt, Direct quantification of HONO formation rates on urban surfaces, dans *XXVI EGS General Assembly 2001*, edited by EGS, Nice, France, 2001.

Albert, A., et E.P. Serjeant, *The Determination of Ionization Constants*, Chapman and Hall, London and New York, 1984.

Alfassi, Z.B., R.E. Huie, et P. Neta, Substituent effects on rates of one-electron oxidation of phenols by the radicals ClO_2, NO_2, and SO_3^-, *J. Phys. Chem.*, *90*, 4156-4158, 1986.

Alicke, B., A. Geyer, A. Hofzumahaus, F. Holland, S. Konrad, H.W. Paetz, J. Schaefer, J. Stutz, A. Volz-Thomas, et U. Platt, OH formation by HONO photolysis during the BERLIOZ experiment, *J. Geophys. Res.*, *108* (D4), PHO 3/1-PHO 3/17, 2003.

Alicke, B., U. Platt, et J. Stutz, Impact of nitrous acid photolysis on the total hydroxyl radical budget during the Limitation of Oxidant Production/Pianura Padana Produzione di Ozono study in Milan, *J. Geophys. Res.*, *107* (D22), LOP9/1-LOP9/17, 2002.

Ammann, M., M. Kalberer, D.T. Jost, L. Tobler, E. Rossler, D. Piguet, H.W. Gäggeler, et U. Baltensperger, Heterogeneous production of nitrous acid on soot in polluted air masses, *Nature*, *395* (6698), 157-160, 1998.

Ammann, M., E. Rössler, R. Strekowski, et C. George, Uptake of NO2 on aqueous solutions containing phenoxy type compounds - Implication for HONO formation in the atmosphere, *Phys. Chem Chem. Phys.*, *In preparation*, 2004.

Anastasio, C., B.C. Faust, et C.J. Rao, Aromatic carbonyl compounds as aqueous-phase photochemical sources of hydrogen peroxide in acidic sulfate aerosols, fogs, and clouds .1. Non-phenolic methoxybenzaldehydes and methoxyacetophenones with reductants (phenols), *Environmental Science & Technology*, *31* (1), 218-232, 1997.

Arens, F., L. Gutzwiller, U. Baltensperger, H.W. Gäggeler, et M. Ammann, Heterogeneous Reaction of NO_2 on Diesel Soot Particles, dans *Environ. Sci. Technol.*, pp. 2191-2199, 2001.

Arens, F., L. Gutzwiller, H.W. Gaggeler, et M. Ammann, The reaction of NO2 with solid anthrarobin (1,2,10-trihydroxy- anthracene), *Physical Chemistry Chemical Physics*, *4* (15), 3684-3690, 2002.

Atkinson, R., Gas-Phase Tropospheric Chemistry of Organic-Compounds, *Journal of Physical and Chemical Reference Data*, R1-&, 1994.

Atkinson, R., D.L. Baulch, R.A. Cox, J.N. Crowley, R.F. Hampson, J.A. Kerr, R.G. Hynes, M.E. Jenkin, M.J. Rossi, et J. Troe, Summary evaluated kinetic and photochemical data for atmospheric chemistry:, *IUPAC Subcomittee for Gas Kinetik Data Evaluation*, *Web-Edition*, 2004.

Aumont, B., F. Chervier, et S. Laval, Contribution of HONO sources to the NOx/HOx/O3 chemistry in the polluted boundary layer, *Atmospheric Environment*, *37*, 487-498, 2003a.

Aumont, B., F. Chervier, et S. Laval, Contribution of HONO sources to the NOx/HOx/O3 chemistry in the polluted boundary layer, *Atmos. Environ.*, *37* (4), 487-498, 2003b.

Baker, J., S.F.M. Ashbourn, et R.A. Cox, Heterogeneous reactivity of nitrous acid on submicron sulfuric acid aerosol, *Physical Chemistry Chemical Physics*, *1* (4), 683-690, 1999.

Baraltosh, S., S.K. Chattopadhyay, et P.K. Das, A Laser Flash-Photolysis Study of Paraquat Reduction by Photogenerated Aromatic Ketyl Radicals and Carbonyl Triplets, *Journal of Physical Chemistry*, *88* (7), 1404-1408, 1984.

Behnke, W., C. George, V. Scheer, et C. Zetzsch, Production and decay of ClNO2 from the reaction of gaseous N2O5 with NaCl solution : bulk and aerosol experiments, *J. Geophys. Res.*, *102*, 3795-3804, 1997a.

Behnke, W., C. George, V. Scheer, et C. Zetzsch, Production and Decay of Clno2, from the Reaction of Gaseous N2O5 with NaCl Solution - Bulk and Aerosol Experiments, *J. Geophys. Res.*, *102* (D3), 3795-3804, 1997b.

Behnke, W., H.U. Krüger, V. Scheer, et C. Zetzsch, Formation of ClNO2 and HONO in the presence of NO2, O2 and wet aerosols, *J. Aerosol Sci.*, *S23*, 933-936, 1992.

Beine, H.J., I. Allegrini, R. Sparapani, A. Ianniello, et F. Valentini, Three years of springtime trace gas and particle measurements at Ny-Alesund, Svalbard, *Atmos. Environ.*, *35* (21), 3645-3658, 2001.

Brown, S.S., R.W. Wilson, et A.R. Ravishankara, Absolute intensities for third and fourth overtone absorptions in HNO3 and H2O2 measured by cavity ring down spectroscopy, *Journal of Physical Chemistry A*, *104* (21), 4976-4983, 2000.

Calvert, J.G., G. Yarwood, et A.M. Dunker, An evaluation of the mechanism of nitrous acid formation in the urban atmosphere, dans *Res. Chem. Intermed.*, pp. 463-502, 1994.

Canonica, S., B. Hellrung, et J. Wirz, Oxidation of phenols by triplet aromatic ketones in aqueous solution, *J. Phys. Chem. A*, *104* (6), 1226-1232, 2000.

Canonica, S., U. Jans, K. Stemmler, et J. Hoigne, Transformation Kinetics of Phenols in Water - Photosensitization by Dissolved Natural Organic Material and Aromatic Ketones, *Environmental Science & Technology*, *29* (7), 1822-1831, 1995.

Chan, W.H., R.J. Nordstrom, J.G. Calvert, et J.H. Shaw, Kinetic Study of HONO Formation and Decay Reactions in Gaseous Mixtures of HONO, NO, NO2, H2O and N2, *Environ. Sci. Tech.*, *10*, 674-682., 1976.

Cheung, J.L., Y.Q. Li, J. Boniface, Q. Shi, P. Davidovits, D.R. Worsnop, J.T. Jayne, et C.E. Kolb, Heterogeneous interactions of NO2 with aqueous surfaces, *J. Phys. Chem. A*, *104* (12), 2655-2662, 2000a.

Cheung, J.L., Y.Q. Li, J. Boniface, Q. Shi, P. Davidovits, D.R. Worsnop, J.T. Jayne, et C.E. Kolb, Heterogeneous interactions of NO2 with aqueous surfaces, *J. Phys. Chem. A*, *104* (12), 2655-2662, 2000b.

Chughtai, A.R., S.A. Gordon, et D.M. Smith, Kinetics of the hexane soot reaction with NO2/N2O4 at low concentration, dans *Carbon*, pp. 405-16, 1994.

Cooney, D.O., S. Kim, et E.J. Davis, Analyses of mass transfer in hemodialyzers for laminar blood flow and homogeneous dialysate, *J. Chem. Eng. Sci.*, *29*, 1731-1738, 1974.

Cox, R.A., The Photolysis of Gaseous Nitrous acid, *J. Photochem.*, *3*, 175-188., 1974.

Cox, R.A., et M.E. Jenkin, Kinetics of the formation of nitrous acid from the thermal reaction of nitrogen dioxide and water vapor, dans *Comm. Eur. Communities, [Rep.] EUR*, pp. 300-8, 1987.

Danckwerts, P.V., *Gas-Liquid Reactions*, McGraw-Hill, New York, 1970a.

Danckwerts, P.V., *Gas-liquid reactions*, xiii, 276 pp., McGraw-Hill Book Co., New York,, 1970b.

Das, P.K., et S.N. Bhattacharyya, Laser Flash-Photolysis Study of Electron-Transfer Reactions of Phenolate Ions with Aromatic Carbonyl Triplets, *Journal of Physical Chemistry*, *85* (10), 1391-1395, 1981.

Das, P.K., M.V. Encinas, et J.C. Scaiano, Laser Flash-Photolysis Study of the Reactions of Carbonyl Triplets with Phenols and Photochemistry of Para- Hydroxypropiophenone, *Journal of the American Chemical Society*, *103* (14), 4154-4162, 1981.

De Santis, F., et I. Allegrini, Heterogeneous reactions of sulfur dioxide and nitrogen dioxide on carbonaceous surfaces, dans *Atmos. Environ., Part A*, pp. 3061-4, 1992.

Fickert, S., F. Helleis, J.W. Adams, G.K. Moortgat, et J.N. Crowley, Reactive uptake of ClNO2 on aqueous bromide solutions, *J. Phys. Chem. A*, *102*, 10689-10696, 1998.

Fine, P.M., G.R. Cass, et B.R.T. Simoneit, Chemical characterization of fine particle emissions from fireplace combustion of woods grown in the northeastern United States, *Environ. Sci. Technol.*, *35* (13), 2665-2675, 2001.

Finlayson-Pitts, B.J., et J.N. Pitts, *Atmospheric chemistry : fundamentals and experimental techniques*, xxviii, 1098 pp., Wiley, New York, 1986.

Finlayson-Pitts, B.J., et J.N. Pitts, *Chemistry of the Upper and Lower Atmosphere: Theory, Experiments and Applications*, Academic Press, San Diego, 2000.

Finlayson-Pitts, B.J., L.M. Wingen, A.L. Sumner, D. Syomin, et K.A. Ramazan, The heterogeneous hydrolysis of NO2 in laboratory systems and in outdoor and indoor atmospheres: An integrated mechanism, *Phys. Chem. Chem. Phys.*, *5* (2), 223-242, 2003.

Forni, L.G., V.O. Mora-Arellano, J.E. Packer, et R.L. Willson, Nitrogen dioxide and related free radicals: electron-transfer reactions with organic compounds in solutions containing nitrite or nitrate, *J. Chem. Soc. Perkin Trans.*, *II*, 1-6, 1986.

Fuzzi, S., S. Dcesari, M.C. Facchini, E. Matta, M. Mircea, et E. Tagliavini, A simplified model of the water soluble organic component of atmospheric aerosols, *Geophys. Res. Lett.*, *28* (21), 4079-4082, 2001.

Gallet, C., et C. Keller, Phenolic composition of soil solutions: comparative study of lysimeter and centrifuge waters, *Soil Biology & Biochemistry*, *31* (8), 1151-1160, 1999.

Gerecke, A., A. Thielmann, L. Gutzwiller, et M.J. Rossi, The Chemical-Kinetics of Hono Formation Resulting from Heterogeneous Interaction of NO_2 with Flame Soot, *Geophys. Res. Lett.*, *25* (13), 2453-2456, 1998.

Gorman, A.A., et M.A.J. Rodgers, The Quenching of Aromatic Ketone Triplets by Oxygen - Competing Singlet Oxygen and Biradical Formation, *Journal of the American Chemical Society*, *108* (17), 5074-5078, 1986.

Graedel, T.E., et C.J. Weschler, Chemistry within aqueous atmospheric aerosols and raindrops, *Reviews Geophysical Space Physics*, *19* (4), 505-539, 1981.

Graham, B., O.L. Mayol-Bracero, P. Guyon, G.C. Roberts, S. Decesari, M.C. Facchini, P. Artaxo, W. Maenhaut, P. Koll, et M.O. Andreae, Water-soluble organic compounds in biomass burning aerosols over Amazonia - 1. Characterization by NMR and GC-MS, *Journal of Geophysical Research-Atmospheres*, *107* (D20), art. no.-8047, 2002.

Grannas, A.M., P.B. Shepson, et T.R. Filley, Photochemistry and nature of organic matter in Arctic and Antarctic snow, *Global Biogeochemical Cycles*, *18* (1), art. no.-GB1006, 2004.

Gutzwiller, L., F. Arens, et M. Ammann, The HONO formation Capacity of Diesel Exhaust, dans *EC/EUROTRAC-2 joint Workshop*, edited by M.J. Rossi, et E.-V. Rossi, pp. 189, EPFL Lausanne, Lausanne, Switzerland, 2000.

Gutzwiller, L., F. Arens, et M. Ammann, New HONO source involving semi-volatile exhausts organics, dans *A Changing Atmosphere, 8th European Symposium on the Physico-chemical behaviour of pollutants*, edited by F. Raes, Torino, Italy, 2001.

Gutzwiller, L., F. Arens, U. Baltensperger, H.W. Gäggeler, et M. Ammann, Significance of semi-volatile diesel exhaust organics for secondary HONO formation, *Environ. Sci. Technol.*, *36*, 677-682, 2002a.

Gutzwiller, L., C. George, E. Rössler, et M. Ammann, Reaction kinetics of NO_2 with resorcinol and 2,7-naphthalenediol in the aqueous phase at different pH, *J. Phys. Chem. A*, *106*, 12045-12050, 2002b.

Hanson, D.R., et E.R. Lovejoy, Heterogeneous Reactions in Liquid Sulfuric Acid: HOCl + HCl as a Model System, *J. Phys. Chem.*, *100*, 6397-6405, 1996.

Hanson, D.R., et A.R. Ravishankara, Heterogeneous chemistry of bromine species in sulfuric acid under stratospheric conditions, *Geophys. Res. Lett.*, *22* (4), 385-8, 1995.

Harris, G.W., W.P.L. Carter, A.M. Winer, J.N. Pitts, Jr., U. Platt, et D. Perner, Observations of nitrous acid in the Los Angeles atmosphere and implications for predictions of ozone-precursor relationships, *Environ. Sci. Technol.*, *16* (7), 414-19, 1982.

Harrison, R.M., et A.-M.N. Kitto, Evidence for a surface source of atmospheric nitrous acid, *Atmos. Environ.*, *28* (6), 1089-94, 1994.

Harrison, R.M., J.D. Peak, et G.M. Collins, Tropospheric cycle of nitrous acid, *Journal of Geophysical Research*, *101* (D9), 14429-14439, 1996a.
Harrison, R.M., J.D. Peak, et G.M. Collins, Tropospheric cycle of nitrous acid, *J. Geophys. Res.*, *101* (D9), 14429-14439, 1996b.
Heland, J., J. Kleffmann, R. Kurtenbach, et P. Wiesen, A New Instrument To Measure Gaseous Nitrous Acid (HONO) in the Atmosphere, *Environ. Sci. Technol.*, *35* (15), 3207-3212, 2001.
Herrmann, H., B. Ervens, H.W. Jacobi, R. Wolke, P. Nowacki, et R. Zellner, CAPRAM2.3: A chemical aqueous phase radical mechanism for tropospheric chemistry, *J. Atmos. Chem.*, *36* (3), 231-284, 2000.
Hoffer, A., G. Kiss, M. Blazso, et A. Gelencser, Chemical characterization of humic-like substances (HULIS) formed from a lignin-type precursor in model cloud water, *Geophysical Research Letters*, *31* (6), art. no.-L06115, 2004.
Hurley, J.K., H. Linschitz, et A. Treinin, Interaction of Halide and Pseudohalide Ions with Triplet Benzophenone-4-Carboxylate - Kinetics and Radical Yields, *Journal of Physical Chemistry*, *92* (18), 5151-5159, 1988.
Inbar, S., H. Linschitz, et S.G. Cohen, Quenching, Radical Formation, and Disproportionation in the Photo-Reduction of 4-Carboxybenzophenone by 4- Carboxybenzhydrol, Hydrazine, and Hydrazinium Ion, *Journal of the American Chemical Society*, *103* (24), 7323-7328, 1981.
Jenkin, M.E., R.A. Cox, et D.J. Williams, Laboratory studies of the kinetics of formation of nitrous acid from the thermal reaction of nitrogen dioxide and water vapor, dans *Atmos. Environ.*, pp. 487-98, 1988.
Kalberer, M., K. Tabor, A. Ammann, Y. Parrat, E. Weingartner, D. Piguet, E. Rössler, D.T. Jost, A. Türler, H.W. Gäggeler, et U. Baltensperger, Heterogeneous chemical processing of 13NO2 by monodisperse carbon aerosols at very low concentrations, *J. Phys. Chem.*, *100* (38), 15487-15493, 1996.
Kleffmann, J., K.H. Becker, M. Lackhoff, et P. Wiesen, Heterogeneous conversion of NO2 on carbonaceous surfaces, *Phys. Chem. Chem. Phys.*, *1* (24), 5443-5450, 1999.
Kleffmann, J., K.H. Becker, et P. Wiesen, Heterogeneous NO_2 conversion processes acid surfaces: possible atmospheric implications, dans *Atmos. Environ.*, pp. 2721-2729, 1998a.
Kleffmann, J., K.H. Becker, et P. Wiesen, Investigation of the heterogeneous NO2 conversion on perchloric acid surfaces, *Journal of the Chemical Society Faraday Transactions*, *94* (21), 3289-3292, 1998b.
Kleffmann, J., T. Benter, et P. Wiesen, Heterogeneous Reaction of Nitric Acid with Nitric Oxide on Glass Surfaces under Simulated Atmospheric Conditions, *J. Phys. Chem. A*, *108* (27), 5793-5799, 2004.
Kleffmann, J., J. Heland, R. Kurtenbach, J.C. Lörzer, et P. Wiesen, A new instrument (LOPAP) for the detection of nitrous acid (HONO), *Environ. Sci. Pollut. Res.*, *9* (4), 48-54, 2002.
Kleffmann, J., R. Kurtenbach, J. Lörzer, P. Wiesen, N. Kalthodd, B. Vogel, et H. Vogel, Measured and simulated vertical profiles of nitrous acid-Part I: Field measurements, *Atmospheric Environment*, *37*, 2949-2955, 2003a.
Kleffmann, J., R. Kurtenbach, J. Lörzer, P. Wiesen, N. Kalthoff, B. Vogel, et H. Vogel, Measured and simulated vertical profiles of nitrous acid - Part I: Field measurements, *Atmos. Environ.*, *37* (21), 2949-2955, 2003b.
Kolb, C.E., D.R. Worsnop, M.S. Zahniser, P. Davidovits, D.R. Hanson, A.R. Ravishankara, L.F. Keyser, M.T. Leu, L.R. Williams, M.J. Molina, et M.A. Tolbert, Laboratory Studies of Atmospheric Heterogeneous Chemistry; Current Problems in Atmospheric Chemistry, in *Advances in Physical Chemistry Series*, edited by J.R. Barker, World scientific, Singapore, 1994.

Kurtenbach, R., K.H. Becker, J.A.G. Gomes, J. Kleffmann, J.C. Lörzer, M. Spittler, P. Wiesen, R. Ackermann, A. Geyer, et U. Platt, Investigations of emissions and heterogeneous formation of HONO in a road traffic tunnel, *Atmos. Environ.*, *35* (20), 3385-3394, 2001.

Lahoutifard, N., M. Ammann, L. Gutzwiller, B. Ervens, et C. George, The impact of multiphase reactions of NO2 with aromatics: a modelling approach, *Atmospheric Chemistry and Physics*, *2*, 215-226, 2002.

Lammel, G., et J.N. Cape, Nitrous acid and nitrite in the atmosphere, dans *Chem. Soc. Rev.*, pp. 361-370, 1996.

Lary, D.J., D.E. Shallcross, R. Toumi, et M.W. Chase, Carbonaceous aerosols and their potential role in atmospheric chemistry, *Journal of Geophysical Research Atmospheres*, *104* (D13), 15929-15940, 1999.

Lee, J.H., et I.N. Tang, Accommodation Coefficient of Gaseous NO2 on Water Surfaces, *Atmos. Environ.*, *22*, 1147-1151., 1988.

Lee, Y.N., et S.E. Schwartz, Evaluation of the rate of uptake of nitrogen dioxide by atmospheric and surface liquid water, dans *JGR, J. Geophys. Res., [Sect.] C*, pp. 11971-83, 1981a.

Lee, Y.N., et S.E. Schwartz, Reaction kinetics of nitrogen dioxide with liquid water at low partial pressure, dans *J. Phys. Chem.*, pp. 840-8, 1981b.

Loeff, I., J. Rabani, A. Treinin, et H. Linschitz, Charge-Transfer and Reactivity of N-Pi-Asterisk and Pi-Pi- Asterisk Organic Triplets, Including Anthraquinonesulfonates, in Interactions with Inorganic Anions - a Comparative-Study Based on Classical Marcus Theory, *Journal of the American Chemical Society*, *115* (20), 8933-8942, 1993.

Lögager, T., et K. Sehested, Formation and decay of peroxynitric acid: a pulse radiolysis study, *J. Phys. Chem.*, *97* (39), 10047-52, 1993.

Lovejoy, E.R., L.G. Huey, et D.R. Hanson, *J. Geophys. Res.*, *100*, 18775, 1995.

Madronich, S., Photodissociation in the Atmosphere .1. Actinic Flux and the Effects of Ground Reflections and Clouds, *Journal of Geophysical Research-Atmospheres*, *92* (D8), 9740-9752, 1987.

Mark, G., H.-G. Korth, H.-P. Schuchmann, et C. von Sonntag, The photochemistry of aqueous nitrate ion revisited, *J. Photochem. Photobiol., A*, *101* (2-3), 89-103, 1996.

Mayol-Bracero, O.L., P. Guyon, B. Graham, G. Roberts, M.O. Andreae, S. Decesari, M.C. Facchini, S. Fuzzi, et P. Artaxo, Water-soluble organic compounds in biomass burning aerosols over Amazonia - 2. Apportionment of the chemical composition and importance of the polyacidic fraction, *Journal of Geophysical Research-Atmospheres*, *107* (D20), art. no.-8091, 2002.

McKenzie, L.M., W.M. Hao, G.N. Richards, et D.E. Ward, Measurement and Modeling of Air Toxins from Smoldering Combustion of Biomass, *Environmental Science & Technology*, *29* (8), 2047-2054, 1995.

Melhuish, W.H., Quantum Efficiencies of Fluorescence of Organic Substances - Effect of Solvent and Concentration of Fluorescent Solute, *Journal of Physical Chemistry*, *65* (2), 229-&, 1961.

Mertes, S., et A. Wahner, Uptake of nitrogen dioxide and nitrous acid on aqueous surfaces, *J. Phys. Chem.*, 1994.

Miao, J.L., W.F. Wang, J.X. Pan, C.Y. Lu, R.Q. Li, et S.D. Yao, The scavenging reactions of nitrogen dioxide radical and carbonate radical by tea polyphenol derivatives: a pulse radiolysis study, *Radiation Phys. Chem.*, *60* (3), 163-168, 2001.

Murov S. L, C., I., Hug, G., L., *Handbook of Photochemistry*, 1993.

Murphy, D.M., et D.W. Fahey, Mathematical treatment of the wall loss of a trace species in denuder and catalytic converter tubes, *Analytical Chemistry*, *59*, 2753-2759, 1987.

Olariu, R.I., I. Barnes, K.H. Becker, et B. Klotz, Rate coefficients for the gas-phase reaction of OH radicals with selected dihydroxybenzenes and benzoquinones, *Int. J. Chem. Kin.*, *32* (11), 696-702, 2000.

Park, J.Y., et Y.N. Lee, Aqueous Solubility and Reactivity of Nitrous Acid, *Symposium on Acid Rain , American Chemical Society Meeting*, *437-440.*, 1986.

Parker, C.A., et T.A. Joyce, Formation Efficiency and Energy of Perylene Triplet, *Chemical Communications* (4), 108-&, 1966.

Perner, D., et U. Platt, Detection of nitrous acid in the atmosphere by differential optical absorption, *Geophys. Res. Lett.*, *6* (12), 917-20, 1979.

Ramazan, K.A., D. Syomin, et B.J. Finlayson-Pitts, The photochemical production of HONO during the heterogeneous hydrolysis of NO2, *Phys. Chem. Chem. Phys.*, *6* (14), 3836-3843, 2004.

Ren, X., H. Harder, M. Martinez, R.L. Lesher, A. Oliger, J.B. Simpas, W.H. Brune, J.J. Schwab, K.L. Demerjian, Y. He, X. Zhou, et H. Gao, OH and HO2 chemistry in the urban atmosphere of New York City, *Atmos. Environ.*, *37* (26), 3639-3651, 2003.

Rogaski, C.A., D.M. Golden, et L.R. Williams, Reactive uptake and hydration experiments on amorphous carbon treated with NO2, SO2, O3, HNO3, and H2SO4, dans *Geophys. Res. Lett.*, pp. 381-384, 1997.

Rogge, W.F., L.M. Hildemann, M.A. Mazurek, G.R. Cass, et B.R.T. Simoneit, Sources of fine organic aerosol. 9. Pine, oak and synthetic log combustion in residential fireplaces, *Environ. Sci. Technol.*, *32* (1), 13-22, 1998.

Rohrer, F., B. Bohn, T. Brauers, D. Brüning, J.-F. Johnen, A. Wahner, et J. Kleffmann, Characterisation of the Photolytic HONO-Source in the Atmosphere Simulation Chamber SAPHIR, *Atmos. Chem. Phys. Discuss.*, *4*, 7881-7915, 2004.

Saliba, N.A., M. Mochida, et B.J. Finlayson-Pitts, Laboratory studies of sources of HONO in polluted urban atmospheres, *Geophys. Res. Lett.*, *27* (19), 3229-3232, 2000.

Scheer, V., A. Frenzel, W. Behnke, C. Zetzsch, L. Magi, C. George, et P. Mirabel, Uptake of nitrosyl chloride, *J. Phys. Chem. A*, *101*, 9359-9366, 1997.

Schwartz, S.E., Mass-transport considerations pertinent to aqueous phase reactions of gases in liquid-water clouds, in *Chemistry of Multiphase Atmospheric Systems, NATO ASI Ser.*, edited by W. Jaesche, pp. 415-471, Springer-Verlag, Berlin, 1986.

Schwartz, S.E., et Y.N. Lee, Laboratory Study of NO2 Reaction with Dispersed and Bulk Liquid Water, *Atmos. Environ.*, *29* (18), 2557-2559, 1995.

Simoneit, B.R.T., J.J. Schauer, C.G. Nolte, D.R. Oros, V.O. Elias, M.P. Fraser, W.F. Rogge, et G.R. Cass, Levoglucosan, a tracer for cellulose in biomass burning and atmospheric particles, *Atmos. Environ.*, *33*, 173-182, 1999.

Stockwell, W.R., F. Kirchner, M. Kuhn, et S. Seefeld, A new mechanism for regional atmospheric chemistry modeling, *J. Geophys. Res.*, *102* (D22), 25847-25879, 1997.

Strekowski, R.S., et C. George, Measurement of Henry's Law Constants for Acetone, 2-Butanone, 2,3-Butanedione and Isobutyraldehyde Using a Horizontal Flow Reactor, *submitted to J. Chem. Eng. Data*, 2005.

Tabor, K., L. Gutzwiller, et M.J. Rossi, Heterogeneous Chemical-Kinetics of NO2 on Amorphous-Carbon at Ambient-Temperature, *J. Phys. Chem.*, *98* (24), 6172-6186, 1994.

Tan, K.H., *Humic matter in soil and the environment: principles and controversies*, 360 pp., Marcel Dekker, Inc, New York, Basel, 2003.

Trick, S., Formation of Nitrous Acid on Urban Surfaces - A Physical-Chemical Perspective, University of Heidelberg, Heidelberg, 2004.

Vogel, B., H. Vogel, J. Kleffmann, et R. Kurtenbach, Measured and simulated vertical profiles of nitrous acid - Part II. Model simulations and indications for a photolytic source, *Atmos. Environ.*, *37* (21), 2957-2966, 2003a.

Vogel, B., H. Vogel, J. Kleffmann, et R. Kurtenbach, Measured and simulated vertical profiles of nitrous acid-Part II. Model simulations and indications for a photolytic source, *Atmospheric Environment*, *37*, 2957-2966, 2003b.

Vogt, R., et B.J. Finlayson-Pitts, Tropospheric Hono and Reactions of Oxides of Nitrogen with NaCl, *Geophys. Res. Lett.*, *21* (21), 2291-2294, 1994.

Zhan, Z., S. Yao, W. Lin, W.F. Wang, Y. Jin, et N. Lin, Mechanism of Reaction of Nitrogen Dioxide Radical with Hydroxycinnamic Acid Derivatives: A Pulse Radiolysis Study, *Free Rad. Res.*, *29*, 13-16, 1998.

Zhou, X., H.J. Beine, R.E. Honrath, J.D. Fuentes, W. Simpson, P.B. Shepson, et J.W. Bottenheim, Snowpack photochemical production of HONO: A major source of OH in the Arctic boundary layer in springtime, *Geophys. Res. Lett.*, *28* (21), 4087-4090, 2001.

Zhou, X., K. Civerolo, H. Dai, G. Huang, J. Schwab, et K. Demerjian, Summertime nitrous acid chemistry in the atmospheric boundary layer at a rural site in New York State, *J. Geophys. Res.*, *107* (D21), ACH13/1-ACH13/11, 2002a.

Zhou, X., H. Gao, Y. He, G. Huang, S.B. Bertman, K. Civerolo, et J. Schwab, Nitric acid photolysis on surfaces in low-NOx environments: significant atmospheric implications, *Geophys. Res. Lett.*, *30* (23), ASC 12/1-ASC 12/4, 2003.

Zhou, X., Y. He, G. Huang, T.D. Thornberry, M.A. Carroll, et S.B. Bertman, Photochemical production of nitrous acid on glass sample manifold surface, *Geophys. Res. Lett.*, *29* (14), 26/1-26/4, 2002b.

Annexe I. Liste de publications issues du projet

1.	C George, R S Strekowski , J Kleffmann, K Stemmler et M Ammann Photoenhanced Uptake of Gaseous NO_2 on Solid Organic Compounds: A photochemical source of HONO *Faraday Discuss.*, 130, 195, 2005. 1ère étude de ce type
2.	M. Ammann, E. Rössler, R. Strekowski et Ch. George Uptake of NO_2 on aqueous solutions containing phenoxy type compounds - Implication for HONO formation in the atmosphere *Phys. Chem. Chem. Phys.,* 12,2513-2518, 2005.
3.	K. Stemmler, M. Ammann, Chantal Donders, J. Kleffmann, Ch. George Photochemistry on Humic Acids and Soil: An Important Source of Atmospheric Nitrous Acid *Nature*, soumise, 2005

Annexe II. Liste de présentations issues du projet

2005

Faraday Discussion 130 - Atmospheric Chemistry, 11-13 avril, Leeds, Angleterre

C George, R S Strekowski , J Kleffmann, K Stemmler et M Ammann (présentation orale, conférencier invité)
Photoenhanced Uptake of Gaseous NO_2 on Solid Organic Compounds: A photochemical source of HONO
Autres conférenciers invités: A.R. Ravishankara, J. Abbatt, J. Burrows,…

PRIMEQUAL 2 – Séminaire de Programme, 10-11 juin, Reims, France

R. Strekowski et Ch. George (présentation orale)
Étude de la contribution de l'aérosol organique en tant que source d'acide nitreux.

Réunion annuelle du Groupe Français de Cinétique et Photochimie, 22-23 juin, Bordeaux, France

R. Strekowski et Ch. George (présentation orale)
Formation hétérogène de HONO.

2005

EGU General Assembly, 24-29 avril, Vienne, Autriche.

K. Stemmler, A. Ammann, J. Kleffmann, Ch. George (présentation orale)
A new Source of Nitrous Acid: NO_2 Photochemistry on various organic Surfaces

Annexe III. Copies des publications issues du projet

M. Ammann, E. Rössler, R. Strekowski et Ch. George, Uptake of NO_2 on aqueous solutions containing phenoxy type compounds - Implication for HONO formation in the atmosphere, *Phys. Chem. Chem. Phys.*, 12,2513-2518, 2005.

Nitrogen dioxide multiphase chemistry: Uptake kinetics on aqueous solutions containing phenolic compounds

Markus Ammann, *[a] Elfriede Rössler, [a] Rafal Strekowski[b,#] and Christian George[b]

[a] *Laboratory for Radio and Environmental Chemistry, Paul Scherrer Institute, 5232 Villigen, Switzerland Markus Ammann, OFLA 106, Paul Scherrer Institute, 5232 Villigen, Switzerland, Tel: ++41 56 310 4049, fax: ++41 56 310 4435, markus.ammann@psi.ch*

[b] *Laboratoire d'Application de la Chimie à l 'Environnement (UCBL-CNRS) 43 boulevard du 11 Novembre 1918, F-69622 Villeurbanne, France. Fax:+33 (0)4 72 44 8114; Tel: +33 (0)4 72 43 1489, E-mail: christian.george@univ-lyon1.fr*

The uptake coefficients of NO_2 on aqueous solutions containing guaiacol, syringol and catechol were determined over the pH range from 1 to 13 using the wetted wall flowtube technique. The measured uptake coefficients were used to determine the rate coefficients for the reaction of the physically dissolved NO_2 with the neutral and deprotonated forms of phenolic compounds listed above. These organic compounds are ubiquitous not only in biomass burning plumes but also in soils, where they form part of the building blocks of humic acids. The NO_2 uptake kinetics on solutions containing guaiacol, syringol or catechol were observed to be strongly pH dependent with uptake coefficients increasing from below 10^{-7} , under acidic conditions, to more than 10^{-5} at pH values above 10. This behaviour illustrates the different reactivity between the neutral phenolic species and the phenoxide ions. The corresponding second order rate coefficients were typically observed to increase from 10^5 M^{-1} s^{-1} for the neutral compounds to a minimum of 10^8 M^{-1} s^{-1} for the phenoxide ions.

Introduction

Lignin is a major structural constituent of vegetation. Microbial degradation or pyrolysis in biomass burning processes, especially in smouldering fires, leads to emissions of a wide range of hydroxy and methoxy substituted aromatic compounds. Catechol, syringol and guaiacol are three major lignin derived metabolites that are representative of this family of compounds and are readily detected in soils (plant litter) and in biomass burning plumes. Their further oxidative degradation leads to radical cations, which in turn undergo polymerization into humic acid type compounds, an important soil forming process [*Tan*, 2003] and of potential atmospheric importance [*Hoffer et al.*, 2004]. Smoke from biomass combustion is one of the largest yet least characterized contributors to atmospheric fine particle levels on local, regional and global scales [*Mayol-Bracero et al.*, 2002; *Rogge et al.*, 1998]. Catechol (o-dihydroxybenzene), guaiacol (o-methoxyphenol), syringol (2,6-dimethoxyphenol) and similar compounds have been detected in biomass burning plumes [*Graham et al.*, 2002] or ambient air influenced by corresponding anthropogenic activities, e.g., residential fires [*Simoneit et al.*, 1999]. Individual ratios of these species to CO have been estimated about 10^{-4} in wild fire emissions [*McKenzie et al.*, 1995]. In soils, capillary water within the top organic soil layer contains typically between 0.1 and 1 mg l^{-1} of phenolic monomers and about 10 mg l^{-1} of phenols in total (including polyphenols) [*Gallet et Keller*, 1999].

In aqueous solution, nitrogen dioxide (NO_2) may undergo electron transfer reactions with phenoxide anions, which have been previously investigated for methylphenols and hydroxybenzenes [*Alfassi et al.*, 1986], catechins [*Miao et al.*, 2001] and hydroxycinnamic acid derivatives [*Zhan et al.*, 1998]. The primary reactant is the deprotonated species, the phenoxide ion, leading to strongly pH dependent overall kinetics.

The primary reaction products of gaseous NO_2 with these organic compounds are the corresponding phenoxy type radical (or the corresponding radical cations) or nitrite anions. In an acidic aqueous environment, the nitrite ion may be subsequently protonated and released to the gas phase as HONO, or undergo secondary chemistry, eventually leading to NO and/or N_2O [*Baker et al.*, 1999; *Kleffmann et al.*, 1998b] or nitrated organics. In atmospheric chemistry, HONO plays an important role as OH radical source due to its photolysis [*Harrison et al.*, 1996a]. Field studies indicate that HONO is mainly formed heterogeneously from NO_2 on ground or airborne surfaces such as aerosol particles and cloud droplets. Previous modelling studies have mostly considered the self-reaction of NO_2 in an aqueous solution as a source of HONO on humid surfaces, the kinetics of which, however, is relatively slow. Recent field measurements also indicate substantial day-time HONO concentrations possibly due to hitherto unknown photochemistry on the ground, rendering HONO an even more significant day-time OH source. [*Aumont et al.*, 2003a; *Kleffmann et al.*, 2003a; *Vogel et al.*, 2003b]

In a recent study, we have reported measurements of NO_2 uptake into solutions of m-dihydroxybenzene (resorcinol) and 2,7-dihydroxynaphthalene, both occurring as photo oxidation products of aromatic compounds in the atmosphere, in the pH range from 3 to 11 using the wetted wall flowtube technique [*Gutzwiller et al.*, 2002b]. In a multiphase modelling study, we have addressed the atmospheric impact of these reactions, as far as their kinetics was known at that time, on the levels of HONO in the gas-phase and nitrite in the aerosol phase under typical urban conditions [*Lahoutifard et al.*, 2002]. That study indicated that the significance of these reactions depends heavily on the total amount of aromatics appearing in the aqueous phase and on aerosol pH. Therefore, in environments with a high content of these compounds combined with the presence of neutralizing minerals, such as in an aerosol from burning of biomass or above soils, a much higher impact of these species on HONO or nitrite may be expected. In the present study, we have expanded our kinetic experiments to three major lignin derived metabolites i.e., guaiacol, syringol and catechol.

Experimental

Wetted-wall flowtube technique. The uptake of gaseous NO_2 into aqueous solutions containing guaiacol, syringol or catechol was studied using the wetted wall flowtube (WWFT) technique [*Danckwerts*, 1970a; *Fickert et al.*, 1998; *Hanson et Ravishankara*, 1995; *Murphy et Fahey*, 1987; *Scheer*

et al., 1997]. Experiments reported here were conducted in both involved laboratories using two very similar set-ups. Where necessary, the setups operated in Lyon, France, and Villigen, Switzerland, will be referred to as LACE and PSI, respectively. The WWFT is a well established experimental approach that has been used to study the transport of gases into liquids for many years [for further examples see ref [*Finlayson-Pitts et Pitts*, 2000] and references therein]. The WWFT method takes advantage of the fact that the well described mass transport equation in cylindrical co-ordinates can be applied. The uptake kinetics were determined from the measured loss rate of gas-phase NO_2 flowing along a vertically aligned flowtube, the wall of which was covered by a film of an aqueous solution allowed to flow slowly under the effect of gravity. Thereby, the observed loss of NO_2 from the gas phase is used to obtain the reactive uptake coefficient, defined as the probability that a gas kinetic collision of a gaseous NO_2 molecule with the liquid surface leads to reactive loss within the liquid. At the bottom of the tube, the reagent solution is pumped out to waste or to a sample vial for further analysis.

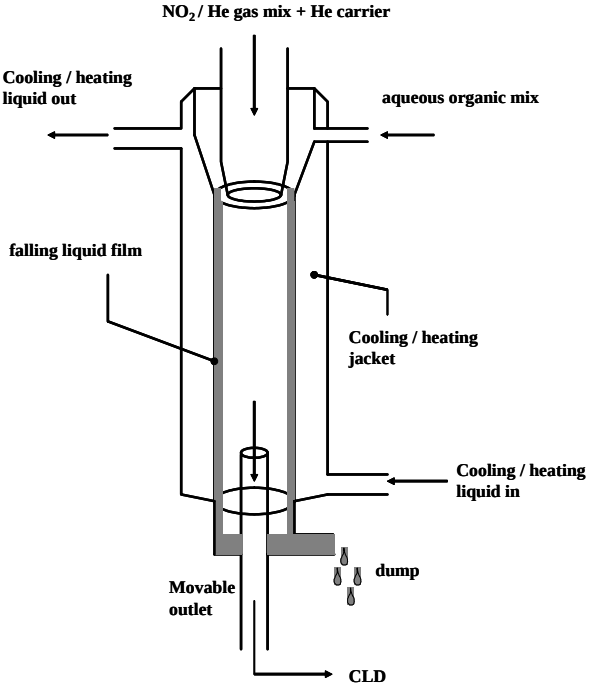

Figure 1. Schematic representation of the vertically mounted wetted-wall reactor used to measure the uptake of NO_2 on aqeuous films.

The instruments operated in our laboratories have been described in detail in our previous studies for PSI [*Gutzwiller et al.*, 2002b; *Strekowski et George*, 2005] and LACE [*Gutzwiller et al.*, 2002b; *Strekowski et George*, 2005] and are designed for the measurement of uptake coefficients in the range of 10^{-5} to 10^{-8} at ambient pressure.

The NO_2 reactant gas concentration was measured at the exit of the flowtube as a function of the distance (time) that the NO_2 gas was in contact with the aqueous film. The NO_2 reactant gas was monitored using a quadrupole mass analyser (at LACE) or a chemiluminescence detector (Monitorlabs, ML9841) (at PSI).

The use of different detectors is accompanied with different NO2 working concentrations. The latter were in the range 10-100 ppm for the MS experiments (LACE) and 10-100 ppb for the chemiluminescence experiments (PSI). In both cases, the NO_2 concentrations were obtained by diluting a certified NO_2 gas mix with the appropriate carrier gas.

Under the typical experimental conditions used for the concentration of the NO_2 gas, the NO_2 dimer (i.e., N_2O_4) is not expected to play a major role in the uptake kinetics. This was confirmed by varying the NO_2 gas phase concentrations. No difference in the uptake was observed.

The solutions used to produce the aqueous film were prepared by allowing a known quantity (weight or volume) of the organic compound to be dissolved in a known volume of water. Under the typical experimental conditions employed the organic solution concentrations used were in the range 10^{-5} to 10^{-1} mol L^{-1}. The freshly prepared standard organic solutions were used without further analysis.

At PSI, the reagent solutions were prepared with degassed Millipore water located in a glovebag continuously flushed with nitrogen (99.999%) to avoid any contact of the solution with oxygen, prior to the reaction. The solutions were pumped to the WWFT directly from within the glovebag. At PSI, the pH values between 6 and 11 were set using phosphate buffers, values below pH 6 were prepared using sulfuric acid, values of 13 were adjusted using potassium hydroxide. The pH of the effluent solutions was routinely checked directly at the exit of the flowtube. The buffers had no effect on the NO_2 uptake (see results).

At LACE, the pH of the solutions were adjusted by adding either sulphuric acid or sodium hydroxide but were not buffered, nor degassed, in order to address the uptake kinetics kinetics under different conditions those used at PSI.

In this study, only the gas phase was analysed i.e., the appearance of nitrite ions could not be monitored.

As the selected approach is based on flow experiments, the aqueous film was constantly and rapidly (within seconds) renewed preventing accumulation of reaction products. It is therefore assumed that the latter are not affecting our kinetic experiments. Again the absence of effect due to changes in the gas phase concentration of NO_2 is supporting this assumption.

The schematic of the experimental approach is shown in Figure 1. Some experimental details that are relevant to this work are given below. An upright Pyrex tube with an internal volume of approximately 314 cm^3 was used in all experiments. The Pyrex reactor was about 100 cm (LACE) and 60cm (PSI) long, and the inner diameter was 1.0 cm (LACE) and 1.2 cm (PSI) . It was maintained at a constant temperature (298.0±0.5 K) by circulating a 1:1 ethanol+methanol mixture from a thermostatically controlled bath through the outer jacket. The reactant NO_2 gas and the carrier gas (nitrogen for PSI and helium for LACE) were introduced into the reactor via a static 9.5 mm o.d. Teflon insert that has been mechanically fitted to leave a space of less than 0.5 mm between its outer diameter and the inner wall of the reactor. This allowed for a little reservoir of the aqueous solution to be formed just above the inner reactor tube. A peristaltic pump was used to pump the aqueous solution into the reservoir. Once enough liquid accumulated in the reservoir, gravity allowed for the aqueous solution to fall and coat the inner wall of the reactor. This point is discussed in detail in the section below. The gases were extracted from the flowtube by a moveable outlet (6mm o.d.).

Water vapour was added to the total flow by allowing the carrier gas to pass through a flask containing deionized H_2O. Controlling humidity in the wetted wall reactor was necessary to avoid any potential evaporation of water from the falling liquid film that could in turn result in cooling.

Uptake Coefficients. The flow dynamics of a liquid film allowed to fall under the effect of gravity in a cylindrical tube has already been discussed in detail by Danckwerts [*Danckwerts*, 1970a]. The thickness of the film f was calculated using the following equation (1).

In equation (1) above, η ρ and F_l are the viscosity, density and liquid flow rate of the falling liquid film, respectively. Under typical experimental conditions employed in this work the liquid flow rate was in the range 2 - 6 ml min^{-1} and the resulting film thickness was in the range from 6.1×10^{-3} to 1.2×10^{-2} cm.

In order to ensure that the mass transport in the gas phase is described by molecular diffusion processes alone i.e., without the effects of turbulence possibly produced by the film's surface ripples, the falling liquid flow has to be laminar. This was ensured by keeping the liquid flow rates as low as possible. Under the experimental conditions employed in this work the presence of ripples on film surfaces was never observed. Another indicator for the presence of turbulence in the liquid film is described by the Reynolds's number, N_{Re} [equation (2)].

$$N_{Re} = \frac{F_l \rho}{\pi d_{tube} \eta} \tag{2}$$

In this work, the calculated Reynolds's number was smaller than 3, a value far below the limit of 250-400 where turbulent transport is favoured. Therefore, it was assumed that gas phase transport can be described by diffusion alone.

The trace gas loss rate in the flowtube can be measured as a function of the position (distance) of the movable outlet *i.e.*, as a function of the gas / liquid exposure time t. The length l of the interaction zone can be varied up to l=80 cm at LACE and l=40cm at PSI. The entrance section (10cm) of the flowtube, where the laminar flow profile and gas-liquid equilibration occurs, was never used for analysis.

$$\frac{n-\Delta n}{n} = \exp\left[-k_w t\right] \tag{3}$$

As shown in equation (3) above, the loss rate can be described with a first order rate law with respect to the gas phase concentration of the reactant. In equation (3) t is the average gas residence time and k_w is the first order rate coefficient for the reaction at the liquid film surface. We assume in equation (3) that the loss rate can be described with a first order rate law. To a first approximation the rate coefficient $k_w$can be calculated by integrating both sides of equation (3) above.

$$k_w = \frac{\gamma < c >}{2 r_{tube}} \tag{4}$$

In equation (4), r_{tube}, γ, and <c> are the flowtube radius, uptake coefficient and average molecular velocity, respectively. However, equation (4) does not hold if gas phase diffusion limitations are present, *i.e.*, when radial gas concentration profiles build up. To take into account gas phase diffusion, the Cooney-Kim-Davis (CKD) equation (5) [*Cooney et al.*, 1974] was used as described in detail by Behnke *et al.*: [*Behnke et al.*, 1997a; *Behnke et al.*, 1992]

$$(n-\Delta n)/n = B_1 \exp(-\Lambda_1^2 z^*) + B_2 \exp(-\Lambda_2^2 z^*) + \ldots \tag{5}$$

In equation (5) above, B_i and Λ_i are functions of the Sherwood number N_{shw} [see equation (6) below] and z* is a dimensionless reaction length.

$$N_{shw} = \frac{r_{tube} < c >}{4 D_g} \times \left(\frac{\gamma}{1-\gamma/2}\right) \tag{6}$$

In equation (6), γ is the corrected uptake coefficient. The dimensionless reaction length z^* can be calculated using equation (7) listed below, where l is the reaction length, D_g is the

binary gas diffusion coefficient, *T* is the temperature and F_g is the gas flow rate ($cm^3\ s^{-1}$), which was in the range from 3-8 $cm^3\ s^{-1}$ and 5.8 $cm^3\ s^{-1}$ for LACE and PSI, respectively.

$$z^* = l \times \frac{D_{g,0}}{2F_g^0} \times \frac{T}{T_0} \tag{7}$$

The subscript "0" refers to standard conditions. Values of B_i and Λ_i were taken from the table reported by Murphy and Fahey [*Murphy et Fahey*, 1987] and interpolated from the four nearest values of N_{shw} using a cubic polynomial.

Applying equation (5) to the results obtained in this work was shown to give results in excellent agreement with the mathematical approach developed by Brown [*Brown et al.*, 2000]. Comparison of the method given by equation (5) with the simple exponential approach given by equation (3) was used to check to what degree uptake coefficients obtained in this work were affected by gas phase diffusion limitations. For the PSI experiments, where the highest measured values for the uptake coefficients were around 10^{-5}, the deviation from the simple exponential behaviour induced by diffusion in the gas-phase was observed to be about 20% (i.e., once corrected, the uptake coefficient increased by 20%. For the LACE experiments, the observed deviation was observed to be mostly below 5%. This difference is believed to be mainly due to different carrier gases used, i.e., helium and nitrogen, for the LACE end PSI experiments, recpectively. Gas phase diffusion proceeds at higher rates in helium than in nitrogen. Nevertheless, all experimental results presented below have either not been affected by gas phase limitations or have been corrected for the effect of slow gas phase diffusion. Note that we have cross-checked the overall procedure by performing the experiments with ABTS (2,2'-azino-bis(3-ethylbenziazoline-6-sulfonic acid) for reference using the PSI setup.

Results

All results listed in this section were obtained at 298 K.

The flowtube technique used in this work in principle allows for sensitive measurements of very small uptake coefficients (as low as a few times 10^{-8}). Accordingly, uptake of the poorly water soluble NO_2 into pure water was detectable, always with uptake coefficients on the order of 10^{-7} or below. This is due to the slow hydrolysis reaction of NO_2, which proceeds through a complex reaction mechanism. Also, due to its second-order character, the uptake coefficient of NO_2 is depending on its gas phase concentration, increasing the complexity of this system. As these experiments were performed with the MS experiments (i.e., with high NO_2 concentrations of about 50 ppm), they were certainly much influenced by this second order chemistry. Uptake of NO_2 by water has been previously studied in more detail [*Cheung et al.*, 2000b], and it is not our aim to provide here more insights into this complex chemistry. We underline that the uptake coefficients of NO_2 on water, as observed in the course of these experiments, were always smaller (by at least a factor 5) than those measured on aqueous solutions containing organic compounds described below, at all pH. Note also that for the experiments at PSI, which were performed at much lower NO_2 concentration, the low uptake coefficient of 10^{-7} and below on the aqueous solutions without organics was confirmed at each pH. Each series of measurements at different

$$f = \left(\frac{3\eta F_l}{\pi g d_{tube} \rho}\right)^{1/3} \tag{1}$$

concentrations of the organic compound was followed by one with the pure buffer solution (after thoroughly cleaning the flowtube).

Uptake on solutions containing aromatics.

The chemical system becomes (apparently) simpler when adding increasing concentrations of phenolic compounds to the aqueous solution. Figure 2 shows the uptake coefficients of NO_2 on catechol containing solutions at different pH. It is obvious that the uptake rate is drastically increased compared to water which means that this compound introduces a new reactive pathway (in the solution) that enhances the uptake of NO_2.

Apart from the disproportionation reaction mentioned, the following three reactions of the phenolic compounds (named generically as ArOH) have to be considered for the present system:

$NO_2 + ArOH \rightarrow HONO + ArO^{\cdot}$ (R1)

$NO_2 + ArO^- \rightarrow NO_2^- + ArO^{\cdot}$ (R2)

where ArOH is the undissociated form of the phenolic compounds, ArO^- is the deprotonated form.

The following simplified equation can be applied to our data, if the uptake without added ArOH is negligible, in order to extract $Hk^{1/2}$ values[*Kolb et al.*, 1994]:

$$\gamma = \frac{4HRT\sqrt{kD}}{< c >} \quad (8)$$

where H is the NO_2 Henry's law constant, R the gas constant, D the NO_2 aqueous phase diffusion coefficient, T the temperature and k is the pseudo first order rate constant. Equation (8) is also based on the assumption of an uptake proceeding at steady–state but does not require attainment of the Henry's law equilibrium over the entire depth of the film. It assumes however an equilibrated surface concentration which is rapidly attained.

Figure 2 shows a plot of the uptake coefficient versus the square root of the concentration of the NO_2 scavenger (i.e., catechol in this particular case) according to equation (8). It can be seen that the uptake coefficients exhibit indeed a linear dependence that almost goes through the origin of such a plot. This shows that the uptake is effectively and exclusively driven by the reaction of NO_2 with the aromatics i.e., there is no competition with the hydrolysis described shortly above. Indeed, all uptake coefficients on aromatic containing solutions were at least a factor of 5 higher than on water (under the same experimental conditions employed). Based on the second order rate coefficient reported by Cheung et al.[*Cheung et al.*, 2000b], the first order loss rate constant of NO_2 due to the hydrolysis reaction is at least a factor of 10 less than the loss rate constant derived from the observed uptake coefficient, which was due to reactions (R1) to (R3).

Under the conditions chosen in this study, uptake into the liquid was limited by the combined effects of reaction and diffusion in

$$k_X^{II} = \left[\frac{\gamma \cdot \frac{< c >}{4}}{H_{NO2} \cdot R \cdot T} \right]^2 \cdot \frac{1}{[X] D_{NO2}} \quad (9)$$

the liquid phase. It was assumed that the mass accommodation coefficient, α, is much larger than the uptake coefficient, γ. Then, the overall second order rate constant k_X^{II} for reactions R1 and R2 in the aqueous phase was calculated from the measured γ values using equation (9):

where k_X^{II} denotes the overall second order rate constant in the liquid phase, [X] the concentration of the liquid phase reactant, H_{NO_2} the Henry's law constant for NO_2 (0.014 M/atm [*Cheung et al.*, 2000a], <c> its mean thermal molecular velocity (37 000 cm s^{-1} at 298 K). D_{NO_2} is the diffusion coefficient in the liquid phase (1.23×10^{-5} $cm^2 s^{21}$.[*Cheung et al.*, 2000a] We used ABTS (2,2'-azino-bis(3-ethylbenziazoline-6-sulfonic acid) as reference to check the overall procedure and obtained a value of k_{II} of 2.48×10^7 (9.4×10^6) $M^{-1}s^{-1}$ in the pH range of 1 to 9, which is in good agreement with the often used literature value of 2.2×10^7 $M^{-1}s^{-1}$ in the pH range of 6.5 to 9. [*Forni et al.*, 1986]

Figure 3 shows a compilation of the uptake coefficients γ of NO_2 into ArOH containing solutions as a function of ArOH concentration and pH for all compounds measured at PSI. No dependence of γ of the NO_2 concentration was observed in the range of 20 to 2000 ppbv of NO_2. The values of the uptake coefficients are contained in the range from 2×10^{-7} to 6×10^{-5} for the whole set of experiments. Figure 3 also contains the data obtained at LACE for catechol at pH=12 (open stars at concentrations larger than 10^{-4} mol L^{-1}). It can be seen that they fit reasonably well to the PSI data at the same pH. As the experiments made at LACE were done at higher NO_2 concentration with unbuffered solutions they potentially carry a large uncertainty in the solution. Therefore, these data were not considered for the calculation of the aqueous phase second order rate constants performed below.

Table I Overview of reactions and measured rate constants

	species		*CASno*	*Reaction*	k^{II} ($M^{-1}s^{-1}$) *pK published values*	*this work*
	catechol	1,2-dihydroxybenzene	120-80-9	$C_6H_4(OH)_2 + H2O = C_6H_4(OH)O^- + H_3O^+$	pK_1 = 9.3 a	**9.1**
1a				$C_6H_4(OH)_2 + NO_2 = C_6H_4(OH)O + HONO$	$k_{1,1}$	**$1x10^4$**
1b				$C_6H_4(OH)O^- + NO_2 = C_6H_4(OH)O + NO_2^-$	$k_{1,2}$	**$1.3x10^8$**
	guaiacol	2-methoxyphenol	90-05-1	$C_6H_4(OCH_3)OH + H_2O = C_6H_4(OCH_3)O^- + H_3O^+$	pK_2 =9.9 b	**9.8**
2°				$C_6H_4(OCH_3)OH + NO_2 = C_6H_4(OCH_3)O + HONO$	$k_{2,1}$	**< 10^4**
2b				$C_6H_4(OCH_3)O^- + NO_2 = C_6H_4(OCH_3)O + NO_2^-$	$k_{2,2}$	**$1.5x10^8$**
	syringol	2,6-dimethoxyphenol	91-10-1	$C_6H_3(OCH_3)_2OH + H_2O = C_6H_3(OCH_3)_2O^- + H_3O^+$	pK_3 =10.2 c	**9.8**
3°				$C_6H_3(OCH_3)_2OH + NO_2 = C_6H_3(OCH_3)O + HONO$	$k_{3,1}$	**$1.5x10^5$**
3b				$C_6H_3(OCH_3)_2O^- + NO_2 = C_6H_3(OCH_3)O + NO_2^-$	$k_{3,2}$	**$4.5x10^8$**
4b	**quinol**	1,4-benzenediol	123-31-9	$C_6H_4(OH)O^- + NO_2 = C_6H_4(OH)O + NO_2^-$	$k_{4,2} = 1.1x10^9$ d	
5b	**m-guaiacol**	3-methoxyphenol	150-19-6	$C_6H_4(OCH_3)O^- + NO_2 = C_6H_4(OCH_3)O + NO_2^-$	$k_{5,2} = 1.8x10^7$ e	
6b	**mequinol**	4-methoxyphenol	150-76-5	$C_6H_4(OCH_3)O^- + NO_2 = C_6H_4(OCH_3)O + NO_2^-$	$k_{6,2} = 2.1x10^8$ f	
7b	**resorcinol**	1,3-benzenediol	108-46-3	$C_6H_4(OH)O^- + NO_2 = C_6H_4(OH)O + NO_2^-$	$k_{7,2} = 1.3x10^7$ g	

; other literature range 9.0-9.5
literature range 9.2-10.0

1986
1990

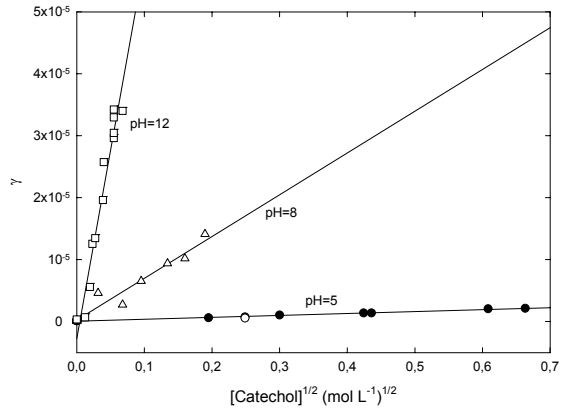

Figure 2. Uptake coefficients measured on catechol solutions as a function of its concentration and pH. These data were obtained at LACE at 298 K with a NO_2 concentration of 90 ppm (open symbols) or 30 ppm (closed circles).

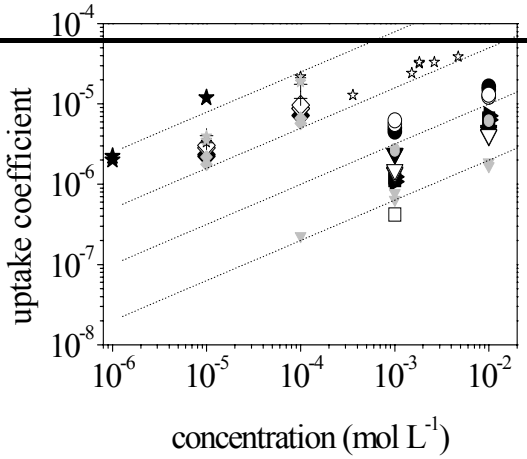

Figure 3: Uptake coefficient γ at the aqueous surface (after correction for diffusion in the gas-phase), measured at 298 K at PSI, plotted as a function of aqueous phase concentration of ArOH. The black solid, black open and grey solid symbols refer to syringol, catechol and guaiacol, respectively. The symbol types refer to the pH of the aqueous solution: (Δ) pH=1, (□) pH=3, (∇) pH=6, (○) pH=7, (◊) pH=9, (*) pH=12, (+) pH=13. The dotted lines indicate the slope of the square root dependency expected for uptake limited by diffusion in the liquid phase.

As given in equation (9), under the assumption of uptake limited by diffusion in the liquid phase, γ is proportional to the square root of the ArOH concentration, resulting in a slope of ½ on the double logarithmic plot of figure 3, indicated by the parallel solid lines. The fact that in most cases the same symbols plot parallel to these lines indicates that the data are in agreement with this assumption. An exception seem to be the data points obtained at pH 1, where secondary reactions of HONO (decomposition into NO and NO_2) might have led to an underestimation of $\tilde{\gamma}$. For syringol, at pH 1, the fits of equation

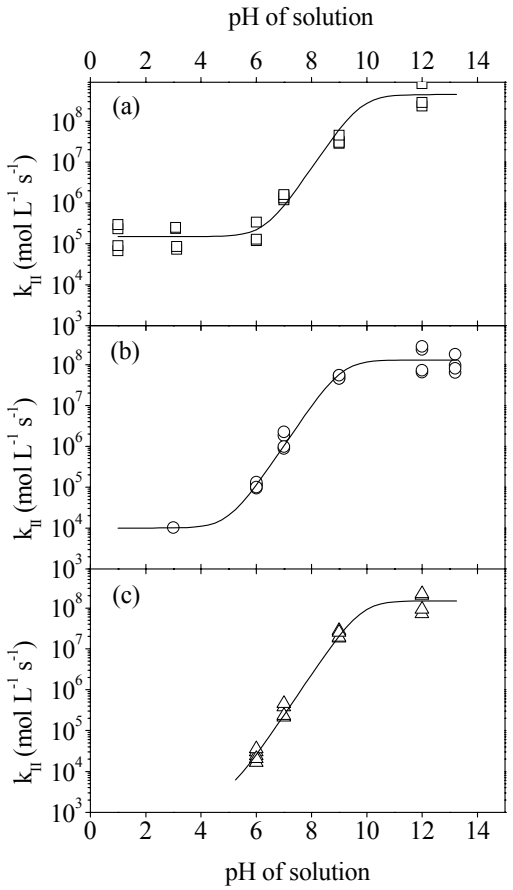

Figure 4: Overall aqueous phase second order rate constant of NO_2 with ArOH solution plotted as a function of pH. Squares, circles, triangles refer to syringol, catechol, guaiacol, respectively. The solid lines were obtained by fitting equation (14) to the measured data..

(5) to the observed loss curves showed some deviation from the behaviour expected for a simple first order loss process at the surface.

An obvious factor strongly affecting the uptake coefficient is the pH of the solutions. Increasing the pH led to higher uptake coefficients, as this was previously reported for other compounds. This is due to the increasing fraction of the more reactive deprotonated species at higher pH. To include the acid-base equilibria in the second order rate constant, k_X^{II} can also be expressed as a superposition of the rate constants of the neutral and deprotonated species, respectively:

$$k_X^{II} = (1 - \theta_{X1}) \cdot k_{X1} + \theta_{X1} \cdot k_{X2} \qquad (10)$$

Θ_X denotes the fraction of X, which is deprotonated at a given pH (see Table 1 for published pK values). Knowing the values of pK_a for the acids, the relative amount θ_{Ξ^-} of the singly dissociated species at a certain pH can be calculated using the Henderson-Haselbalch formula:[*Albert et Serjeant*, 1984]

.

$$\theta_1 = \frac{1}{1+10^{(pK_{a1}-pH)}} \qquad (11)$$

Equation (10) was used to fit the k^X_{II} values as a function of pH with k_X^1, k_X^2 and pK_X as adjustable parameters.

k_X^{II} values obtained from the measured uptake coefficients are plotted in Figure 4. The reactivity obviously follows deprotonation as a function of pH due to the orders of magnitude higher reactivity of the deprotonated species than the neutral species. The solid lines in Figure 4 are a fit of equation 10 to the measured data. The data at lowest and highest pH allowed to constrain mostly k_{X1} and k_{X2}, respectively, whereas the data at intermediate pH are most sensitive to the pK_X value. The results are given in Table 1. The pK values are clearly in agreement with previously reported values. The rate constants for the monoanions are also in the range of those few structurally similar species already reported in the literature, which are summarized in Table 1 one for comparison.

Conclusions and atmospheric implications

Using the wetted wall flowtube technique, the uptake rates and liquid phase kinetics of catechol, syringol and guiacol with NO_2 were investigated over the pH range 1 to 13 and for different initial reactant concentrations. These substances serve as reactants in the reduction of NO_2 to nitrite, which is the liquid phase base associated to atmospheric nitrous acid. The results were interpreted using a simple model taking into account the deprotonation of these three weak organic acids. The present results might serve as input into atmospheric box model aiming at assessing the importance of heterogeneous HONO formation due to semi-volatile organic compounds as postulated in one of our recent studies.[*Arens et al.*, 2002] Also these kinetics support the outcomes of an exploratory study by Lahoutifard et al. [*Lahoutifard et al.*, 2002], where a multiphase model was applied to simulate the chemistry of dissociated hydroxyl-substituted aromatics occurring in liquid aerosol particles, in the early morning, under polluted conditions. That chemistry produces nitrite ions in the liquid phase with kinetics (that were almost missing at the time of their study), which, depending on the pH, may lead to HONO out-gassing. The strength of this source was explored, and it was shown that it leads to HONO even for very dilute liquid droplets under moderate acidic conditions, and increases in importance when the aromatic content of the droplets is increased. The influence of these reactions on daytime photochemistry is still minor with a notable impact only at heavily polluted locations or in biomass burning plumes, in which the title compounds may represent about 1 % of water soluble organic aerosol mass [*Graham et al.*, 2002]. On the other hand, structurally similar compounds are also present in the soil water with concentrations in the 10mg/l (10^{-4} M) range at typical soil water pH of 4 to 5 [*Gallet et Keller*, 1999]. Uptake coefficients of NO_2 into such an aqueous phase of 10^{-6} seem reasonable (see Figure 3) and by far exceed that for the heterogeneous hydrolysis of NO_2. It remains to be investigated to what degree the non-aqueous soil fraction contributes to this chemistry as these phenolic species may also occur in adsorbed form on minerals and humic acids, or form even part of the latter [*Tan*, 2003]. Some insight into this may be derived from the study by Arens et al. [*Arens et al.*, 2002] on solid 1,2,10-trihydroxyanthracene, on which HONO formation scaled with the relative humidity with uptake coefficients also in the 10^{-6} range.

Acknowledgement

The support by the French program PRIMEQUAL2 for the project SHONO and by the Swiss National Science Foundation are gratefully acknowledged

[#] N*ow at Université de Provence, TRACES, Centre de Saint Jérôme, Case 512, 13397 Marseille cedex 20, France. Tél.: (+33) (0)4 91 28 89 00, E-mail : Rafal.Strekowski@up.univ-mrs.fr*

References

1 K. H. Tan *Humic matter in soil and the environment: principles and controversies*; Marcel Dekker, Inc: New York, Basel, 2003.

2 A. Hoffer; Kiss, G.; Blazso, M.; Gelencser, A. *Geophysical Research Letters,* 2004, **31**, art. no.

3 W. F. Rogge; Hildemann, L. M.; Mazurek, M. A.; Cass, G. R.; Simoneit, B. R. T. *Environ. Sci. Technol.,* 1998, **32**, 13.

4 O. L. Mayol-Bracero; Guyon, P.; Graham, B.; Roberts, G.; Andreae, M. O.; Decesari, S.; Facchini, M. C.; Fuzzi, S.; Artaxo, P. *Journal of Geophysical Research-Atmospheres,* 2002, **107**, art. no.

5 B. Graham; Mayol-Bracero, O. L.; Guyon, P.; Roberts, G. C.; Decesari, S.; Facchini, M. C.; Artaxo, P.; Maenhaut, W.; Koll, P.; Andreae, M. O. *Journal of Geophysical Research-Atmospheres,* 2002, **107**, art. no.

6 B. R. T. Simoneit; Schauer, J. J.; Nolte, C. G.; Oros, D. R.; Elias, V. O.; Fraser, M. P.; Rogge, W. F.; Cass, G. R. *Atmos. Environ.,* 1999, **33**, 173.

7 L. M. McKenzie; Hao, W. M.; Richards, G. N.; Ward, D. E. *Environmental Science & Technology,* 1995, **29**, 2047.

8 C. Gallet; Keller, C. *Soil Biology & Biochemistry,* 1999, **31**, 1151.

9 Z. B. Alfassi; Huie, R. E.; Neta, P. *J. Phys. Chem.,* 1986, **90**, 4156.

10 J. L. Miao; Wang, W. F.; Pan, J. X.; Lu, C. Y.; Li, R. Q.; Yao, S. D. *Radiation Phys. Chem.,* 2001, **60**, 163.

11 Z. Zhan; Yao, S.; Lin, W.; Wang, W. F.; Jin, Y.; Lin, N. *Free Rad. Res.,* 1998, **29**, 13.

12 J. Kleffmann; Becker, K. H.; Wiesen, P. *Journal of the Chemical Society Faraday Transactions,* 1998, **94**, 3289.

13 J. Baker; Ashbourn, S. F. M.; Cox, R. A. *Physical Chemistry Chemical Physics,* 1999, **1**, 683.

14 R. M. Harrison; Peak, J. D.; Collins, G. M. *Journal of Geophysical Research,* 1996, **101**, 14429.

15 B. Aumont; Chervier, F.; Laval, S. *Atmospheric Environment,* 2003, **37**, 487.

16 J. Kleffmann; Kurtenbach, R.; Lörzer, J.; Wiesen, P.; Kalthodd, N.; Vogel, B.; Vogel, H. *Atmospheric Environment,* 2003, **37**, 2949.

17 B. Vogel; Vogel, H.; Kleffmann, J.; Kurtenbach, R. *Atmospheric Environment,* 2003, **37**, 2957.

18 L. Gutzwiller; George, C.; Rössler, E.; Ammann, M. *J. Phys. Chem. A,* 2002, **106**, 12045.

19 N. Lahoutifard; Ammann, M.; Gutzwiller, L.; Ervens, B.; George, C. *Atmospheric Chemistry and Physics,* 2002, **2**, 215.

20 P. V. Danckwerts *Gas-Liquid Reactions*; McGraw-Hill: New York, 1970.

21 D. M. Murphy; Fahey, D. W. *Analytical Chemistry,* 1987, **59**, 2753.

22 D. R. Hanson; Ravishankara, A. R. *Geophys. Res. Lett.,* 1995, **22**, 385.

23 V. Scheer; Frenzel, A.; Behnke, W.; Zetzsch, C.; Magi, L.; George, C.; Mirabel, P. *J. Phys. Chem. A,* 1997, **101**, 9359.

24 S. Fickert; Helleis, F.; Adams, J. W.; Moortgat, G. K.; Crowley, J. N. *J. Phys. Chem. A,* 1998, **102**, 10689.

25 B. J. Finlayson-Pitts; Pitts, J. N. *Chemistry of the Upper and Lower Atmosphere: Theory, Experiments and Applications*; Academic Press: San Diego, 2000.

26 R. S. Strekowski; George, C. *submitted to J. Chem. Eng. Data,* 2005.

27 D. O. Cooney; Kim, S.; Davis, E. J. *J. Chem. Eng. Sci.,* 1974, **29**, 1731.

28 W. Behnke; Krüger, H. U.; Scheer, V.; Zetzsch, C. *J. Aerosol Sci.,* 1992, **S23**, 933.

29 W. Behnke; George, C.; Scheer, V.; Zetzsch, C. *J. Geophys. Res.,* 1997, **102**, 3795.

30 S. S. Brown; Wilson, R. W.; Ravishankara, A. R. *Journal of Physical Chemistry A,* 2000, **104**, 4976.

31 J. L. Cheung; Li, Y. Q.; Boniface, J.; Shi, Q.; Davidovits, P.; Worsnop, D. R.; Jayne, J. T.; Kolb, C. E. *J. Phys. Chem. A,* 2000, **104**, 2655.

32 C. E. Kolb; Worsnop, D. R.; Zahniser, M. S.; Davidovits, P.; Hanson, D. R.; Ravishankara, A. R.; Keyser, L. F.; Leu, M. T.; Williams, L. R.; Molina, M. J.; Tolbert, M. A. Laboratory Studies of Atmospheric Heterogeneous Chemistry; Current Problems in Atmospheric Chemistry. In *Advances in Physical Chemistry Series*; J. R. Barker, Ed.; World scientific, Singapore, 1994; Vol. 3.

33 J. L. Cheung; Li, Y. Q.; Boniface, J.; Shi, Q.; Davidovits, P.; Worsnop, D. R.; Jayne, J. T.; Kolb, C. E. *J. Phys. Chem. A,* 2000, **104**, 2655.

34 L. G. Forni; Mora-Arellano, V. O.; Packer, J. E.; Willson, R. L. *J. Chem. Soc. Perkin Trans.,* 1986, **II**, 1.

35 A. Albert; Serjeant, E. P. *The Determination of Ionization Constants*; Chapman and Hall: London and New York, 1984.

36 F. Arens; Gutzwiller, L.; Gaggeler, H. W.; Ammann, M. *Physical Chemistry Chemical Physics,* 2002, **4**, 3684.

.

C George, R S Strekowski , J Kleffmann, K Stemmler et M Ammann, Photoenhanced Uptake of Gaseous NO_2 on Solid Organic Compounds: A photochemical source of HONO, *Faraday Discuss.*, 130, 195, 2005.

Photoenhanced Uptake of Gaseous NO_2 on Solid Organic Compounds: A photochemical source of HONO

C George [a]*, R S Strekowski [a(#)], J Kleffmann [b], K Stemmler [c] and M Ammann [c]

[a] *Laboratoire d'Application de la Chimie à l 'Environnement (UCBL-CNRS) 43 boulevard du 11 Novembre 1918, F-69622 Villeurbanne, France. Fax:+33 (0)4 72 44 8114; Tel: +33 (0)4 72 43 1489, E-mail: christian.george@univ-lyon1.fr*

[b] *Physikalische Chemie/FB C, Bergische Universität Wuppertal, 42097 Wuppertal, Germany. Fax:+49 202 439 2505; Tel: +49 202 439 3534, E-mail: kleffman@uni-wuppertal.de*

[c] *Labor für Radio- und Umweltchemie, Paul Scherrer Institut, 5232 Villigen, Switzerland. Fax:+41 56 310 4435; Tel: +41 56 310 4049, E-mail: markus.ammann@psi.ch;konrad.stemmler@psi.ch.*

***This submission was created using the RSC Article Template* (*DO NOT DELETE THIS TEXT*)**
(*LINE INCLUDED FOR SPACING ONLY - DO NOT DELETE THIS TEXT*)

In several recent field campaigns the existence of a strong daytime source of nitrous acid was demonstrated. The mechanism of this source remains unclear. Accordingly, in the present laboratory study, the effect of light (in the range 300-500nm) on the uptake kinetics of NO_2 on various surfaces taken as proxies for organic surfaces encountered in the troposphere (as organic aerosol but also ground surfaces) was investigated. In this collaborative study, the uptake kinetics and product formation rate were measured by different flow tube reactors in combination with a sensitive HONO instrument. Uptake on light absorbing aromatic compounds was significantly enhanced when irradiated with light of 300 – 420 nm, and HONO was formed with high yield when the gas was humidified. Especially organic substrates containing a combination of electron donors, such as phenols, and of compounds yielding excited triplet states, such as aromatic ketones, showed a high reactivity towards NO_2. Adding a stronger absorber, such as 4-benzoylbenzoate, further enhanced the reactivity of the substrate. Based on the results reported a mechanism is suggested, in which photosensitised electron transfer is occurring. The results show that HONO can be efficiently formed during the day in the atmosphere at much longer wavelengths compared to the recently proposed nitrate photolysis.

Introduction

Since the initial detection of nitrous acid (HONO) in the atmosphere by Perner and Platt [*Perner et Platt*, 1979], many studies have shown that nitrous acid may accumulate during night-time before undergoing photolysis in the early morning:

$$HONO + h\nu \rightarrow NO + OH \qquad (1),$$

which creates an important morning OH radical burst [*Harris et al.*, 1982; *Harrison et al.*, 1996b]. In recent studies[*Alicke et al.*, 2003; *Alicke et al.*, 2002; *Aumont et al.*, 2003b; *Ren et al.*, 2003; *Vogel et al.*, 2003a; *Zhou et al.*, 2002a], a significant contribution of the HONO photolysis to the integrated OH yield of up to 60 % was calculated.. As both products of reaction (1) are key players in the processes leading to photochemical pollution, it is essential to understand and identify all sources of tropospheric nitrous acid.

Despite many studies, to date the formation mechanism of HONO in the atmosphere is still not completely understood. It appears that all gas phase reactions are too slow to explain night-time HONO formation [*Calvert et al.*, 1994]. In addition, direct emissions can only partly explain atmospheric HONO levels [9].[*Kurtenbach et al.*, 2001]. Accordingly, different heterogeneous formation pathways have been postulated. For example, it has been suggested that HONO is formed by the heterogeneous conversion of nitrogen dioxide (NO_2) on soot surfaces [*Ammann et al.*, 1998; *Gerecke et al.*, 1998]. However, recent studies demonstrated that this non-catalytic reaction cannot explain current HONO levels in the atmosphere [*Arens et al.*, 2001; *Kleffmann et al.*, 1999]. Based on correlation studies, it was proposed that the heterogeneous reaction of NO and NO_2 on particle surfaces is a significant atmospheric HONO source [*Calvert et al.*, 1994]. However, field studies [*Harrison et Kitto*, 1994] and a laboratory investigation in which the reaction was studied under humidity levels and NO_x concentrations prevailing in the atmosphere [*Kleffmann et al.*, 1998a] indicate that this reaction is unimportant. Laboratory studies have also proposed that the reaction of NO with adsorbed nitric acid (HNO_3) represents a potential HONO source [*Saliba et al.*, 2000], however, a recent study which was performed at atmospheric humidity levels and NO_y concentrations much lower than the ones used in all other studies, demonstrates that this reaction is too slow to be of importance in the atmosphere [*Kleffmann et al.*, 2004].

Although it is commonly proposed that HONO is mainly formed by heterogeneous processes during the night, i.e. by the conversion of NO_2 on humid surfaces [*Lammel et Cape*, 1996], the exact mechanism of the NO_2 conversion is still under discussion and remains unclear. In most studies, the following heterogeneous reaction was postulated [*Finlayson-Pitts et al.*, 2003]:

$$2\ NO_2 + H_2O \rightarrow HONO + HNO_3 \qquad (2)$$

On the other hand, in a recent study, the reaction of NO_2 with organics dissolved in aqueous solutions was proposed [*Gutzwiller et al.*, 2002a]. In an aqueous solution, NO_2 may undergo electron transfer reactions with phenoxide ions, which have been previously investigated for methylphenols and hydroxybenzenes [*Alfassi et al.*, 1986; *Gutzwiller et al.*, 2002b], catechins [*Miao et al.*, 2001] and hydroxycinnamic acid derivatives [*Zhan et al.*, 1998]. The most important reactant is the deprotonated species, the phenoxide ion, leading to strongly pH dependent overall kinetics. The primary reaction product is the corresponding phenoxy type radical and nitrite ion or HONO [*Gutzwiller et al.*, 2002b]. A similar mechanism was shown to occur on solid 1,2,10-trihydroxyanthracene, where HONO has

been observed as a primary product [*Arens et al.*, 2002]. The kinetics seem to be driven by the presence of adsorbed water associated with this sparingly soluble compound, and the reaction rates remain relatively low, possibly due to the very small tendency of this weak acid to form the phenoxide ion under the experimental conditions employed.

These phenolic compounds are ubiquitously present in the environment. Hydroxybenzenes may be formed as intermediates in the photooxidation of aromatic compounds in the gas phase [*Atkinson*, 1994; *Olariu et al.*, 2000]. A variety of guaiacols, catechols and syringols are formed during combustion of biomass, mainly from lignin pyrolysis [*Fine et al.*, 2001; *Rogge et al.*, 1998]. Furthermore, the microbial decomposition of vegetation leads to a large number of polyphenols along with their acid and aldehyde derivatives at significant conentrations in the soil [*Gallet et Keller*, 1999].

The significance of the (dark) chemistry of NO_2 with these organic compounds in a polluted atmospheric aerosol heavily depends on the total amount of aromatics appearing in the aqueous phase and on aerosol pH [*Lahoutifard et al.*, 2002] and might be important in a biomass burning plume [*Ammann et al.*, 2004]. The significance in an aqueous or non-aqueous environment with a high content of these species combined with the presence of neutralizing minerals or organic acids, such as above soils, still needs to be investigated.

While the night time formation of HONO in the atmosphere may be reasonably well explained by direct emissions and heterogeneous conversion of NO_2 on ground surfaces with the different mechanisms mentioned above, measured concentrations significantly exceeded modelled values during the day [9]. Accordingly, a strong daytime source was postulated in recent studies to explain daytime concentrations of HONO over snow [e.g.][*Zhou et al.*, 2001], ground and vegetation surfaces [*Kleffmann et al.*, 2003b; *Vogel et al.*, 2003a; *Zhou et al.*, 2002a; *Zhou et al.*, 2003; *Zhou et al.*, 2002b]. The source strength of this daytime source was estimated to be 200-1800 pptv/h [*Ren et al.*, 2003; *Zhou et al.*, 2003] or to be ~20 times faster than all night-time sources of HONO [*Kleffmann et al.*, 2003b]. The photolysis of nitrate and/or nitric acid on surfaces was postulated to explain these high daytime concentrations of HONO [*Zhou et al.*, 2002a; *Zhou et al.*, 2003]. However, the exact mechanism of this photolytic HONO source still remains to be unanswered, e.g. the photolysis frequency of adsorbed HNO_3 was reported to be two orders of magnitude faster compared to the gas and the liquid phase, which is still unclear [*Ramazan et al.*, 2004; *Zhou et al.*, 2003]. In addition, in a recent study in a large simulation chamber, the photolysis of HNO_3/nitrate was excluded to explain the observed photolytic HONO formation [*Rohrer et al.*, 2004].

Therefore, we investigated the effect of light (in the range 300-500 nm) on the uptake kinetics of NO_2 on various surfaces taken as proxies for organic surfaces encountered in the troposphere. In this collaborative study, the uptake kinetics and product formation rates were measured using different flow tube reactors in combination with different analytical methods for NO_x and HONO detection. We will show that there is a substantial effect of light on the NO_2 uptake kinetics on organic surfaces and on the formation of nitrous acid.

Experimental

The heterogeneous interactions of gaseous NO_2 were studied on bulk surfaces by exposing different concentrations of gaseous NO_2 mixtures to selected solid organic films. The experimental approach is based on measuring the reactant gas concentration i.e., NO_2 gas, at the exit of a cylindrical flow reactor as a function of the distance (time) that the NO_2 gas is in contact with the solid organic surface. This flow tube method was used in two different configurations, one by coupling the reactor to a quadrupole mass spectrometer to detect NO_2 in the range of 10 to 100 ppm, and one by coupling a simpler version of the reactor

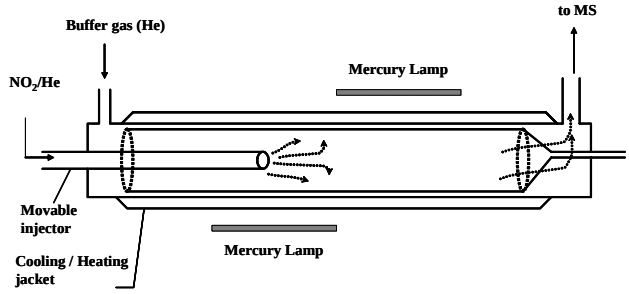

Figure 1. Schematic representation of the horizontal wall flow tube experimental approach used to measure the uptake of NO_2 on solid organic films.

to the LOPAP instrument (LOPAP: Long Path Absorption Photometer) and a chemiluminescence detector to detect HONO and NO_X in the lower ppb range.

a) Horizontal Coated Wall Reactor with MS Detection

The horizontal flow tube approach used in this study (see Figure 1) is similar to the one used in previous studies of heterogeneous reactions[*Hanson et Lovejoy*, 1996; *Lovejoy et al.*, 1995]. However, the horizontal reactor used in this work has been adapted with two UV lamps to study the effect of irradiation on the uptake of NO_2 gas on organic surfaces and the possible generation of nitrous acid (HONO). This point is discussed further in the section below.

A Pyrex tube with an internal volume of approximately 80 cm^3 and an inner diameter of 1.5 cm (S/V = 2.7 cm^{-1}) was used in all experiments. The cell was maintained at a constant temperature (±0.5 K) using a Huber CC130 thermostatically controlled bath by circulating a 1:1 ethanol+methanol mixture through the outer jacket. A Type J thermocouple (OMEGA Engineering, Inc.) with a stainless steel jacket was inserted into the reactor through a vacuum seal, allowing measurement of the temperature under precise experimental conditions employed. The geometry of the flow tube reactor was such that it allowed for the helium carrier and the reactant flows to enter at one end and the quadrupole mass spectrometer to be located downstream at the opposite end.

All experiments were carried out at atmospheric pressure with the linear flow rate through the reactor in the range 3 to 10 cm s^{-1}. The flow tube was mounted horizontally and the organic layer was contained within the inner flow tube. In certain experiments, water vapour was added to the carrier He gas upstream to control the humidity. All experiments were performed under atmospheric pressure and the temperature range was T=278 K to 308 K. The reactant NO_2 gas was introduced into the reactor via a 0.635 cm o.d. and 50 cm long movable, Pyrex injector equipped with a fritted end. The gas phase NO_2 reactant was monitored directly (i.e., the reactant gas was introduced directly into the differentially pumped chamber without any pre-treatment or pre-concentration) using a quadrupole mass spectrometer. The molecular mass signal of the NO_2 reactant gas (m/z= 46) was monitored.

The uptake coefficients for NO_2 were determined by measuring the quantity of the NO_2 reactant gas absorbed by the organic film [*Danckwerts*, 1970a; *Hanson et Lovejoy*, 1996]. The trace gas loss in the flow tube can be measured as a function of the position (distance) of the movable inlet tube (injector) i.e., as a function of the gas / solid exposure time t. The maximum length l of the interaction zone (maximum length that the injector could be retracted) was about 30 cm. As shown in equation (I) below,

the measured loss rate can be interpreted in terms of a first order process with respect to the gas phase concentration of the reactant.

$$\frac{n-\Delta n}{n} = \exp\left[-k_w t\right] \quad (I)$$

In equation (I) t is the average carrier gas residence time and k_w is the first order rate coefficient for the reaction at the film surface. The first order rate coefficient k_w is related to the uptake coefficient by

In equation (II), r_{tube}, γ, and <c> are the flow tube radius, uptake coefficient and average molecular velocity, respectively.

Initial concentrations of each component in the reaction mixture were determined from measurements of the appropriate mass flow rates, vapour pressure, and the total pressure. The mass flow rates were determined using Brooks electronic mass flow meters which had ranges of 20 to 1000 standard cm^3 min^{-1} (SCCM). The NO_2/He standard mix and the He buffer gas were allowed to flow directly from their high pressure storage tanks. Water vapour was added by bubbling the helium gas through a flask containing deionized H_2O.

Two mercury HPK lamps (Cathodeon), with an arc length of about 5 cm were mounted parallel above and below the horizontal reactor. The two lamps were about 3 cm, away from the thermostated pyrex flowtube. These lamps and the flowtube were surrounded by an aluminium jacket in order to increase the homogeneity of the light inside the reactor.

The solid organic film was prepared using two complementary methods. In the first method, the organic solid was heated in an air tight flask while a small flow of nitrogen gas was allowed to pass through. Then, the organic vapour carried by the nitrogen carrier was "injected" using Teflon tubing and deposited directly on the colder insert (see Figure 1) inner surface. In the second method, a known quantity of the organic was dissolved in methanol. Then, a 5 ml aliquot of the organic+methanol solution was placed inside the rotating insert. The insert was then dried by allowing a small flow of nitrogen to pass through the tube.

b) Flow tube experiments with LOPAP and Chemiluminiscence NO_x Detector

Further investigations were performed at lower, atmospherically more relevant NO_2 concentrations in synthetic air by using the sensitive direct analysis of the produced HONO by a HONO-analyzer (Long Path Absorption Photometer: LOPAP; described below) or alternatively by an indirect detection of the produced HONO by means of a NO/NO_x-chemiluminescence detector (CLD, Ecophysics, model CLD77AM coupled to a molybdenum converter at 400°C reducing HONO and NO_2 to NO), in combination with a sodium carbonate denuder tube for removing HONO from the gas stream. This molybdenum converter/chemiluminescence detection system principally measures the NO_y-species NO, NO_2, and HONO with an equal analytical response. The sodium carbonate denuder tube (50 cm × 0.8 cm ID glass tube) may either be switched into the sampling line to measure the sum of the species NO and NO_2 or may be bypassed that the CLD signal accounts for the sum of the species NO, NO_2 and HONO. The HONO concentration can therefore be expressed as the difference of the CLD-signal without and with carbonate denuder in the sampling line[*Gutzwiller et al.*, 2002b]. The NO concentration can be obtained from the detector signal, when the molybdenum converter is bypassed.

The photoreactor employed was a 50 cm × 0.8 cm ID Duran glass tube installed in an air cooled lamp housing holding 7 fluorescence lamps in a circular arrangement surrounding the reactor tube. The lamps used are Phillips Cleo Compact tanning lamps (44 cm × 2.6 cm), which emit light as a continuous band in the 300-420 nm (λmax = 354 nm) spectral region (90 % of the light power) and in the discrete Hg-lines at 436 nm, 546 nm, and 578 nm (9.8 % of the light power). The spectral irradiance E(λ) reaching the reactor surface was measured with a LI-COR 1800 hemisperical, cosine corrected spectroradiometer. The total irradiance (250-800 nm) is 150 Watt m^{-2} at the reactor surface. The inner surface of the tubular flow reactor was coated with a film of organic compounds. This surface was sandblasted to prevent droplet formation during the coating procedure and could therefore reach a relatively homogeneous distribution of the organic test compound on the reactor walls. The organic coatings on the reactor wall were produced by gently drying 0.5 ml aliquots of solutions of the organic compounds (either

$$k_w = \frac{\gamma < c >}{2r_{tube}} \quad (II)$$

aqueous solutions or solutions in ethanol or dichloromethane; depending on the solubility of the solute) dispersed on the reactor walls in a nitrogen stream at room temperature.

The carrier gas flow (synthetic air) and the NO_2 addition, from a 959 ppb mixture in synthetic air (Carbagas AG, Switzerland), were controlled by mass flow controllers. Usually total flows rates of about 2.5 liters per minute at ambient pressure were used leading to gas residence times of about 0.5 seconds in the photoreactor. The reactor temperature was 30-32 °C during irradiation. The NO_2 concentrations were adjusted normally around 20 ppb, a typical average concentration found in the atmosphere in densely populated areas within Europe. All experiments were performed at about 20 % relative humidity. In order to prevent HONO eventually present in the NO_2-supply from entering the coated wall flow tube, an additional carbonate denuder was placed upstream of the flow reactor.

LOPAP instrument

For the measurement of nitrous acid (HONO) a new, very sensitive instrument (LOPAP: Long Path Absorption Photometer) was used, which is described in detail elsewhere [*Heland et al.*, 2001; *Kleffmann et al.*, 2002]. Briefly, HONO is sampled in a stripping coil by a fast chemical reaction and converted into an azo dye which is photometrically detected by long path absorption inside a special Teflon tube. During the measurements the instrument had an integrated time resolution of ~2.5 min and a detection limit of 5 pptV. Due to the two-channel concept of the instrument all tested interferences including the combined one of NO_2 and unknown semi-volatile diesel exhaust components [*Gutzwiller et al.*, 2002a] can be neglected [*Kleffmann et al.*, 2002]. In a recent intercomparison campaign with a DOAS instrument in which the same air masses were analysed for the first time, an excellent agreement was obtained [*Trick*, 2004] also during the day.

Reagents

The following organic test reagents were obtained from the commercial suppliers with the purity given below and used without further purification: 4-benzoylbenzoic acid (4-BBA, Fluka; ≥ 98%), perylene (PER, Fluka; ≥ 99%), 4-hydroxy-3,5-dimethoxy benzoic acid (syringic acid, SYR, Fluka; ≥ 97%), 3,7-dihydroxy-2-naphtoic acid (3,7-DHNA, Fluka; ≥ 95%), potassium iodide (Fluka; ≥ 99%), 3,4-dihydroxy-phenylacetic acid (3,4-DHPA, Fluka ; ≥ 98%), Catechol (Aldrich, 99%), anthracene (Aldrich, 99%), benzophenone (Aldrich, 99%), anthrarobin (Aldrich, 85%). The solvents used are analytical grade, and water was purified with a Millipore Milli-Q water system to a resistivity ≤0.054 μS cm^{-1}.

Results and Discussion

Uptake of NO_2 under dry and dark conditions

The uptake on bare glass was beyond the sensitivity of our horizontal coated wall reactor with MS detection, which means that the uptake coefficient was below the detection limit of a few times 10^{-7}. Only a physical adsorption was observed i.e., the surface exposed by the glass flow tube was rapidly covered and saturated by NO_2 molecules. At this stage, no more uptake occurred on this surface. As the surface could be exposed stepwise to gas phase NO_2, we could measure adsorption and desorption isotherms. By this we could observe a fully reversible uptake on the glass surfaces i.e., in the dark and at low relative humidity i.e., rh below 1%), there was no reaction on the bare glass surface.

The uptake of NO_2 in the dark was also studied on various pure organic surfaces i.e., on catechol, anthracene, benzophenone, anthrarobin.

As an example, the raw data during a NO_2 uptake experiment on a pure catechol surface is shown in Figure 2. When the organic surface was exposed to gaseous NO_2, we first observed a rapid decrease of the MS signal at m/z 46 (i.e., corresponding to the NO_2 molecular mass) which recovered to its original level within a few minutes. This timescale was of course depending on the actual flow rate used in the experiment and the NO_2 concentration. However, as the recovery of the MS signal was rapid, low flow rates, of about 150 mL min^{-1}, were typically used. Even under these conditions, the gas phase concentration of NO_2 first decreased and recovered very rapidly to its original level after exposure to an organic surface.

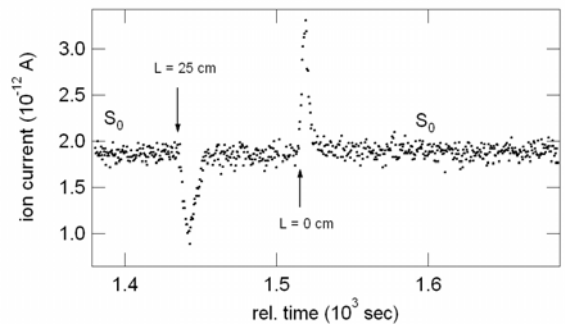

Figure 2. Typical NO_2 signal (m/z= 46) observed for the uptake of NO_2 gas on solid catechol under "dark" conditions. Experimental conditions are 0% RH; p=760 Torr; T=298 K; $[NO_2]_0$=4.9 x 10^{14} molecules cm^3. A decrease in the NO_2 signal is observed when the injector is moved back to L=25 cm. The signal is observed to recover to its original S_0 level within seconds. Once the inlet is moved all the way in (L=0 cm) so that the catechol surface is not exposed to the absorbent gas, the signal is observed to increase to greater than S_0 since the absorbed NO_2 gas desorbs from the catechol surface into the carrier gas and adds to the carrier gas.

This means that the organic surfaces were very rapidly saturated with NO_2 molecules, ason the bare glass surface. In our setup the NO_2 injector can be pulled back at its original position in which the organic surface is only flushed with the carrier gas (i.e., helium in these experiments). When this was done, we observed a rapid increase of the MS signal at m/z 46, which then decayed back to its original level. This corresponds to the desorption of physically adsorbed NO_2 molecules. By integrating the area below these peaks, we can determine the number of molecules being adsorbed or being desorbed. We observed that theses quantities are, within experimental uncertainty, equal which means again that under dry conditions, NO_2 only physically adsorbs on these pure organic surfaces (as on the bare glass tube but in slightly smaller amounts).

As NO_2 only physically adsorbs on these catechol surfaces, we were unable to determine any reliable uptake coefficients, which were below or too close to our detection limit of a few times 10^{-7}.

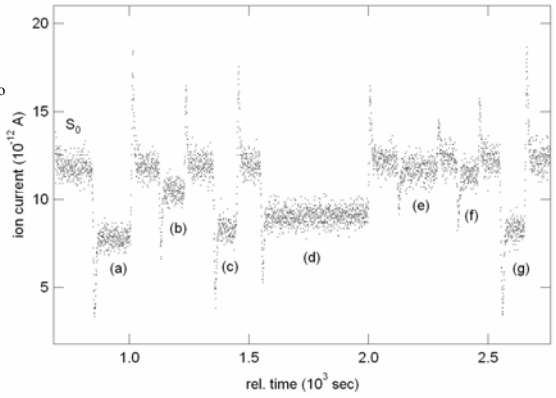

Figure 3. Typical NO_2 signal (m/z= 46) observed for the uptake of NO_2 gas on solid catechol in the presence of light. Experimental conditions are 0% RH, p=760 Torr and T=298 K. $[NO_2]_0$= 1 x 10^{15} molec. cm^3 ; injector length L (in cm) is (a) 32.5; (b) 13.8; (c) 26.0; (d) 19.8; (e) 6.5; (f) 10.5; (g) 33.8. γ = 2.1 x 10^{-6}

Similar observations have been made on a surface made of anthrarobin (1,2,10-trihydroxyanthracene) i.e., NO_2 only physically adsorbs on these surfaces with uptake coefficients, which were below or too close to our detection limit of a few times 10^{-7}.

On anthracene surfaces, we observed a similar behaviour but we observed also a small dark reaction. In this case, when NO_2 was exposed to the organic surface, its gas phase concentration rapidly decayed and then started to recover to its original level. However, with anthracene, NO_2 never reached again its initial concentration, within our experimental conditions, but reached a plateau which is an evidence that at long enough gas/solid contact times, the uptake is driven by a slow dark reaction. However, this was observed to slow down at long reaction times i.e., the plateau is not totally time independent, which means that there is a deactivation of the surface during the course of the experiment. Similar observations were made in the case of benzophenone, for which an uptake coefficient of 0.3×10^{-6} was determined. All results are summarised in Table I.

Humidity and dark chemistry

While all experiments described above were performed under dry conditions (i.e., rh < 1%), we observed that adding water vapour into the gas flow lead to an increased uptake of NO_2 by at least a factor of 3 when the humidity was increased to more than 40 %. And this was observed for all materials studied. It appears certainly that water adsorbs on our films changing the properties of the surfaces and its ability to react with NO_2. Visual inspection showed that some of the films deliquesced at high humidity. It seems clear that the total amount of water taken up into the film has an influence on its reactivity, as the presence of an aqueous phase could enhance the liquid phase mechanisms with NO_2 [*Arens et al.*, 2002; *Gutzwiller et al.*, 2002b]. However, also in this case a time dependent uptake was observed i.e., the surface was deactivated slowly with increasing reaction time, similar to the observations made by Arens et al. [*Arens et al.*, 2002] on solid anthrarobin.

Surface photochemistry

Figure 3 shows the raw data for an uptake experiment on a catechol surface when the pyrex flowtube was irradiated by the output of the mercury lamps . This has to be compared with data shown in Figure 2 (corresponding experiment but in the dark). It is obvious that in the dark only physical adsorption is occuring while under irradiation the uptake of NO_2 is driven by a chemical reaction on the solid film. In fact, in this later case the uptake coefficient is no longer time dependent, as the NO_2 concentration, when exposed to the irradiated flowtube, decreases rapidly and reaches a plateau after a few seconds. Here the quantity of NO_2 that has reacted is depending "only" on the surface exposed to the gas phase. The uptake coefficient measured in this case is about 10^{-6} i.e., at least an order of magnitude larger than without light.

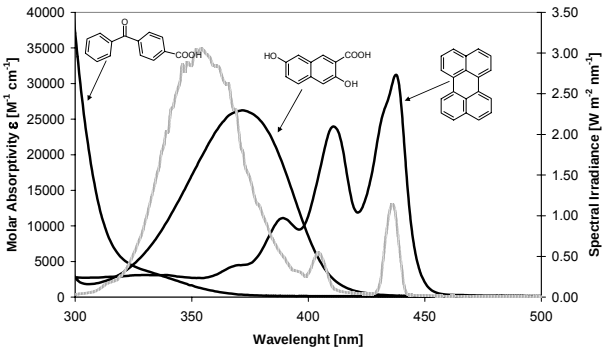

Fig. 4 Absorption spectra (molar absorptivities ε) of the investigated organic light absorbers 4-benzoylbenzoic acid (4-BBA), 3,7-dihydroxy-2-naphtoic acid (3,7-DHNA) and perylene (PER), overlaid with with the spectral irradiance of the light source (Philips Cleo Compact fluorescence lamps, grey line). 4-BBA and 3,7-DHNA are recorded in phosphate buffered aqueous solution (pH=7), PER is recorded in dichlormethane.

The light induced effects for the other organics are less pronounced but mainly visible through the removal of any time dependence in the uptake coefficient. The main effect of light was therefore to eliminate any sign of deactivation of the surfaces within the experimental time scales.

Not only the magnitude and time dependence of the uptake of NO_2 was increased under irradiation, we also observed MS-signals from a potential gas phase product. The observation is that both MS-signal traces for m/z= 30 (NO^+-ion) and m/z= 46 (NO_2^+-ion) are well correlated in the presence of unreacted NO_2 at varying concentrations. However, when NO_2 was reacted with irradiated organic films the signal at m/z= 30 rose, whereas the sinal at m/z= 46 decayed. This was interpreted as a product signal that was interfering with the signal of mass 30, whereas mass 46 was not influenced. Potential reaction products showing mass signals at m/z=30 are NO (from a surface photolysis of NO_2) or HONO (from reduction of NO_2).

To determine if the product formed was HONO or NO, we inserted a sodium carbonate coated trap in the gas line between the flow tube and the MS that would remove any traces of HONO from the gas phase. With the trap in-line, the mass 30 follows mass 46 which can be taken as an indirect evidence that HONO is photochemically formed during the interactions of NO_2 and the various organics films. Note however, that the production of HONO was only observed when the gas was humidified.

It is however very difficult from these experiments to draw any conclusions about the reaction mechanism simply because we are unable to distinguish between photochemistry of adsorbed NO_y species and photochemistry involving the organic compounds. Aditionally these experiments were performed at higher NO_2 concentrations than typically found in atmospheric environments.

While the experiments with mass spectrometric detection revealed that HONO might be a product of a photoenhanced reaction of NO_2 with the organic species investigated, further experiments were performed with specific and sensitive HONO detection, at low concentrations of NO_2. Three different types of light absorbing organic species have been investigated. These are 4-benzoylbenzoic acid (4-BBA) and its sodium salt, 3,7-dihydroxy-2-naphtoic acid (3,7-DHNA) and perylene (PER). 4-BBA is an analogue of benzophenone, bearing an extra organic acid substituent. This compound has been used instead of benzophenone, as it is less volatile and therefore the produced films are more stable during the experiments. 4-BBA was selected as it is known to form excited triplet states in high yields when irradiated in the UV-A spectral region in benzene and in water containing solutions [*Inbar et al.*, 1981; *Murov S. L*,

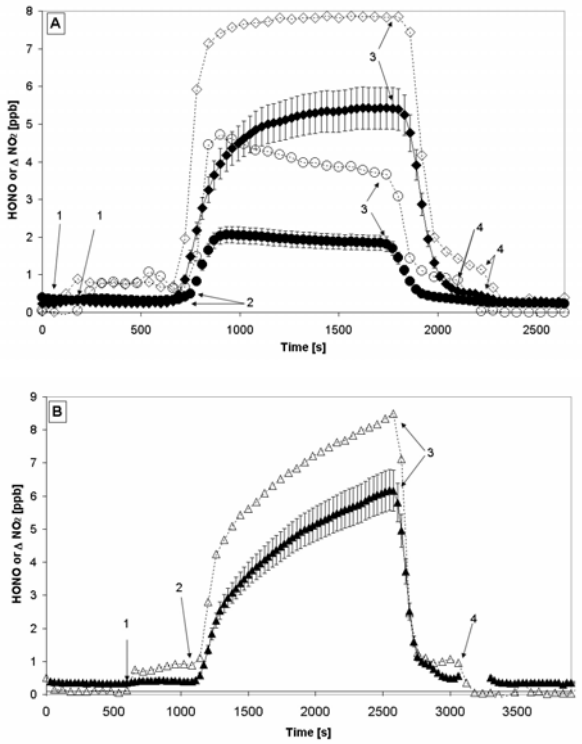

Fig. 5 Concentration of the reaction product HONO and change of the NO_2 concentration during irradiation (300-420 nm) of organic films. Results from three different experiments are shown. **Panel A:** An experiment where a film of 4-benzoyl-benzoate sodium salt (1 mg on 125 cm^2 sandblasted Duran glass) is irradiated (filled circles: HONO concentration; empty circles: loss of NO_2, i.e. $NO_2(t=0)$-$NO_2(t)$) and an experiment where a mixed film of 4-benzoyl-benzoate sodium salt (1 mg on 125 cm^2 glass surface) and syringic acid (0.5 mg on 125 cm^2 glass surface) is irradiated (filled diamonds: HONO concentration; empty diamonds: loss of NO_2, i.e. $NO_2(t=0)$-$NO_2(t)$). **Panel B:** An irradiation of 3,7-dihydroxy-2-naphtoic acid (1 mg on 125 cm^2 glass surface; filled triangles: HONO concentration; empty triangles: loss of NO_2, i.e. $NO_2(t=0)$-$NO_2(t)$).

The numbers given in the figures represent the following steps in the course of the experiments: (1) The coated reactor was switched into the NO_2 stream ($NO_2(t=0)$= 19 ppb); (2) the light source (300-420 nm) was switched on; (3) the light source was switched off; and (4) the coated reactor was removed from the NO_2 stream.

1993]. Contrary PER was selected as a mechanistical probe molecule, as it has a high fluorescence quantum yield in benzene solutions or alcohol solutions and hardly forms excited triplet states [*Melhuish*, 1961; *Murov S. L*, 1993; *Parker et Joyce*, 1966]. However, in our experiments these absorbers are investigated as pure organic films, which were exposed to humid air (relative humidity of about 20%), therefore the triplet and fluorescence yields of the absorbers may be significantly altered from those reported in the literature for benzene or aqueous solutions. A third UV-A absorbing species 3,7-DHNA was chosen, as hydroxylated aromatic compounds are known to react with NO_2 in aqueous solution or on wetted surfaces to form nitrite ions and aryloxy radicals in a dark reaction [*Alfassi et al.*, 1986; *Ammann et al.*, 2004; *Arens et al.*, 2002; *Gutzwiller et al.*, 2002b]. Our aim was to test if this reaction could be enhanced in presence of light. In Figure 4 the absorption spectra of the three compounds are shown in comparison with the spectral irradiance measured at the reactor surface.

Two additional model compounds m 3,4-dihydroxyphenylacetic acid (3,4-DHPAA) and 4-hydroxy-3,5-dimethoxybenzoic acid (syringic acid, SYR) were selected as electron donors. Both compounds are electron donor substituted phenols, which are on

the one hand capable to reduce NO_2 in aqueous solutions [*Ammann et al.*, 2004] and which on the other hand can reduce photochemically excited triplet states of aromatic ketones, such as 4-BBA [*Canonica et al.*, 1995; *Das et Bhattacharyya*, 1981; *Das et al.*, 1981]. Both compounds hardly absorb light in the

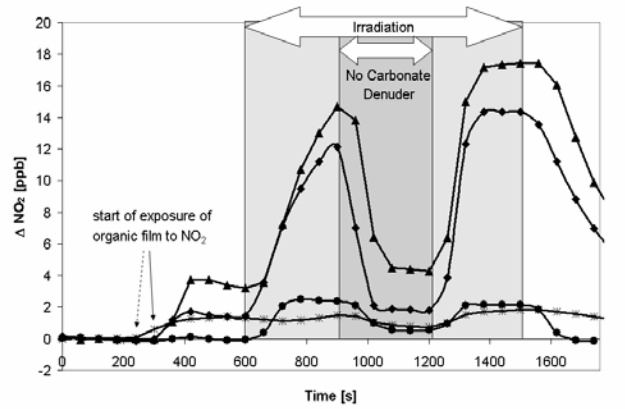

Figure 6: Change of the NO_2 concentration during irradiation (300-420 nm) of different organic films. The displayed unit Δ NO_x is the loss of NO_x in the coated wall reactor and in the carbonate denuder (i.e. $NO_x(t=0)$-$NO_x(t)$). The figure illustrates the steps of a typical experiments using the carbonate denuder technique for the CLD-detection of NO_2 and HONO. At time 300 s the coated wall reactor was switched into a stream of NO_2 in synthetic air (20 ppb). At time 600 s the reactor is illuminated until time 1500 s. At times 900 s to 1200 s the carbonate denuder preventing HONO from entering the CLD detector is bypassed. The concentration steps starting at the times 900 s and 1200 s are a indirect measure of the HONO concentration in the reactor effluent. Results from four different experiments are shown: (•) Exposure of a film of 4-benzoylbenzoic acid (1 mg per 125 cm^2 surface); (*) Exposure of a film of 3,4-dihydroxyphenylacetic acid (1 mg per 125 cm^2 surface); (▲) Exposure of a internally mixed film of 4-benzoylbenzoic and 3,4-dyhydroxyphenylacetic acid (1 mg and 0.5 mg per 125 cm^2 surface, respectively); (♦) Exposure of a internally mixed film of 4-benzoylbenzoic and 3,4-dyhydroxyphenylacetic acid (1 mg of both compounds per 125 cm^2 surface).

spectral region above 300 nm. For comparison an inorganic electron donor, potassium iodide, was examined additionally.

In Table II the observation of the change of the NO_2 concentration and the formation of HONO have been summarized for the experiments with different organic films. All experiments have been performed at a relative humidity of about 20 % in synthetic air at atmospheric pressure.

Figure 5 shows the concentration evolution of NO_2 and HONO during a typical experiment, where NO_2 was measured with the chemiluminescence detector and HONO was measured with the long path absorption photometer (LOPAP).

It is obvious from Table II and Figure 5, that a significant depletion of NO_2 occurred on the organic substrate surfaces during irradiation. The direct measurement of gaseous HONO with the LOPAP-analyser clearly shows that a large fraction of NO_2 taken up was converted into HONO, in line with the experiments shown above and with an earlier study on dark reactions of NO_2 on anthrarobin (Arens et al., 2002). A small production of HONO was also observed during dark exposure of the organic films towards NO_2, but the HONO-yield increased by more than an order of magnitude during irradiation. It appears that the photochemical production of HONO is strongly dependent on the type of organic species examined. For perylene no photochemical production of HONO was observed, whereas 4-BBA and 3,7-DHNA are efficiently reacting with NO_2 and produced significant amounts of HONO during irradiation. From Figure 5 it can be seen that for 4-BBA the yield of HONO only accounts for roughly 50 % of the reacted NO_2. For 3,7-DHNA the observed gaseous HONO accounts for about 75 % of the reacted NO_2. As shown in Table II and discussed below for some mixed organic coatings containing 4-BBA nearly 100 % of the reacted NO_2 is converted into HONO.

Another difference between 4-BBA and 3,7-DHNA is that 4-BBA shows the highest reactivity at the beginning of the irradiation, whereas the reactivity of 3,7-DHNA increases during the course of an irradiation. Therefore it appears that 3,7-DHNA is converted into more reactive product species during the course of its photochemical degradation.

The model electron donors used in this study, SYR, 3,4-DHPAA, and potassium iodide, are able to react directly with NO_2 in a dark reaction yielding nitrite or nitrous acid. This can be seen clearly for the experiment with potassium iodide coating, where a considerable dark reaction occurred. However, the reaction was not significantly photoenhanced under our irradiation conditions. For the phenolic compounds, SYR and 3,4-DHPAA a slight HONO-production occurred upon irradiation. As these compounds are hardly absorbing under the given light conditions, this is somewhat surprising and might be related to impurities present in these compounds or on the reactor wall or to absorbing species formed during the exposure of the compounds to the NO_2/synthetic air mixture in the reactor.

Proposed reaction mechanism

Using the combination of a Pyrex flow tube and a mercury lamp, we are initiating photochemistry at wavelengths longer than 300 nm. Indeed, the triple Pyrex walled flow tube would have filtered out any wavelength shorter than 300 nm. In addition, the output of the lamp will be mainly around 366 nm. For the experiments illuminated with the Philips Cleo Compact Fluorescence lamps the spectral irradiance at the reactor surface has been measured (see Figure 4). Under the assumption of an isotropic radiation in the reactor (e.g. the flow tube is surrounded by 7 fluorescence lamps in a cyclic arrangement mounted in a reflecting aluminium box) the actinic flux in the reactor is estimated after the procedure of Madronich [*Madronich*, 1987] as four times the measured 2π-spectral irradiance, neglecting any influence of the glass reactor walls. Using the actinic flux derived this way and using the IUPAC recommendations for the cross-sections and quantum yields [*Atkinson et al.*, 2004], we would calculate the photolysis frequencies $J(NO_2)$ as 0.046 s^{-1}, J(HONO) as 0.011 s^{-1} and $J(HNO_3)$ as 1.8×10^{-6} s^{-1} for the respective gaseous species. For the aqueous nitrate ion, a somewhat higher photolysis frequency of $J(NO_{3\,aq}^-)= 2.5\times10^{-6}$ s^{-1} is expected based on the literature absorption spectra and quantum yields [*Graedel et Weschler*, 1981]. We also determined $J(NO_2)$ experimentally by the photolysis of NO_2 in air and the measurement of the reaction product NO as 0.024 ± 0.007 s^{-1}. Therefore, our model overestimates the actual actinic fluxes in the reactor by roughly a factor of 2, which might have resulted mainly from neglecting of absorbance and the light reflection of the Duran glass flow tube and the simplified representation of the radiation conditions in the reactor. Nevertheless, the calculated photolysis frequencies indicate that direct HNO_3/NO_3^- photolysis should be insignificant even when we would assume that 10 % of the initial NO_2 concentration would hypothetically react to HNO_3 in the dark and accumulate on the reactor wall and would then photo-dissociate with a hypothetical unity quantum yield to form HONO, as suggested by Ramazan et al. [*Ramazan et al.*, 2004]. In our experiments this explanation is likely not valid, as the reservoir of adsorbed HNO_3 would be too limited to explain the HONO-formation, is unlikely in our experiments, due to the multi-step soaking and rinsing procedure used to clean our reactors. In addition, it was clearly demonstrated that no nitrate is formed in the electron transfer reactions between hydroxylated aromatic compounds and NO_2 in the dark [*Arens et al.*, 2002]. This excludes nitrate formation on the organic substrates before irradiation.

The photolysis of gaseous NO_2 and HONO seems to be unimportant under the given flow tube conditions (0.5 s residence time). This is in agreement with our finding that NO is not produced in significant amounts in our experiments.

No significant photoenhancement of the reaction of NO_2 with the clean glass surface was observed under humid conditions, in good agreement with previous studies, which showed that reaction (2) is not photoenhanced [*Ramazan et al.*, 2004; *Rohrer et al.*, 2004]. Due to the fact that the mechanism operated down to very low concentrations of NO_2, the involvement of N_2O_4 (and subsequent photochemistry) is unlikely.

The stoichiometry of the formation of HONO from NO_2 in the 4-BBA photosensitized reaction (see Table II) with a HONO yield up to 100 % shows that the reaction cannot be explained as a catalysed disproportionation of NO_2 on wet surfaces (equation 2, see introduction) as soon as suitable electron donors are present in the system, Therefore, the primary electron donor must be a constituent of the organic films.

From the data presented in Table I and II and Figures 5 and 6 it appears that NO_2 is transformed in an efficient and coating specific photoreaction on organically coated glass surfaces. Very reactive coatings were obtained from 4-BBA, especially when it was mixed with an electron donor, such as a phenolic compound. In the given experiments the light is primarily absorbed by 4-BBA and therefore we suggest a mechanism, where this benzophenone derivate acts as a photosensitizer for the reduction of NO_2. The proposed reaction mechanism is depicted in Figure 7. It is based on the findings from photochemical experiments in solution [*Das et Bhattacharyya*, 1981; *Das et al.*, 1981; *Murov S. L*, 1993], which conclude that the photoexcitation of benzophenones produces excited triplet states of benzophenone in near unity yield. These triplet states act as one electron oxidants and react with electron donor substituted phenols in near diffusion controlled rates [*Baraltosh et al.*, 1984; *Canonica et al.*, 2000; *Canonica et al.*, 1995]. The resulting products are phenoxy radicals and reduced benzophenones (diphenyl ketyl radicals). Therefore this photosensitized reaction generates reactive radical intermediates which are thought to be reactive towards NO_2. The ketyl radical of benzophenone is a short lived reductant, which is generally assumed to react with dissolved oxygen in aerated aqueous solution experiments [*Canonica et al.*, 2000; *Gorman et Rodgers*, 1986] to form O_2^-/HO_2 radicals. Such reaction systems have been investigated by Anastasio et al. [*Anastasio et al.*, 1997], who irradiated mixtures of aromatic ketones and aldehydes in dilute aqueous solution. They observed a distinct formation of H_2O_2, when phenolic compounds were added to the solution of the aromatic ketone photosensitizers, and proposed that H_2O_2 is formed from the disproportionation of O_2^-/HO_2 radicals resulting from the reaction of the intermediate ketyl radicals with oxygen (equations 3 and 4).

$$PhOH + O_2 \xrightarrow{\text{sensitizer}+h\nu} PhO\bullet + HO_2 \qquad (3)$$

$$2HO_2 / O_2^- \rightarrow H_2O_2 + O_2 \qquad (4)$$

The aromatic photosensitizer molecules were only slowly consumed in the reactions and acted therefore as photocatalysts mediating the reduction of oxygen by phenols. However the yields of H_2O_2 were lower by a factor of 2.5 than expected from the given mechanism and the oxidation rate of the phenols. This indicates that dissolved O_2 might not be viewed as the sole possible final electron acceptor in such reaction systems. As indicated in Figure 7 beneath oxygen also organic constituents and in our case NO_2 could act as final electron acceptors. It also seems possible, that NO_2 can be reduced by the intermediate HO_2/O_2^-radical produced from reaction (3), as both reactions (5) and (6) [*Lögager et Sehested*, 1993]

$$O_2^- + NO_2 \rightarrow O_2NOO^- \qquad (5)$$

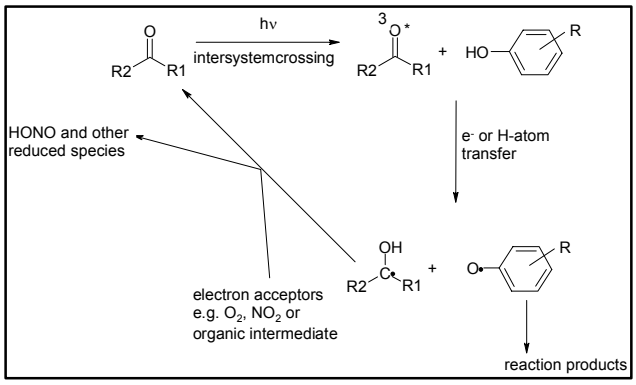

Figure 7: Proposed reaction mechanism for the photoreduction of NO_2 to HONO in the presence of 4-BBA (absorbing

$$k(5)= 4.5\times10^9\ M^{-1}\ s^{-1}$$

$$HO_2 + NO_2 \rightarrow O_2NOOH \qquad (6)$$

$$k(6)= 1.8\times10^9\ M^{-1}\ s^{-1}$$

are significantly faster than the disproportionation reactions of HO_2/O_2^- over the whole pH range, but it is not clear how fast the reaction products the peroxynitric acid/peroxynitrate decay into $HONO/NO_2^-$ and O_2 under our reaction conditions, as in aqueous solution only the deprotonated form (pK_a= 5.85) decayed rapidly (lifetime τ= 1 s)[Logager and Sehested, 1993]. Therefore, we propose that NO_2 is reduced in the present system by reductants produced during the photosensitized oxidation of phenols. These reductants might be the ketyl radical formed from 4-BBA, the superoxide/hydroperoxyl radical formed from the reaction of the ketyl radical with oxygen or reduced intermediates stemming from subsequent reactions of the ketyl radicals with organic constituents (phenol degradation intermediates) present in the organic films.

The experiments employing iodide as the electron donor were conducted to investigate an alternative route to produce the ketyl radical of 4-BBA. [*Hurley et al.*, 1988; *Loeff et al.*, 1993]. Iodide reacts with excited triplets of 4-BBA in a near diffusion controlled rate to form a charge-transfer exciplex which can react (in presence of high concentrations of iodide) with an additional iodide ion and subsequently dissociate into the ketyl radical and a diiodide ion (equation 7 and 8).

$$4-BBA + I^- \xrightarrow{h\nu} {}^3[4-BBA^-I] \qquad (7)$$

$${}^3[4-BBA^-I] + I^- \rightarrow 4-BBA^- + I_2^- \qquad (8)$$

The results from these experiments (Table II) show that the phototransformation of NO_2→ HONO is also effective, when the electron donor is not a phenolic compound. This indicates that neither radical oxidation intermediates of the phenols nor products of the phenolic oxidation (for example quinones) are necessary for the photoreduction of NO_2→HONO. This is a strong indication that the diphenylketyl radical (protonated and/or deprotonated form) is a key species in the reduction of NO_2. Furthermore, the experiment with iodide showed that energy transfer reaction between triplet 4-BBA and the probe phenols in the ground state (equation 9) is not essential in the reaction system. This type of energy transfer reaction might occur if the lowest triplet state energy of the phenols is lower than that of 4-BBA (68.3 kcal/mol [*Hurley et al.*, 1988]).

Measurements by Canonica et al. [*Canonica et al.*, 1995] for some selected substituted phenols showed that they had higher triplet energies than 4-BBA.

$$^3 4-\mathrm{BBA} + \mathrm{PhOH} \rightarrow 4-\mathrm{BBA} + {}^3\mathrm{PhOH} \qquad (9)$$

In order to obtain a more quantitative understanding of the ongoing reactions the overall quantum yields of the HONO-formation are estimated by using the solution UV/VIS-absorption spectra and the spectral irradiance measured at the outer surface of the reactor as presented in Figure 4. The estimated total photon absorptions of 0.5 mg PER-, 1 mg 4-BBA- and 1 mg 3,7-DHNA-films are 1.6×10^{-6}, 1.0×10^{-6} and 4.6×10^{-6} Einstein per second, respectively. Therefore, the highest overall quantum yields reached in the present study (for the mixtures of 4-BBA and 3,4-DHPAA and 20 ppb of NO_2) are estimated to be around 4.1×10^{-5}. This overall quantum yield is of course depending on the exact parameters in our experiments, as for example the NO_2 concentrations, the thickness and homogeneity of the organic films, but should give an impression about the effectiveness of the observed photoreactions. Clearly, the low quantum yields for the HONO-production leave room for a multitude of photophysical processes and photochemical reactions of the excited 4-BBA molecules and the conversion of $NO_2 \rightarrow$HONO is not more than a side reaction. The proposed mechanism is therefore rather uncertain, but it explains a number of the observed characteristics of the reaction, i.e. (i) the higher reactivity of the 4-BBA-mixtures than of the perylene mixtures, (ii) the acceleration of the photoreaction of 4-BBA with NO_2 in presence of non-absorbing electron donors, (iii) the low photo enhancement of the reaction of NO_2 with the electron donors in absence of 4-BBA and (iv) the high conversion yields of $NO_2 \rightarrow$HONO indicating that the reducing agent is photoproduced in the organic film.

Atmospheric implications

Based on experimental evidence presented in this study, photoinduced conversion of NO_2 into HONO has been observed on organic films, which exceeds the rate of the dark reaction by one order of magnitude (see Fig. 5) and that of reaction (2) by even more than one order of magnitude under our experimental conditions. Uptake coefficients observed here easily reach the 10^{-6} range or higher, with HONO yields between 50 and close to 100% with an artificial irradiance comparable to the irradiance in the wavelength interval of 300-400 nm at the Earth surface under 0° Zenith angle. From field measurements, it was recently estimated that there is an unknown daytime source of HONO which exceeds the night time source by a factor of 20 [*Kleffmann et al.*, 2003b]. Since the night time formation could be very well explained by emission and heterogeneous HONO formation on ground surfaces by reaction (2) [*Vogel et al.*, 2003a], a photoinduced enhancement of the rate of HONO formation by at least one order of magnitude observed in this study, would help to explain the missing daytime source. The species under study here are representatives of decomposition products of major structural components of vegetation and are ubiquitously distributed in the environment. In addition, the absorbing species necessary to provide excited molecules for initiating the primary electron transfer process from the phenolic species may be found among the oxidation products of the same species family, i.e., the natural oxidation chain produces the necessary ingredients of the suggested mechanism continuously. Note that such species are also present in the atmospheric aerosol, from the photochemical degradation of aromatics or as components of biomass burning aerosol.

Grannas et al. [*Grannas et al.*, 2004] report significant contributions of vanillyl phenols, syringyl phenols, cinnamyl phenols, p-hydroxyacetophenone, p-hydroxybenzaldehyde (lignin derived metabolites) to the organic carbon content in the arctic snow-pack. It seems therefore likely that the mechanism suggested here is also operating under those conditions. It could then even explain the high HONO yields observed in Arctic regions, since these high yields are in contradiction to the known photochemisty of nitrate. In the laboratory, the effective yield for nitrite formation was found to be two orders of magnitude smaller compared to the NO_2 formation [*Mark et al.*, 1996], whereas in arctic regions HONO/NO_2 ratios up to 1:2 are observed [*Beine et al.*, 2001]. So probably, the NO_2 formed in the nitrate photolysis is efficiently converted into HONO even on polar snow surfaces by the mechanism suggested here.

Acknowledgement

The support by the French program PRIMEQUAL2 for the project SHONO and by the Swiss National Science Foundation are gratefully acknowledged

(#) Now at Université de Provence, TRACES, Centre de Saint Jérôme, Case 512, 13397 Marseille cedex 20, Tel. : (+33)(0)4 91 28 86 43. E-mail : Rafal.Strekowski@up.univ-mrs.fr

References

Ackermann, R., A. Geyer, K.-H. Naumann, H. Saathoff, U. Schurath, S. Trick, et U. Platt, Direct quantification of HONO formation rates on urban surfaces, dans *XXVI EGS General Assembly 2001*, edited by EGS, Nice, France, 2001.

Albert, A., et E.P. Serjeant, *The Determination of Ionization Constants*, Chapman and Hall, London and New York, 1984.

Alfassi, Z.B., R.E. Huie, et P. Neta, Substituent effects on rates of one-electron oxidation of phenols by the radicals ClO_2, NO_2, and SO_3^-, *J. Phys. Chem.*, *90*, 4156-4158, 1986.

Alicke, B., A. Geyer, A. Hofzumahaus, F. Holland, S. Konrad, H.W. Paetz, J. Schaefer, J. Stutz, A. Volz-Thomas, et U. Platt, OH formation by HONO photolysis during the BERLIOZ experiment, *J. Geophys. Res.*, *108* (D4), PHO 3/1-PHO 3/17, 2003.

Alicke, B., U. Platt, et J. Stutz, Impact of nitrous acid photolysis on the total hydroxyl radical budget during the Limitation of Oxidant Production/Pianura Padana Produzione di Ozono study in Milan, *J. Geophys. Res.*, *107* (D22), LOP9/1-LOP9/17, 2002.

Ammann, M., M. Kalberer, D.T. Jost, L. Tobler, E. Rossler, D. Piguet, H.W. Gäggeler, et

U. Baltensperger, Heterogeneous production of nitrous acid on soot in polluted air masses, *Nature*, *395* (6698), 157-160, 1998.

Ammann, M., E. Rössler, R. Strekowski, et C. George, Uptake of NO2 on aqueous solutions containing phenoxy type compounds - Implication for HONO formation in the atmosphere, *Phys. Chem Chem. Phys.*, *In preparation*, 2004.

Anastasio, C., B.C. Faust, et C.J. Rao, Aromatic carbonyl compounds as aqueous-phase photochemical sources of hydrogen peroxide in acidic sulfate aerosols, fogs, and clouds .1. Non-phenolic methoxybenzaldehydes and methoxyacetophenones with reductants (phenols), *Environmental Science & Technology*, *31* (1), 218-232, 1997.

Arens, F., L. Gutzwiller, U. Baltensperger, H.W. Gäggeler, et M. Ammann, Heterogeneous Reaction of NO_2 on Diesel Soot Particles, dans *Environ. Sci. Technol.*, pp. 2191-2199, 2001.

Arens, F., L. Gutzwiller, H.W. Gaggeler, et M. Ammann, The reaction of NO2 with solid anthrarobin (1,2,10-trihydroxy-anthracene), *Physical Chemistry Chemical Physics*, *4* (15), 3684-3690, 2002.

Atkinson, R., Gas-Phase Tropospheric Chemistry of Organic-Compounds, *Journal of Physical and Chemical Reference Data*, R1-&, 1994.

Atkinson, R., D.L. Baulch, R.A. Cox, J.N. Crowley, R.F. Hampson, J.A. Kerr, R.G. Hynes, M.E. Jenkin, M.J. Rossi, et J. Troe, Summary evaluated kinetic and photochemical data for atmospheric chemistry:, *IUPAC Subcomittee for Gas Kinetik Data Evaluation*, *Web-Edition*, 2004.

Aumont, B., F. Chervier, et S. Laval, Contribution of HONO sources to the NOx/HOx/O3 chemistry in the polluted boundary layer, *Atmospheric Environment*, *37*, 487-498, 2003a.

Aumont, B., F. Chervier, et S. Laval, Contribution of HONO sources to the NOx/HOx/O3 chemistry in the polluted boundary layer, *Atmos. Environ.*, *37* (4), 487-498, 2003b.

Baker, J., S.F.M. Ashbourn, et R.A. Cox, Heterogeneous reactivity of nitrous acid on submicron sulfuric acid aerosol, *Physical Chemistry Chemical Physics*, *1* (4), 683-690, 1999.

Baraltosh, S., S.K. Chattopadhyay, et P.K. Das, A Laser Flash-Photolysis Study of Paraquat Reduction by Photogenerated Aromatic Ketyl Radicals and Carbonyl Triplets, *Journal of Physical Chemistry*, *88* (7), 1404-1408, 1984.

Behnke, W., C. George, V. Scheer, et C. Zetzsch, Production and decay of ClNO2 from the reaction of gaseous N2O5 with NaCl solution : bulk and aerosol experiments, *J. Geophys. Res.*, *102*, 3795-3804, 1997a.

Behnke, W., C. George, V. Scheer, et C. Zetzsch, Production and Decay of Clno2, from the Reaction of Gaseous N2O5 with NaCl Solution - Bulk and Aerosol Experiments, *J. Geophys. Res.*, *102* (D3), 3795-3804, 1997b.

Behnke, W., H.U. Krüger, V. Scheer, et C. Zetzsch, Formation of ClNO2 and HONO in the presence of NO2, O2 and wet aerosols, *J. Aerosol Sci.*, *S23*, 933-936, 1992.

Beine, H.J., I. Allegrini, R. Sparapani, A. Ianniello, et F. Valentini, Three years of springtime trace gas and particle measurements at Ny-Alesund, Svalbard, *Atmos. Environ.*, *35* (21), 3645-3658, 2001.

Brown, S.S., R.W. Wilson, et A.R. Ravishankara, Absolute intensities for third and fourth overtone absorptions in HNO3 and H2O2 measured by cavity ring down spectroscopy, *Journal of Physical Chemistry A*, *104* (21), 4976-4983, 2000.

Calvert, J.G., G. Yarwood, et A.M. Dunker, An evaluation of the mechanism of nitrous acid formation in the urban atmosphere, dans *Res. Chem. Intermed.*, pp. 463-502, 1994.

Canonica, S., B. Hellrung, et J. Wirz, Oxidation of phenols by triplet aromatic ketones in

aqueous solution, *J. Phys. Chem. A*, *104* (6), 1226-1232, 2000.

Canonica, S., U. Jans, K. Stemmler, et J. Hoigne, Transformation Kinetics of Phenols in Water - Photosensitization by Dissolved Natural Organic Material and Aromatic Ketones, *Environmental Science & Technology*, *29* (7), 1822-1831, 1995.

Chan, W.H., R.J. Nordstrom, J.G. Calvert, et J.H. Shaw, Kinetic Study of HONO Formation and Decay Reactions in Gaseous Mixtures of HONO, NO, NO2, H2O and N2, *Environ. Sci. Tech.*, *10*, 674-682., 1976.

Cheung, J.L., Y.Q. Li, J. Boniface, Q. Shi, P. Davidovits, D.R. Worsnop, J.T. Jayne, et C.E. Kolb, Heterogeneous interactions of NO2 with aqueous surfaces, *J. Phys. Chem. A*, *104* (12), 2655-2662, 2000a.

Cheung, J.L., Y.Q. Li, J. Boniface, Q. Shi, P. Davidovits, D.R. Worsnop, J.T. Jayne, et C.E. Kolb, Heterogeneous interactions of NO2 with aqueous surfaces, *J. Phys. Chem. A*, *104* (12), 2655-2662, 2000b.

Chughtai, A.R., S.A. Gordon, et D.M. Smith, Kinetics of the hexane soot reaction with NO2/N2O4 at low concentration, dans *Carbon*, pp. 405-16, 1994.

Cooney, D.O., S. Kim, et E.J. Davis, Analyses of mass transfer in hemodialyzers for laminar blood flow and homogeneous dialysate, *J. Chem. Eng. Sci.*, *29*, 1731-1738, 1974.

Cox, R.A., The Photolysis of Gaseous Nitrous acid, *J. Photochem.*, *3*, 175-188., 1974.

Cox, R.A., et M.E. Jenkin, Kinetics of the formation of nitrous acid from the thermal reaction of nitrogen dioxide and water vapor, dans *Comm. Eur. Communities, [Rep.] EUR*, pp. 300-8, 1987.

Danckwerts, P.V., *Gas-Liquid Reactions*, McGraw-Hill, New York, 1970a.

Danckwerts, P.V., *Gas-liquid reactions*, xiii, 276 pp., McGraw-Hill Book Co., New York,, 1970b.

Das, P.K., et S.N. Bhattacharyya, Laser Flash-Photolysis Study of Electron-Transfer Reactions of Phenolate Ions with Aromatic Carbonyl Triplets, *Journal of Physical Chemistry*, *85* (10), 1391-1395, 1981.

Das, P.K., M.V. Encinas, et J.C. Scaiano, Laser Flash-Photolysis Study of the Reactions of Carbonyl Triplets with Phenols and Photochemistry of Para-Hydroxypropiophenone, *Journal of the American Chemical Society*, *103* (14), 4154-4162, 1981.

De Santis, F., et I. Allegrini, Heterogeneous reactions of sulfur dioxide and nitrogen dioxide on carbonaceous surfaces, dans *Atmos. Environ., Part A*, pp. 3061-4, 1992.

Fickert, S., F. Helleis, J.W. Adams, G.K. Moortgat, et J.N. Crowley, Reactive uptake of ClNO2 on aqueous bromide solutions, *J. Phys. Chem. A*, *102*, 10689-10696, 1998.

Fine, P.M., G.R. Cass, et B.R.T. Simoneit, Chemical characterization of fine particle emissions from fireplace combustion of woods grown in the northeastern United States, *Environ. Sci. Technol.*, *35* (13), 2665-2675, 2001.

Finlayson-Pitts, B.J., et J.N. Pitts, *Atmospheric chemistry : fundamentals and experimental techniques*, xxviii, 1098 pp., Wiley, New York, 1986.

Finlayson-Pitts, B.J., et J.N. Pitts, *Chemistry of the Upper and Lower Atmosphere: Theory, Experiments and Applications*, Academic Press, San Diego, 2000.

Finlayson-Pitts, B.J., L.M. Wingen, A.L. Sumner, D. Syomin, et K.A. Ramazan, The heterogeneous hydrolysis of NO2 in laboratory systems and in outdoor and indoor atmospheres: An integrated mechanism, *Phys. Chem. Chem. Phys.*, *5* (2), 223-242, 2003.

Forni, L.G., V.O. Mora-Arellano, J.E. Packer, et R.L. Willson, Nitrogen dioxide and related free radicals: electron-transfer reactions with organic compounds in solutions containing nitrite or nitrate, *J. Chem. Soc. Perkin Trans.*, *II*, 1-6, 1986.

Fuzzi, S., S. Dcesari, M.C. Facchini, E. Matta, M. Mircea, et E. Tagliavini, A simplified model of the water soluble organic component of atmospheric aerosols,

Geophys. Res. Lett., *28* (21), 4079-4082, 2001.

Gallet, C., et C. Keller, Phenolic composition of soil solutions: comparative study of lysimeter and centrifuge waters, *Soil Biology & Biochemistry*, *31* (8), 1151-1160, 1999.

Gerecke, A., A. Thielmann, L. Gutzwiller, et M.J. Rossi, The Chemical-Kinetics of Hono Formation Resulting from Heterogeneous Interaction of NO_2 with Flame Soot, *Geophys. Res. Lett.*, *25* (13), 2453-2456, 1998.

Gorman, A.A., et M.A.J. Rodgers, The Quenching of Aromatic Ketone Triplets by Oxygen - Competing Singlet Oxygen and Biradical Formation, *Journal of the American Chemical Society*, *108* (17), 5074-5078, 1986.

Graedel, T.E., et C.J. Weschler, Chemistry within aqueous atmospheric aerosols and raindrops, *Reviews Geophysical Space Physics*, *19* (4), 505-539, 1981.

Graham, B., O.L. Mayol-Bracero, P. Guyon, G.C. Roberts, S. Decesari, M.C. Facchini, P. Artaxo, W. Maenhaut, P. Koll, et M.O. Andreae, Water-soluble organic compounds in biomass burning aerosols over Amazonia - 1. Characterization by NMR and GC-MS, *Journal of Geophysical Research-Atmospheres*, *107* (D20), art. no.-8047, 2002.

Grannas, A.M., P.B. Shepson, et T.R. Filley, Photochemistry and nature of organic matter in Arctic and Antarctic snow, *Global Biogeochemical Cycles*, *18* (1), art. no.-GB1006, 2004.

Gutzwiller, L., F. Arens, et M. Ammann, The HONO formation Capacity of Diesel Exhaust, dans *EC/EUROTRAC-2 joint Workshop*, edited by M.J. Rossi, et E.-V. Rossi, pp. 189, EPFL Lausanne, Lausanne, Switzerland, 2000.

Gutzwiller, L., F. Arens, et M. Ammann, New HONO source involving semi-volatile exhausts organics, dans *A Changing Atmosphere, 8th European Symposium on the Physico-chemical behaviour of pollutants*, edited by F. Raes, Torino, Italy, 2001.

Gutzwiller, L., F. Arens, U. Baltensperger, H.W. Gäggeler, et M. Ammann, Significance of semi-volatile diesel exhaust organics for secondary HONO formation, *Environ. Sci. Technol.*, *36*, 677-682, 2002a.

Gutzwiller, L., C. George, E. Rössler, et M. Ammann, Reaction kinetics of NO_2 with resorcinol and 2,7-naphthalenediol in the aqueous phase at different pH, *J. Phys. Chem. A*, *106*, 12045-12050, 2002b.

Hanson, D.R., et E.R. Lovejoy, Heterogeneous Reactions in Liquid Sulfuric Acid: HOCl + HCl as a Model System, *J. Phys. Chem.*, *100*, 6397-6405, 1996.

Hanson, D.R., et A.R. Ravishankara, Heterogeneous chemistry of bromine species in sulfuric acid under stratospheric conditions, *Geophys. Res. Lett.*, *22* (4), 385-8, 1995.

Harris, G.W., W.P.L. Carter, A.M. Winer, J.N. Pitts, Jr., U. Platt, et D. Perner, Observations of nitrous acid in the Los Angeles atmosphere and implications for predictions of ozone-precursor relationships, *Environ. Sci. Technol.*, *16* (7), 414-19, 1982.

Harrison, R.M., et A.-M.N. Kitto, Evidence for a surface source of atmospheric nitrous acid, *Atmos. Environ.*, *28* (6), 1089-94, 1994.

Harrison, R.M., J.D. Peak, et G.M. Collins, Tropospheric cycle of nitrous acid, *Journal of Geophysical Research*, *101* (D9), 14429-14439, 1996a.

Harrison, R.M., J.D. Peak, et G.M. Collins, Tropospheric cycle of nitrous acid, *J. Geophys. Res.*, *101* (D9), 14429-14439, 1996b.

Heland, J., J. Kleffmann, R. Kurtenbach, et P. Wiesen, A New Instrument To Measure Gaseous Nitrous Acid (HONO) in the Atmosphere, *Environ. Sci. Technol.*, *35* (15), 3207-3212, 2001.

Herrmann, H., B. Ervens, H.W. Jacobi, R. Wolke, P. Nowacki, et R. Zellner, CAPRAM2.3: A chemical aqueous phase radical mechanism for tropospheric chemistry, *J. Atmos. Chem.*, *36* (3), 231-284, 2000.

Hoffer, A., G. Kiss, M. Blazso, et A. Gelencser, Chemical characterization of humic-like substances (HULIS) formed from a lignin-type precursor in model cloud water, *Geophysical Research Letters*, *31* (6), art. no.-L06115, 2004.

Hurley, J.K., H. Linschitz, et A. Treinin, Interaction of Halide and Pseudohalide Ions with Triplet Benzophenone-4-Carboxylate - Kinetics and Radical Yields, *Journal of Physical Chemistry*, *92* (18), 5151-5159, 1988.

Inbar, S., H. Linschitz, et S.G. Cohen, Quenching, Radical Formation, and Disproportionation in the Photo-Reduction of 4-Carboxybenzophenone by 4- Carboxybenzhydrol, Hydrazine, and Hydrazinium Ion, *Journal of the American Chemical Society*, *103* (24), 7323-7328, 1981.

Jenkin, M.E., R.A. Cox, et D.J. Williams, Laboratory studies of the kinetics of formation of nitrous acid from the thermal reaction of nitrogen dioxide and water vapor, dans *Atmos. Environ.*, pp. 487-98, 1988.

Kalberer, M., K. Tabor, A. Ammann, Y. Parrat, E. Weingartner, D. Piguet, E. Rössler, D.T. Jost, A. Türler, H.W. Gäggeler, et U. Baltensperger, Heterogeneous chemical processing of 13NO2 by monodisperse carbon aerosols at very low concentrations, *J. Phys. Chem.*, *100* (38), 15487-15493, 1996.

Kleffmann, J., K.H. Becker, M. Lackhoff, et P. Wiesen, Heterogeneous conversion of NO2 on carbonaceous surfaces, *Phys. Chem. Chem. Phys.*, *1* (24), 5443-5450, 1999.

Kleffmann, J., K.H. Becker, et P. Wiesen, Heterogeneous NO_2 conversion processes acid surfaces: possible atmospheric implications, dans *Atmos. Environ.*, pp. 2721-2729, 1998a.

Kleffmann, J., K.H. Becker, et P. Wiesen, Investigation of the heterogeneous NO2 conversion on perchloric acid surfaces, *Journal of the Chemical Society Faraday Transactions*, *94* (21), 3289-3292, 1998b.

Kleffmann, J., T. Benter, et P. Wiesen, Heterogeneous Reaction of Nitric Acid with Nitric Oxide on Glass Surfaces under Simulated Atmospheric Conditions, *J. Phys. Chem. A*, *108* (27), 5793-5799, 2004.

Kleffmann, J., J. Heland, R. Kurtenbach, J.C. Lörzer, et P. Wiesen, A new instrument (LOPAP) for the detection of nitrous acid (HONO), *Environ. Sci. Pollut. Res.*, *9* (4), 48-54, 2002.

Kleffmann, J., R. Kurtenbach, J. Lörzer, P. Wiesen, N. Kalthodd, B. Vogel, et H. Vogel, Measured and simulated vertical profiles of nitrous acid-Part I: Field measurements, *Atmospheric Environment*, *37*, 2949-2955, 2003a.

Kleffmann, J., R. Kurtenbach, J. Lörzer, P. Wiesen, N. Kalthoff, B. Vogel, et H. Vogel, Measured and simulated vertical profiles of nitrous acid - Part I: Field measurements, *Atmos. Environ.*, *37* (21), 2949-2955, 2003b.

Kolb, C.E., D.R. Worsnop, M.S. Zahniser, P. Davidovits, D.R. Hanson, A.R. Ravishankara, L.F. Keyser, M.T. Leu, L.R. Williams, M.J. Molina, et M.A. Tolbert, Laboratory Studies of Atmospheric Heterogeneous Chemistry; Current Problems in Atmospheric Chemistry, in *Advances in Physical Chemistry Series*, edited by J.R. Barker, World scientific, Singapore, 1994.

Kurtenbach, R., K.H. Becker, J.A.G. Gomes, J. Kleffmann, J.C. Lörzer, M. Spittler, P. Wiesen, R. Ackermann, A. Geyer, et U. Platt, Investigations of emissions and heterogeneous formation of HONO in a road traffic tunnel, *Atmos. Environ.*, *35* (20), 3385-3394, 2001.

Lahoutifard, N., M. Ammann, L. Gutzwiller, B. Ervens, et C. George, The impact of multiphase reactions of NO2 with aromatics: a modelling approach, *Atmospheric Chemistry and Physics*, *2*, 215-226, 2002.

Lammel, G., et J.N. Cape, Nitrous acid and nitrite in the atmosphere, dans *Chem. Soc. Rev.*, pp. 361-370, 1996.

Lary, D.J., D.E. Shallcross, R. Toumi, et M.W. Chase, Carbonaceous aerosols and their

potential role in atmospheric chemistry, *Journal of Geophysical Research Atmospheres*, *104* (D13), 15929-15940, 1999.

Lee, J.H., et I.N. Tang, Accommodation Coefficient of Gaseous NO2 on Water Surfaces, *Atmos. Environ.*, *22*, 1147-1151., 1988.

Lee, Y.N., et S.E. Schwartz, Evaluation of the rate of uptake of nitrogen dioxide by atmospheric and surface liquid water, dans *JGR, J. Geophys. Res., [Sect.] C*, pp. 11971-83, 1981a.

Lee, Y.N., et S.E. Schwartz, Reaction kinetics of nitrogen dioxide with liquid water at low partial pressure, dans *J. Phys. Chem.*, pp. 840-8, 1981b.

Loeff, I., J. Rabani, A. Treinin, et H. Linschitz, Charge-Transfer and Reactivity of N-Pi-Asterisk and Pi-Pi- Asterisk Organic Triplets, Including Anthraquinonesulfonates, in Interactions with Inorganic Anions - a Comparative-Study Based on Classical Marcus Theory, *Journal of the American Chemical Society*, *115* (20), 8933-8942, 1993.

Lögager, T., et K. Sehested, Formation and decay of peroxynitric acid: a pulse radiolysis study, *J. Phys. Chem.*, *97* (39), 10047-52, 1993.

Lovejoy, E.R., L.G. Huey, et D.R. Hanson, *J. Geophys. Res.*, *100*, 18775, 1995.

Madronich, S., Photodissociation in the Atmosphere .1. Actinic Flux and the Effects of Ground Reflections and Clouds, *Journal of Geophysical Research-Atmospheres*, *92* (D8), 9740-9752, 1987.

Mark, G., H.-G. Korth, H.-P. Schuchmann, et C. von Sonntag, The photochemistry of aqueous nitrate ion revisited, *J. Photochem. Photobiol., A*, *101* (2-3), 89-103, 1996.

Mayol-Bracero, O.L., P. Guyon, B. Graham, G. Roberts, M.O. Andreae, S. Decesari, M.C. Facchini, S. Fuzzi, et P. Artaxo, Water-soluble organic compounds in biomass burning aerosols over Amazonia - 2. Apportionment of the chemical composition and importance of the polyacidic fraction, *Journal of Geophysical Research-Atmospheres*, *107* (D20), art. no.-8091, 2002.

McKenzie, L.M., W.M. Hao, G.N. Richards, et D.E. Ward, Measurement and Modeling of Air Toxins from Smoldering Combustion of Biomass, *Environmental Science & Technology*, *29* (8), 2047-2054, 1995.

Melhuish, W.H., Quantum Efficiencies of Fluorescence of Organic Substances - Effect of Solvent and Concentration of Fluorescent Solute, *Journal of Physical Chemistry*, *65* (2), 229-&, 1961.

Mertes, S., et A. Wahner, Uptake of nitrogen dioxide and nitrous acid on aqueous surfaces, *J. Phys. Chem.*, 1994.

Miao, J.L., W.F. Wang, J.X. Pan, C.Y. Lu, R.Q. Li, et S.D. Yao, The scavenging reactions of nitrogen dioxide radical and carbonate radical by tea polyphenol derivatives: a pulse radiolysis study, *Radiation Phys. Chem.*, *60* (3), 163-168, 2001.

Murov S. L, C., I., Hug, G., L., *Handbook of Photochemistry*, 1993.

Murphy, D.M., et D.W. Fahey, Mathematical treatment of the wall loss of a trace species in denuder and catalytic converter tubes, *Analytical Chemistry*, *59*, 2753-2759, 1987.

Olariu, R.I., I. Barnes, K.H. Becker, et B. Klotz, Rate coefficients for the gas-phase reaction of OH radicals with selected dihydroxybenzenes and benzoquinones, *Int. J. Chem. Kin.*, *32* (11), 696-702, 2000.

Park, J.Y., et Y.N. Lee, Aqueous Solubility and Reactivity of Nitrous Acid, *Symposium on Acid Rain , American Chemical Society Meeting*, *437-440.*, 1986.

Parker, C.A., et T.A. Joyce, Formation Efficiency and Energy of Perylene Triplet, *Chemical Communications* (4), 108-&, 1966.

Perner, D., et U. Platt, Detection of nitrous acid in the atmosphere by differential optical absorption, *Geophys. Res. Lett.*, *6* (12), 917-20, 1979.

Pires, M., M.J. Rossi, et D.S. Ross, Kinetic and Mechanistic Aspects of the No Oxidation

by O-2 in Aqueous-Phase, *Int. J. Chem. Kin.*, *26* (12), 1207-1227, 1994.

Ramazan, K.A., D. Syomin, et B.J. Finlayson-Pitts, The photochemical production of HONO during the heterogeneous hydrolysis of NO2, *Phys. Chem. Chem. Phys.*, *6* (14), 3836-3843, 2004.

Ren, X., H. Harder, M. Martinez, R.L. Lesher, A. Oliger, J.B. Simpas, W.H. Brune, J.J. Schwab, K.L. Demerjian, Y. He, X. Zhou, et H. Gao, OH and HO2 chemistry in the urban atmosphere of New York City, *Atmos. Environ.*, *37* (26), 3639-3651, 2003.

Rogaski, C.A., D.M. Golden, et L.R. Williams, Reactive uptake and hydration experiments on amorphous carbon treated with NO2, SO2, O3, HNO3, and H2SO4, dans *Geophys. Res. Lett.*, pp. 381-384, 1997.

Rogge, W.F., L.M. Hildemann, M.A. Mazurek, G.R. Cass, et B.R.T. Simoneit, Sources of fine organic aerosol. 9. Pine, oak and synthetic log combustion in residential fireplaces, *Environ. Sci. Technol.*, *32* (1), 13-22, 1998.

Rohrer, F., B. Bohn, T. Brauers, D. Brüning, J.-F. Johnen, A. Wahner, et J. Kleffmann, Characterisation of the Photolytic HONO-Source in the Atmosphere Simulation Chamber SAPHIR, *Atmos. Chem. Phys. Discuss.*, *4*, 7881-7915, 2004.

Saliba, N.A., M. Mochida, et B.J. Finlayson-Pitts, Laboratory studies of sources of HONO in polluted urban atmospheres, *Geophys. Res. Lett.*, *27* (19), 3229-3232, 2000.

Scheer, V., A. Frenzel, W. Behnke, C. Zetzsch, L. Magi, C. George, et P. Mirabel, Uptake of nitrosyl chloride, *J. Phys. Chem. A*, *101*, 9359-9366, 1997.

Schwartz, S.E., Mass-transport considerations pertinent to aqueous phase reactions of gases in liquid-water clouds, in *Chemistry of Multiphase Atmospheric Systems, NATO ASI Ser.*, edited by W. Jaesche, pp. 415-471, Springer-Verlag, Berlin, 1986.

Schwartz, S.E., et Y.N. Lee, Laboratory Study of NO2 Reaction with Dispersed and Bulk Liquid Water, *Atmos. Environ.*, *29* (18), 2557-2559, 1995.

Simoneit, B.R.T., J.J. Schauer, C.G. Nolte, D.R. Oros, V.O. Elias, M.P. Fraser, W.F. Rogge, et G.R. Cass, Levoglucosan, a tracer for cellulose in biomass burning and atmospheric particles, *Atmos. Environ.*, *33*, 173-182, 1999.

Stockwell, W.R., F. Kirchner, M. Kuhn, et S. Seefeld, A new mechanism for regional atmospheric chemistry modeling, *J. Geophys. Res.*, *102* (D22), 25847-25879, 1997.

Strekowski, R.S., et C. George, Measurement of Henry's Law Constants for Acetone, 2-Butanone, 2,3-Butanedione and Isobutyraldehyde Using a Horizontal Flow Reactor, *submitted to J. Chem. Eng. Data*, 2005.

Tabor, K., L. Gutzwiller, et M.J. Rossi, Heterogeneous Chemical-Kinetics of NO2 on Amorphous-Carbon at Ambient-Temperature, *J. Phys. Chem.*, *98* (24), 6172-6186, 1994.

Tan, K.H., *Humic matter in soil and the environment: principles and controversies*, 360 pp., Marcel Dekker, Inc, New York, Basel, 2003.

Trick, S., Formation of Nitrous Acid on Urban Surfaces - A Physical-Chemical Perspective, University of Heidelberg, Heidelberg, 2004.

Vogel, B., H. Vogel, J. Kleffmann, et R. Kurtenbach, Measured and simulated vertical profiles of nitrous acid - Part II. Model simulations and indications for a photolytic source, *Atmos. Environ.*, *37* (21), 2957-2966, 2003a.

Vogel, B., H. Vogel, J. Kleffmann, et R. Kurtenbach, Measured and simulated vertical profiles of nitrous acid-Part II. Model simulations and indications for a photolytic source, *Atmospheric Environment*, *37*, 2957-2966, 2003b.

Vogt, R., et B.J. Finlayson-Pitts, Tropospheric Hono and Reactions of Oxides of Nitrogen with NaCl, *Geophys. Res. Lett.*, *21* (21), 2291-2294, 1994.

Zhan, Z., S. Yao, W. Lin, W.F. Wang, Y. Jin, et N. Lin, Mechanism of Reaction of Nitrogen Dioxide Radical with

Hydroxycinnamic Acid Derivatives: A Pulse Radiolysis Study, *Free Rad. Res.*, *29*, 13-16, 1998.

Zhou, X., H.J. Beine, R.E. Honrath, J.D. Fuentes, W. Simpson, P.B. Shepson, et J.W. Bottenheim, Snowpack photochemical production of HONO: A major source of OH in the Arctic boundary layer in springtime, *Geophys. Res. Lett.*, *28* (21), 4087-4090, 2001.

Zhou, X., K. Civerolo, H. Dai, G. Huang, J. Schwab, et K. Demerjian, Summertime nitrous acid chemistry in the atmospheric boundary layer at a rural site in New York State, *J. Geophys. Res.*, *107* (D21), ACH13/1-ACH13/11, 2002a.

Zhou, X., H. Gao, Y. He, G. Huang, S.B. Bertman, K. Civerolo, et J. Schwab, Nitric acid photolysis on surfaces in low-NOx environments: significant atmospheric implications, *Geophys. Res. Lett.*, *30* (23), ASC 12/1-ASC 12/4, 2003.

Zhou, X., Y. He, G. Huang, T.D. Thornberry, M.A. Carroll, et S.B. Bertman, Photochemical production of nitrous acid on glass sample manifold surface, *Geophys. Res. Lett.*, *29* (14), 26/1-26/4, 2002b.

Table I Summary of the measured uptake coefficients on solid films using the coated wall flowtube /MS combination

Type	RH (%)	γ_{dark} (10^{-6})	γ_{light} (10^{-6})
Benzophenone	dry	0.32	0.65
Benzophenone / Catechol	dry	1.26	2.40
Benzophenone / Catechol	14	1.30	2.51
Benzophenone / Catechol	76	3.6	5.1
Catechol	dry	0.07	1.4
Catechol	42	1.1	1.8
Anthracene	dry	0.66	1.2
Anthracene	56	1.9	2.3
Catechol / Anthracene	dry	< 0.1	0.89
Catechol / Anthracene	46	0.67	1.3
Anthrarobin	14	0.24	0.34

Table II. Reactivity and HONO-yields of the reaction of NO_2 with differently composed organic films in the dark and under irradiation (300-420 nm)

type of organic coating and amount of organic compound used	% removal of initial [NO_2] by dark reaction[b] [%]	% yield of HONO per reacted NO_2 in dark reaction [%]	% removal of initial [NO_2] by light reaction[c,d] [%]	% yield of HONO per reacted NO_2 in light reaction [%]
sodium 4-benzoylbenzoate (1 mg)	4	7	20/17	45/48
4-benzoylbenzoic acid (1 mg)	2	n.a.	12/12	68/71
3,7-dihydroxy-2-napthoic acid (1 mg)	4	11	22/28/38[e]	67/74/77
perylene (0.5 mg)	3	n.a.	~0/0	n.a
syringic acid (1 mg)	6	6	7/7	36/43
3,4-dihydroxyphenylacetic acid (1 mg)	6	n.a.	1/2	n.a
potassium iodide (1 mg)	53	100	~0/0	n.a
external mixture[a]: sodium 4-benzoylbenzoate (1 mg) syringic acid (0.5 mg)	4	4	36/36	61/70
external mixture[a]: sodium 4-benzoylbenzoate (1 mg) 3,4-dihydroxyphenylacetic acid (1 mg)	2	n.a.	42/38	91/90
external mixture[a]: sodium 4-benzoylbenzoate (1 mg) potassium iodide (1 mg)	14	n.a	66/58	93/101
external mixture[a]: perilene (0.5 mg) 3,4-dihydroxyphenylacetic acid (1 mg)	2	n.a.	6/9	57/67
external mixture[a]: perilene (0.5 mg) potassium iodide (1 mg)	20	>80	7/10	n.a
internal mixture[a]: 4-benzoylbenzoic acid (1 mg) 3,4-dihydroxyphenylacetic acid (0.5 mg)	16	n.a	52/63	90/93
internal mixture[a]: 4-benzoylbenzoic acid (1 mg) 3,4-dihydroxyphenylacetic acid(1 mg)	7	n.a.	47/58	95/97

[a]The term external mixture is used when the reactor surface was coated first by the absorber molecule and subsequently by the phenol or potassium iodide. The term internal mixture is used when the reactor was coated from one solution containing both compounds.
[b]The removal of NO_2 due to the dark reaction was measured by exposing the coated wall reactor to the NO_2-mixture and measuring the decrease of the NO_2 concentration.
[c]The removal of NO_2 due to the light reaction was measured by illuminating the NO_2-mixture flowing through the coated wall reactor and comparing the NO_2 concentration before and during the irradiation.
[d]Values after 5 and 10 minutes of irradiation, respectively
[e]Values after 5,10 and 25 minutes of irradiation, respectively